COMILLAS
UNIVERSIDAD PONTIFICIA
ICAI

MASTER'S DEGREE IN INDUSTRIAL ENGINEERING

MASTER'S THESIS

DIVERSITY FOR HUMAN MODELLING IN MADYMO SOFTWARE

DEVELOPMENT OF THE FEMALE 50TH PERCENTILE ACTIVE HUMAN MODEL

Author: Juan Manuel Asensio Gil

Supervisor: Richard Lancashire

Madrid

Declaro, bajo mi responsabilidad, que el Proyecto presentado con el título

Diversity for Human Modelling in Madymo Software

en la ETS de Ingeniería - ICAI de la Universidad Pontificia Comillas en el

curso académico 2021/2022 es de mi autoría, original e inédito y

no ha sido presentado con anterioridad a otros efectos.

El Proyecto no es plagio de otro, ni total ni parcialmente y la información que ha sido

tomada de otros documentos está debidamente referenciada.

Fdo.: Juan Manuel Asensio Gil Fecha: 17/08/2022

Autorizada la entrega del proyecto

EL DIRECTOR DEL PROYECTO

Fdo.: Richard Lancashire Fecha: 17/08/2022

COMILLAS
UNIVERSIDAD PONTIFICIA
ICAI

MASTER'S DEGREE IN INDUSTRIAL ENGINEERING

MASTER'S THESIS

DIVERSITY FOR HUMAN MODELLING IN MADYMO SOFTWARE

DEVELOPMENT OF THE FEMALE 50TH PERCENTILE ACTIVE HUMAN MODEL

Author: Juan Manuel Asensio Gil

Supervisor: Richard Lancashire

Madrid

Acknowledgements

I would like to thank Siemens Digital Industry Software and Simcenter Madymo's Safety and Comfort Modelling Team, for once more giving me the opportunity to work and learn with them.

In particular, I would like to thank my supervisor Richard Lancashire, for his excellent guidance and advice during the development of this project; and Erik Dijkstra and Karan Chatrath for their invaluable support and technical insight.

I would also like to thank the Comillas Pontifical University and the group of professors that conforms it, for the technical and interpersonal skills acquired during my Master's Degrees and my Bachelor's Degree. Said skills have provided me with the necessary tools to face any engineering problem with professionalism, dedication, and integrity.

Additionally, I would like to thank my family and friends for the emotional support received throughout this experience.

DIVERSIDAD EN MODELOS HUMANOS EN EL SOFTWARE MADYMO

Desarrollo del Modelo Humano Activo Femenino percentil 50

Autor: Asensio Gil, Juan Manuel.
Director: Lancashire, Richard.
Entidad Colaboradora: Siemens Industry Software Netherlands B.V.

RESUMEN

El objetivo de este Trabajo Fin de Máster fue el de proporcionar a fabricantes de equipo original (OEM, por sus siglas en inglés) y programas de evaluación de seguridad vehicular, una herramienta para mejorar la seguridad de las mujeres como usuarias de la vía, mediante el desarrollo del Modelo Humano Activo Femenino percentil 50 (FAHM) del programa informático Siemens Simcenter Madymo. En primer lugar, se realizó un análisis de antropometría femenina, en el que se discutieron las principales diferencias biomecánicas entre los hombres y las mujeres. Esto, junto con un análisis de otras soluciones tecnológicas existentes a los modelos del percentil 50 femenino, permitió la selección del modelo base y las principales referencias para este estudio. En segundo lugar, se analizó y se realizó el método de desarrollo de modelado humano más adecuado, centrándose en la respuesta pasiva del modelo. Tanto la parte morfométrica como la parte dinámica se modelaron según la metodología y las referencias establecidas. En tercer lugar, se diseñó y se ejecutó un proceso de validación. Los resultados iniciales mostraron consistencia, coherencia y robustez en la respuesta local y global del modelo. Además, se realizó una comparación local frente al modelo ViVA+, que mostró una respuesta dinámica y cinemática inicial similares para ambos modelos, pero con un comportamiento más rígido del FAHM en la zona abdominal y pélvica. Además, el modelo ViVA+ mostró una recuperación significativamente más rápida de la caja torácica. En todos los casos, las respuestas de ambos modelos estuvieron dentro del mismo orden de magnitud, y las diferencias observadas fueron consistentes. Finalmente, las futuras investigaciones sugeridas incluyen validación adicional enfocándose en las diferencias mencionadas, y la implementación de la respuesta activa y de funciones de riesgo de lesión específicas para la mujer.

Palabras clave: antropometría, biofidelidad, modelo humano, multicuerpo, seguridad femenina

1. Introducción

La literatura recopilada concluyó que la seguridad de las mujeres como usuarias de la carretera es significativamente menor que la de los hombres. Por ejemplo, según [i], las mujeres estadounidenses tienen un 17% más de probabilidades que los hombres de morir en un accidente de tráfico; y, según [ii], las mujeres de todo el mundo tienen un 73% más de probabilidades que los hombres de sufrir lesiones AIS 3+ o superior. Un análisis adicional sugirió que no solo las diferencias fisiológicas relacionadas con el sexo podrían ser responsables, sino también el comportamiento, la cultura y el diseño de los sistemas de seguridad de los vehículos. Las posibles razones propuestas para esto último son la falta general (con 2 excepciones) de representación de la antropometría femenina en el sector de la seguridad de los vehículos, y que los diferentes fabricantes de equipos originales (OEM) y los programas de evaluación de la seguridad vehicular (tanto de

homologación como evaluaciones de consumidores), que forman parte del sector de la seguridad de los vehículos, consideran la seguridad de las mujeres promedio cubierta por la antropometría media masculina.

Por lo tanto, la visión de este estudio fue: proporcionar a estas organizaciones otra herramienta para mejorar tanto el diseño de los vehículos (en cuanto a comodidad y seguridad) como la evaluación de la seguridad de estos, con el fin de aumentar la seguridad de las usuarias de la carretera, así como mejorar la predicción de las lesiones femeninas. En consecuencia, la misión fue: desarrollar un modelo humano multicuerpo percentil 50 femenino. La definición del alcance y los objetivos de esta misión solo incluyó la respuesta pasiva del nuevo modelo, y no la respuesta activa.

2. Descripción de las Tecnologías

Siemens Simcenter Madymo fue el principal programa informático utilizado en este estudio. Se trata de uno de los más utilizados a nivel mundial en cuanto a Dinámica del Multicuerpo, aunque también incluye Método de Elementos Finitos y dinámica de fluidos, y su modelo humano más complejo es el Modelo Humano Activo (percentil 50 masculino, con siglas AHM). En el contexto de este programa informático, la definición de la misión se ajustó de la siguiente manera: desarrollar el Modelo Humano Activo Femenino percentil 50 (con siglas FAHM). Esto implica que este nuevo modelo sería el equivalente femenino del AHM mencionado.

Otros programas informáticos o herramientas específicas utilizados en este Trabajo Fin de Máster fueron: Madymo Scaler Tool (herramienta de escalado), Siemens Jack Scaling (base de datos de antropometría humana), LS-Dyna (solucionador de elementos finitos, utilizado para simulaciones acopladas con Madymo) y Altair HyperMesh (programa informático de modelado de elementos finitos, utilizado para modificaciones morfométricas de las geometrías).

Por último, la configuración computacional seleccionada tanto para Madymo como para LS-Dyna en las simulaciones acopladas mencionadas fue la de Procesamiento en Paralelo a Gran Escala (con siglas mpp).

3. Estado del Arte

Un análisis de la antropometría y el comportamiento biomecánico femenino mostró la existencia de varias diferencias entre hombres y mujeres. Entre ellas, las que son compatibles con la Dinámica de Multicuerpo y se consideran adecuadas y suficientes para una implementación parcial o total en el FAHM, están relacionadas con la distribución del tejido adiposo, la morfometría de la columna cervical, el comportamiento y la musculatura del cuello, la masa de la cabeza y la morfometría de la pelvis. Otras diferencias encontradas, pero no implementadas en este estudio (debido a la falta de datos disponibles) involucraban la fuerza de los ligamentos y tendones, la fuerza biomecánica general, las propiedades óseas generales, las medidas antropométricas del radio, las propiedades corticales de la tibia y la fisiología y el comportamiento del tobillo.

En cuanto a otras aproximaciones tecnológicas existentes a los modelos percentil 50 femenino, se encontraron el ATD virtual EvaRID de Humanetics y el modelo ViVA+. Esto, junto con el anterior análisis de la antropometría femenina, permitió la selección del modelo base (el AHM) y las referencias de este estudio. De estos últimos, las llamadas "referencias principales" incluyeron un estudio interno previo de Madymo sobre el desarrollo de un sistema de cuello femenino específico (denominado MR1) y el modelo escalable percentil 5 femenino de Simcenter Madymo (MR2).

Asimismo, se realizó un proceso de escalado automático mediante la herramienta Madymo Scaler Tool y usando una base de datos de Siemens Jack Scaling para MR2, con el fin de poder usarlo como referencia para la distribución antropométrica femenina promedio. Se consideró que el estudio del National Health and Nutrition Examination Survey (NHANES) de 2011 a 2014 era la base de datos más adecuada (de Siemens Jack Scaling) para este estudio.

4. Desarrollo del modelo

El método de desarrollo de modelo seleccionado fue el de escalado, con excepción de la geometría de la piel (relacionada directamente con la distribución del tejido adiposo), la morfometría pélvica y la implementación de MR1. El enfoque matemático utilizado para el escalado fue el mismo implementado en Madymo Scaler Tool.

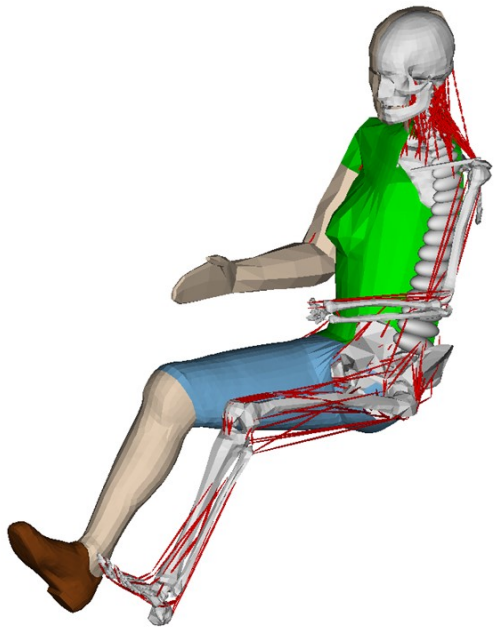

Figura i. Modelo Humano Activo Femenino percentil 50 de Siemens Simcenter Madymo

El primer paso del desarrollo se centró en la parte morfométrica del modelo, a partir de la modificación morfométrica de la pelvis y de la superficie torácica atendiendo a su función dentro de Madymo, y a las herramientas, datos de entrada y recursos disponibles. Posteriormente, se implementó MR1 en el nuevo modelo, necesitando realizar previamente varias modificaciones en cuanto a su estructura. A continuación, se llevó a

cabo el resto de la parte morfométrica, asociada al proceso de escalado. Finalmente, se realizó la parte dinámica del modelo (proceso de escalado puro), obteniéndose posteriormente, el nuevo FAHM (ver Figura i), que dio como resultado una diferencia del 1,2% en altura, y del 4% en masa total con respecto a MR2.

5. Validación del modelo

Validar un modelo es comprobar si dicho modelo se comporta de igual forma al grupo humano al cual representa, tanto cinemáticamente como dinámicamente. Los tipos de pruebas de validación de modelos se pueden categorizar usando dos criterios diferentes. En primer lugar, las pruebas experimentales con cadáveres (PMHS, por sus siglas en inglés) se utilizan para la validación de la respuesta pasiva, mientras que las pruebas experimentales con voluntarios se utilizan para la respuesta activa. En segundo lugar, las pruebas de validación locales (por ejemplo, las pruebas de impacto localizado) se utilizan para la validación de subsistemas del modelo, mientras que la validación global se centra en escenarios comunes específicos (pruebas con trineos y vehículos) y en las principales respuestas del modelo en su conjunto. La combinación que mejor se ajusta a este estudio fue la de las pruebas de validación PMHS, primero nivel local y luego a nivel global.

La normalización de la respuesta fue un elemento clave en el análisis de los datos de validación, y el método de normalización seleccionado fue el del estudio de Mertz de 1984 [iii]. Sin embargo, las curvas obtenidas deben considerarse como una aproximación en el caso de datos experimentales masculinos normalizados a femeninos, especialmente en lo que respecta a la validación local, debido a las diferencias antropométricas observadas entre hombres y mujeres.

Se realizó un primer paso en la validación local, utilizando las ‘pruebas de validación estándar’ y comparando las respuestas del FAHM y del AHM. Se normalizaron los pasillos experimentales de los experimentos cadavéricos para el FAHM. Los resultados mostraron robustez, consistencia y coherencia con los factores de escalado utilizados para cada eje y parte del modelo.

En un segundo paso en la validación local, se comparó el FAHM y el modelo ViVA+ (la validación local del modelo aún no se ha publicado en el momento de la documentación de ese Trabajo Fin de Máster) mediante una versión modificada de las pruebas de validación anteriores. No se incluyeron los pasillos experimentales, debido a los ajustes realizados a las pruebas estándar. Se normalizaron las respuestas del modelo ViVA+. Ambos modelos mostraron una respuesta cinemática inicial similar, pero el desarrollo cinemático del FAHM fue en general más rígido (como se muestra en el ejemplo de la Figura ii). La respuesta dinámica para ambos modelos fue en general similar, pero el FAHM mostró un comportamiento más rígido en la zona abdominal y pélvica. Además, el modelo ViVA+ mostró una recuperación significativamente más rápida de la caja torácica. En todos los casos, las respuestas de ambos modelos estuvieron dentro del mismo orden de magnitud, y las diferencias observadas fueron consistentes.

Por último, se realizó la validación global utilizando un conjunto de pruebas de la 'validación estándar' y comparando, como en la validación local, el AHM y el FAHM con el fin de comprobar la robustez, la coherencia y la consistencia del FAHM. De igual forma, los resultados mostraron una respuesta del FAHM proporcional a los factores de escalado utilizados en su desarrollo.

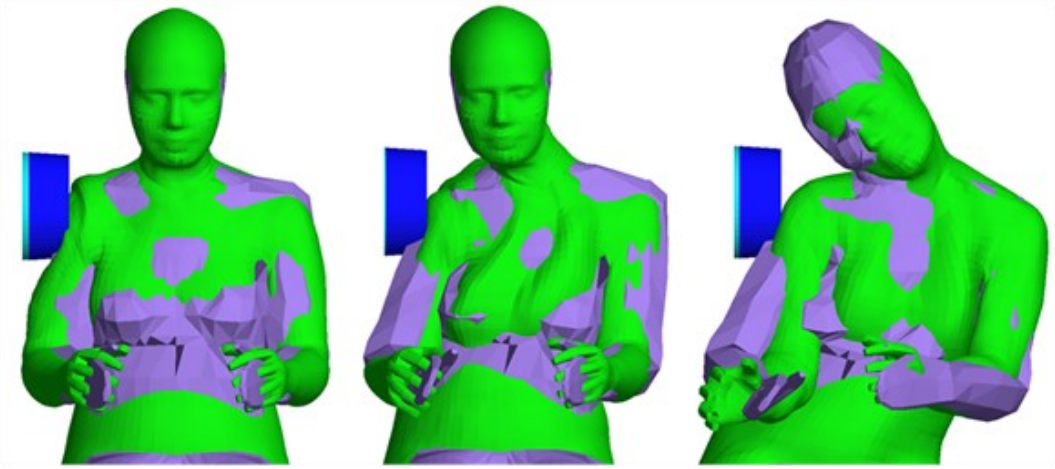

Figure ii. Impacto lateral en hombre a 4.5 m/s. FAHM (morado) vs modelo ViVA+ (verde)

6. Trabajos Futuros y Conclusiones

Los trabajos futuros sugeridos para el FAHM se centran en una validación pasiva adicional, la implementación y validación de una respuesta activa femenina específica, la implementación de características antropométricas adicionales femeninas específicas, y la parametrización completa del modelo para su uso en Madymo Scaler Tool.

En conclusión, este estudio desarrolló un Modelo Humano Activo Femenino percentil 50 utilizando datos de entrada recopilados a partir del análisis antropométrico femenino. Dicho análisis permitió definir el modelo base y las referencias para el desarrollo del modelo. Después del proceso, el modelo mostró consistencia en términos de distribución antropométrica con las referencias mencionadas. Se realizó un primer acercamiento a la validación del FAHM, obteniendo respuestas consistentes, coherentes y robustas tanto a nivel local como global. Además, se realizó una comparación local frente al modelo ViVA+, que mostró respuestas globales similares, aunque se observaron algunas diferencias.

7. Referencias

[i] C. J. Kahane. Injury vulnerability and effectiveness of occupant protection technologies for older occupants and women. (Report No. DOT HS 811 766). 2013. Washington, DC: National Highway Traffic Safety Administration (NHTSA).

[ii] J. Forman, G. S. Poplin, C. G. Shaw, T. L. McMurry, K. Schmidt, J. Ash & C. Sunnevang. Automobile injury trends in the contemporary fleet: Belted occupants

in frontal collisions. 2019. Traffic Injury Prevention. 2019;20(6):607-612. doi: 10.1080/15389588.2019.1630825.

[iii] Mertz, H. A Procedure for Normalizing Impact Response Data. 1984. SAE Technical Paper 840884. Warrendale, PA, USA.

DIVERSITY FOR HUMAN MODELLING IN MADYMO SOFTWARE

Development of the Female 50th percentile Active Human Model

Author: Asensio Gil, Juan Manuel.
Supervisor: Lancashire, Richard.
Collaborating Entity: Siemens Industry Software Netherlands B.V.

ABSTRACT

This aim of this Master´s Thesis was to provide OEMs and vehicle safety assessment programmes with a tool to improve female safety as road users by developing the Siemens Simcenter Madymo´s Female 50th percentile Active Human Model (FAHM). Firstly, a female anthropometry analysis was performed, in which the main biomechanical differences between males and females were discussed. This, together with an analysis of other existent technological approaches to female 50th percentile models, allowed for the selection of the baseline model and the main references for this study. Secondly, the most adequate human model development method was analysed and performed, focusing on the model´s passive response. Both the morphometry and dynamic parts were modelled within the established methodology and references. Thirdly, a validation process was designed and executed. Initial results showed consistency, coherence and robustness in the model´s local and global response. Additionally, a local benchmark against the ViVA+ model showed an overall similar dynamic response and initial kinematics for both models, but with a stiffer behaviour of the FAHM in the abdominal and pelvic area. Furthermore, the ViVA+ model displayed a significantly faster ribcage recovery. In all cases, the responses of both models were within the same order of magnitude, and the observed differences were consistent. Finally, suggested future work include further validation focusing on the mentioned differences, and the implementation of a female-specific active response and injury risk functions.

Keywords: anthropometry, biofidelity, female safety, human body model, multibody

1. Introduction

Gathered literature concluded that female safety as a road user is significantly worse than that of males. For instance, US women have a 17% higher probability than men of dying in a road traffic accident, as stated in [i]; and women worldwide have 73% more probability than men of having AIS 3+ injuries, according to [ii]. A further analysis suggested that not only physiological sex-related differences could be responsible, but also behaviour, culture, and vehicle safety systems design. The possible reasons proposed for the latter are the general lack (with 2 exceptions) of representation of the female anthropometry in the vehicle safety sector, and that the different OEMs and vehicle safety assessment programmes (both type approval and consumer testing) that form part of the vehicle safety sector consider the average female safety covered by the average male anthropometry.

Hence, the vision of this study was: to provide these organizations with another tool to improve vehicle design (regarding comfort and safety) and vehicle safety assessment towards increasing female road users' safety, as well as to improve female injury prediction. Consequently, the mission was: to develop a 50th percentile female MB

HBM. The scope and objectives definition of this mission only included the passive response part of the new model, and not the active response.

2. Description of Technologies

Siemens Simcenter Madymo was the main software used in this study. This is one of the most used software packages worldwide regarding MBD, although it also includes FEM and fluid dynamics, and its most complex human model is the Active Human Model (50^{th} percentile male). In the context of this software, the mission definition was adjusted as: to develop the Female 50^{th} percentile Active Human Model. This implies that this new model would be the female equivalent to the mentioned AHM.

Other software or specific tools used in this Master´s Thesis were Madymo Scaler Tool (scaling tool), Siemens Jack Scaling (human anthropometry database), LS-Dyna (finite element solver, used for coupled simulations with Madymo), and Altair HyperMesh (finite element modelling software, used for geometry morphing).

Lastly, the computation configuration selected for both Madymo and LS-Dyna in the mentioned coupled simulations was the Massively Parallel Processing (mpp).

3. State of the Art

An analysis on female anthropometry and biomechanical behaviour showed the existence of several differences between sexes. Among them, the ones compatible with multibody dynamics and considered as adequate and sufficient for a partial or total implementation in the FAHM were related to adipose tissue distribution, cervical spine morphometry, neck muscle and behaviour, head mass, and pelvis morphometry. Other differences found but not implemented in this study (due to insufficient data available) involved ligament and tendon strength, general biomechanical strength, general bone properties, radius anthropometric measures, tibia cortical bone properties, and ankle physiology and behaviour.

Other existent technological approaches to female 50th percentile models, the Humanetics EvaRID virtual ATD, and the ViVA+ model were found. This, together with the aforementioned female anthropometry analysis allowed for the selection of the baseline model (the AHM) and the references of this study. From the latter, the called ‘main references’ included a previous internal Madymo study on the development of a female-specific neck system (denominated MR1), and the Simcenter Madymo´s facet female 5th percentile scalable model (MR2).

An automatic scaling process via Madymo Scaler Tool and using a database from Siemens Jack Scaling was needed for MR2, in order to use it as a reference for the average female anthropometric distribution. The National Health and Nutrition Examination Survey (NHANES) study from 2011 to 2014 was considered as the most adequate database (from Siemens Jack Scaling) for this study.

4. Model Development

The development method selected was scaling the model, with the exceptions of the skin geometry (directly related to adipose tissue distribution), the pelvis morphometry, and

the implementation of MR1. The mathematical approach to scaling used was that of the Madymo Scaler Tool.

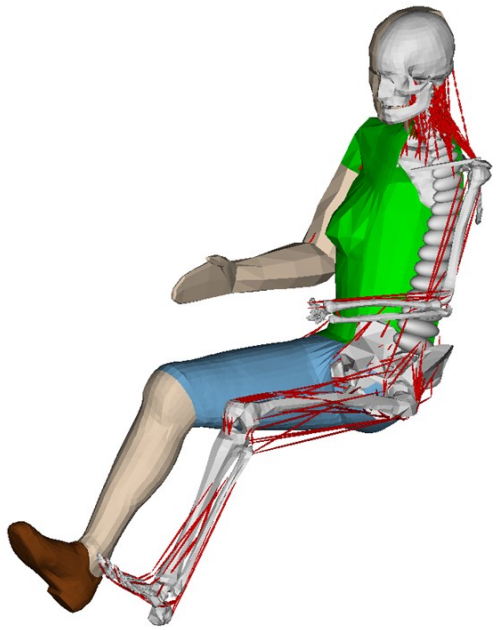

Figure i. Siemens Simcenter Madymo Female 50th percentile Active Human Model

The first step in the development focused on the morphometry part of the model, starting with the morphing of the pelvis and the thorax skin attending to their function within Madymo, and to the available tools, input data, and resources. Afterwards, MR1 was implemented in the new model. Next, the rest of the morphometry part associated with the scaling process was performed. Finally, the dynamic side of the scaling process (purely scaling) was performed, obtaining after, the new FAHM (see Figure i), that resulted in only a 1.2% difference in height, and a 4% difference in total mass with respect to MR2.

5. Model Validation

To validate a model is to check whether said model behaves as the human group it is representing would on average, both kinematically and dynamically. Model validation test types can be categorized using two different criteria. Firstly, Post Mortem Human Subject (PMHS) experimental tests are used for passive response validation, whereas volunteer experimental tests are used for active response. Secondly, local validation testing (blunt impact tests typically) is used for the validation of subsystems of the model, while global validation focuses on specific common scenarios (sled and vehicle tests) and key responses of the whole model. The combination chosen in this study was PMHS validation tests, first locally and then globally.

Response normalization was a key element in the analysis of the validation data, and the selected normalization method was that of the Mertz 1984 study [iii]. However, the obtained curves should be considered as an approximation in the case of male

experimental data into female, especially regarding local validation, due to the observed sex-specific anthropometric differences between males and females.

A first step in local validation was performed, using the 'standard validation tests' and comparing the responses of the FAHM and the AHM. PMHS experimental corridors were normalized for the FAHM. Results showed robustness, consistency, and coherence with the scaling factors used for each absolute axis and model part.

A second step in local validation compared the FAHM and the ViVA+ model (model local validation yet to be published at the time of documentation of this Master´s Thesis) using a modified version of the previous validation tests. Experimental corridors were not included, due to the adjustments made to the tests. ViVA+ model responses were normalized. Both models showed a similar initial kinematic response, but the FAHM kinematic development was stiffer overall (as shown in the example of Figure ii). The dynamic response for both models was overall similar, but the FAHM exhibited stiffer behaviour in the abdominal and pelvic area. Additionally, the ViVA+ model showed a significantly faster ribcage recovery. In all cases, the responses of both models were within the same order of magnitude, and the observed differences were consistent.

Lastly, the global validation was performed using a test set from the 'standard validation tests' and comparing, as in the local validation, the AHM and FAHM for robustness, coherence and consistency. Likewise, the response was as expected, showing the FAHM response as proportional to the scaling factors used in its development.

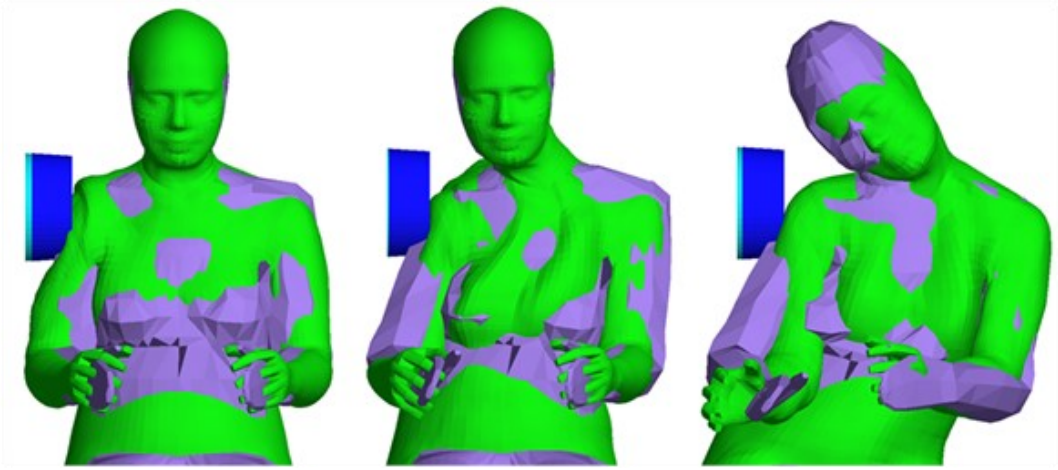

Figure ii. Shoulder blunt impact tests 4.5 m/s. FAHM (purple) vs ViVA+ model (green)

6. Future Work & Conclusions

The suggested future work for the FAHM focus on further passive validation, implementation and validation of female-specific active response, the implementation of additional sex-specific anthropometric features, and the full parametrization of the model for use in the Madymo Scaling Tool.

In conclusion, this study developed a Female 50th percentile Active Human Model, using input data gathered from female anthropometry analysis. Said analysis allowed the baseline model and references for the development of the model to be defined. After said process, the model showed consistency in terms of anthropometric distribution with the mentioned references. A first approach to the FAHM validation was performed, obtaining consistent, coherent and robust responses both locally and globally. Additionally, a local comparison against the ViVA+ model showed overall similar responses, although some differences were observed.

7. References

[i] C. J. Kahane. Injury vulnerability and effectiveness of occupant protection technologies for older occupants and women. (Report No. DOT HS 811 766). 2013. Washington, DC: National Highway Traffic Safety Administration (NHTSA).

[ii] J. Forman, G. S. Poplin, C. G. Shaw, T. L. McMurry, K. Schmidt, J. Ash & C. Sunnevang. Automobile injury trends in the contemporary fleet: Belted occupants in frontal collisions. 2019. Traffic Injury Prevention. 2019;20(6):607-612. doi: 10.1080/15389588.2019.1630825.

[iii] Mertz, H. A Procedure for Normalizing Impact Response Data. 1984. SAE Technical Paper 840884. Warrendale, PA, USA.

Contents

List of Figures

List of Tables

Chapter 1. INTRODUCTION

The purpose of this chapter is to contextualize the current Master's Thesis by presenting its field of study, aim and workflow. The first subchapter serves as a discussion on the injury severity and mortality rate differences existent between males and females after a road traffic accident and its possible sources and risk factors. The second subchapter focuses on two points. On the one hand, on how the present work could impact the abovementioned differences by providing Original Equipment Manufacturers (from now on, OEMs) as well as vehicle safety assessment programmes with a tool to consider average female anthropometry in vehicle design and vehicle safety rating. On the other hand, on the definition of the objectives of this study that enabled the materialization of said tool. To finalize this chapter, the work process carried out throughout this Master's Thesis is described.

1.1 CONTEXTUALIZATION

Female motor vehicle occupants have 17% more probability of dying in a road accident in the United States than male occupants, as per stated in [1]. Additionally, women worldwide have a 142% more probability of AIS 2+ (Abbreviated Injury Scale) injuries and a 73% more probability of AIS 3+ injuries as occupants in road accidents, according to [2]. Furthermore, [3] concludes that women have 3.1 times more risk of impairment from a Whiplash Associated Disorder (from now on, WAD) in the driver position; while [1] states that women are more susceptible to abdominal injuries and extremity fractures than men.

However, it is necessary to analyse the possible sources for these outcomes, since not only the physiological sex-related differences existent between males and females (which are analysed in detail in Chapter 3) influence them. Hence, dividing road safety factors and elements into groups allows an evaluation on the impact of non-anthropometrical factors separately. The most recent and accepted concept regarding the categorization of factors

involved in road safety is the Safe System and its five pillars: safe roads and roadsides, safe vehicles, safe road use, safe speeds, and post-crash response [4].

Safe roads and roadsides

This category refers to any infrastructure element that has a direct or indirect relationship with vehicle mobility, from roads and crash barriers to any static or moving object present in the roadside. Nevertheless, this work has not found any factor in this group that could have a different impact on injury and mortality rate in a road accident depending on the sex of the involved occupants.

Post-crash response

Post-crash response includes not only the reaction time and efficacy of the emergency first responders, but also traffic management at the accident site, and repairing of the infrastructure after it, among others. Assuming the professionalism of said emergency corps, no factor has been found that could affect the observed differences previously described.

Safe speed and safe road use

These two categories can be grouped together for the purpose of this analysis since they both refer to the road user's culture and behaviour, such as type of vehicle driven or average aggressiveness and speed of drivers. For instance, in the United States of America (from now on, USA), women are less aggressive than men when driving, using lighter and smaller (and subsequently less stiff) cars when doing so, as per stated in [5]. Therefore, in a car accident involving an average male driver and an average female driver, the female driver and all the other occupants of that vehicle (male or female) would have higher injury and mortality rates just accounting for the type, size, and stiffness of the vehicle. On the other side, male drivers would be expected to have higher injury and mortality rates when considering aggressiveness alone, since the probability of having an accident is also higher. Similarly, speeding also increases the probability and severity of the accident, and therefore the injury and mortality rates of the users involved. According to [6], men account for 79% of speeding related deaths in 2020 in the USA.

Safe vehicles

Referring this category to the design and safety systems of vehicles, it would seem obvious to conclude that no factors or elements have any effect on sex-related differences existent in car accidents' injury and mortality rates.

However, the following data provided by the Global Health Data Exchange tool of the Institute for Health Metrics and Evaluation [7] raise the necessity for further research:

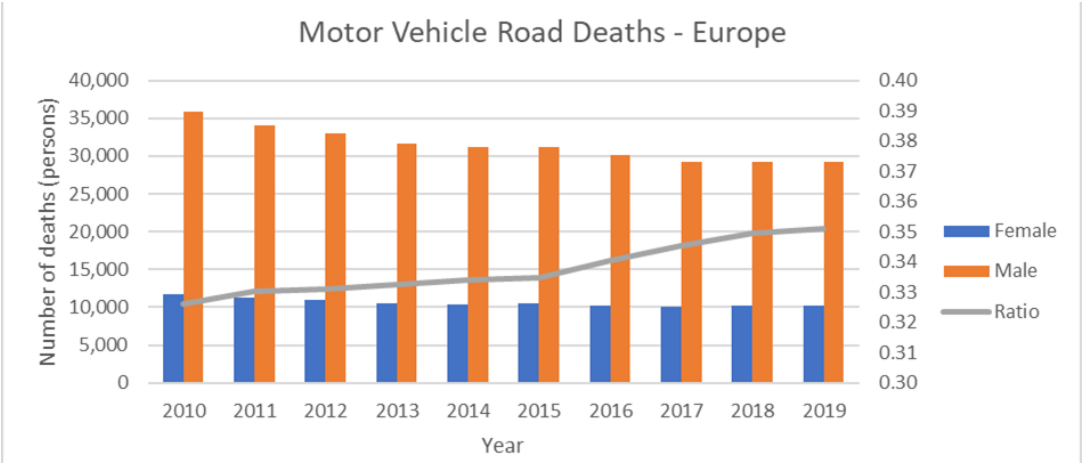

Fig. 1. Motor Vehicle Road Deaths in Europe 2010-2019

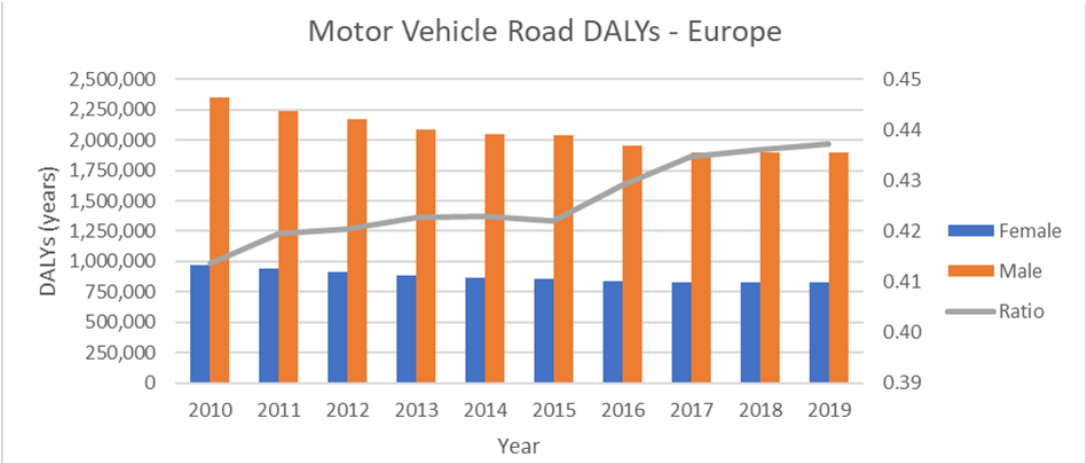

Fig. 2. Motor Vehicle Road DALYs in Europe 2010-2019

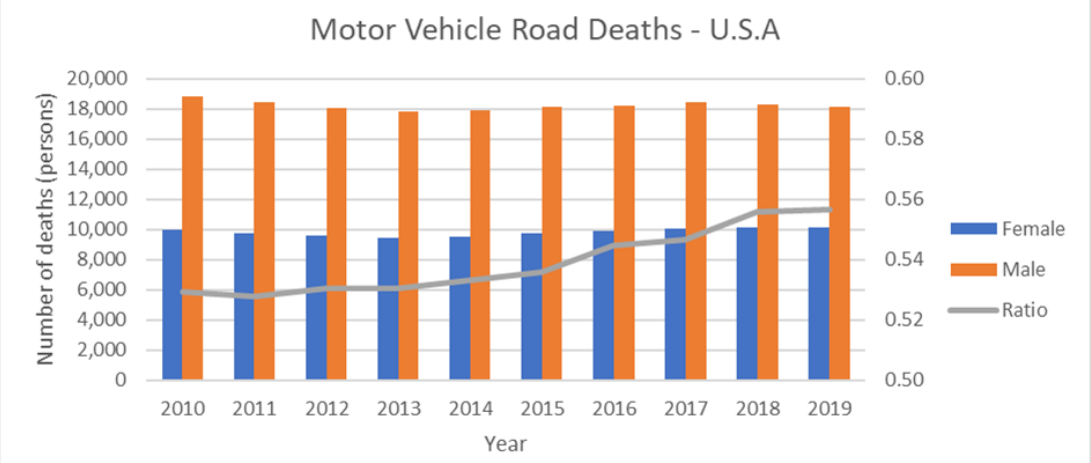

Fig. 3. Motor Vehicle Road Deaths in USA 2010-2019

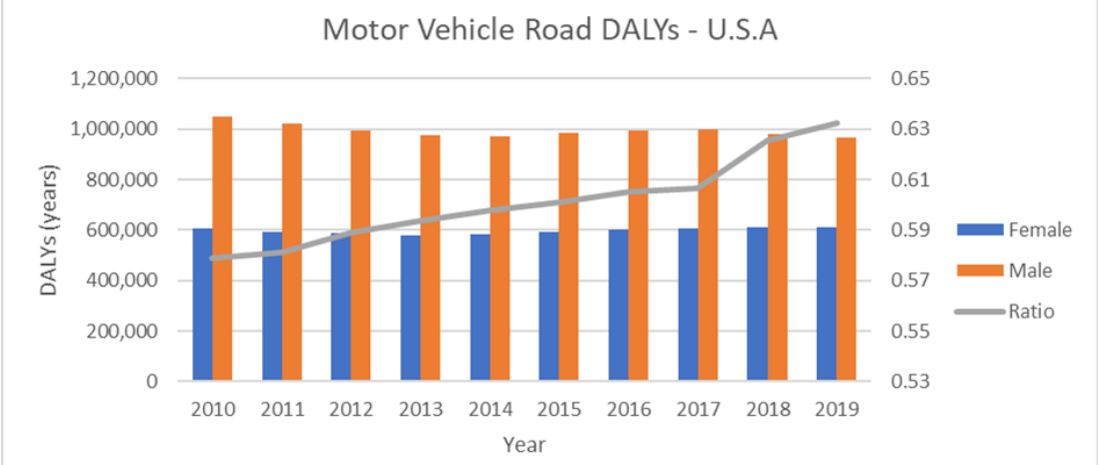

Fig. 4. Motor Vehicle Road DALYs in USA 2010-2019

Fig. 1 to Fig. 4 correspond to motor vehicle deaths and Disability-Adjusted Life Years (from now on, DALYs) in Europe and the USA from 2010 to 2019. DALYs is a parameter that measures the total number of years lost due to illness, disability, or early death. In these figures, female and male data have been separated, and a female/male ratio curve has been included.

These results show how at least since 2010 the female/male ratio is increasing, that is, each year, relatively more females and female DALYs are lost. Only the results for Europe and USA are shown, but this tendency is present globally, following the data obtained in [7].

Assuming no significant cultural or behavioural changes of road users since 2010 that would affect substantially injury and mortality rates for each gender, the existence of sex-related factors in both vehicle design and its safety systems and vehicle safety assessment programmes can be a possible explanation to the observed phenomena.

Delving into vehicle design and vehicle safety systems, several examples where average female physiology is not considered can be found. For instance, vehicle seats' geometry and ergonomics are designed considering only average male physiology, as stated in [8]. Therefore, women have a higher tendency of being out-of-position occupants, a fact that has been demonstrated throughout the present literature to increase injury and death likelihood. Additionally, the high firmness of car seats induces in women higher cervical accelerations in rear-end collisions at low velocities than in men, since they are lighter on average, according to [9] and [10]. Hence, increasing the risk for a neck injury, such as the abovementioned WAD. Other examples may include occupant compartment design, seatbelts, or airbags, although no conclusive literature addressing these matters has been found.

Regarding vehicle safety assessment programmes, [11] concludes that no EU type approval regulation on crash-tests require a female anthropometric dummy, except for one that requires a 5th percentile female Anthropomorphic Test Device (from now on ATD or dummy). This dummy represents only 5% of the shortest and lightest females and is often used as a restrictive case rather than a reference for vehicle safety assessment or design. That is, for instance in the latter case, that the vehicle design in terms of safety uses as the main source the average male anthropometry, and as a verification or lower end, a small percentage of the female population. Furthermore, and as per stated in [12], the average female is not being represented in vehicle safety tests for National Highway Traffic Safety Administration (NHTSA) and Insurance Institute for Highway Safety (IIHS), but only the aforementioned 5th percentile female in some of the tests and rarely as drivers (except for the side-impact tests). Similarly, in the consumer tests performed by Euro NCAP (European New Car Assessment Programme) and other NCAPs, 50th percentile female is not being

used, although the 5th percentile dummy is required in more tests than in the previous examples.

More examples could be presented regarding the low presence of the average female anthropometry in vehicle design and vehicle safety assessment, and also regarding the high negative impact of this factor on female injury and mortality rates after a car accident, although the aim of this safe vehicle factors category analysis has already been achieved.

In conclusion, the purpose of this Contextualization has been to shed some light on the main reasons behind higher mortality and injury rates on females involved in car accidents: differences in physiology across sexes and in behaviour across genders when driving and other related preferences, and the absence of representation of the average female anthropometry in vehicle design and vehicle safety assessment.

1.2 MOTIVATION, VISION AND MISSION

From the mentioned three gender and sex-related factors, this Master's Thesis has focused on the lack of average female representation in the safety part of the automotive sector, since it carries a strong engineering-dependent component.

The reason behind the existence of this factor lays mainly on the general lack of available 50th percentile female ATD (both physical or virtual) or HBM (Human Body Models, only virtual); as well as the general assumption that females are slightly smaller than males and so, covered by protecting males. There are only two known exceptions, one physical ATD (the EvaRID) and an FE (Finite Element) HBM (the ViVA+), which are explained more in detail in Chapter 3.

Hence, the vision of this Master's Thesis was to provide OEMs and vehicle safety assessment programmes (both type approval and consumer testing) with another tool to improve vehicle design (regarding comfort and safety) and vehicle safety assessment towards increasing female road user's safety, as well as to improve female injury prediction.

The mission of this work was to develop a 50th percentile female MB (Multi-Body) HBM. The main advantage of MB HBM (Multi-Body Dynamics solver) over FE HBM (Finite Element Method solver) is the reduced computational cost, making the MB HBM more suitable for Design of Experiments (DOE), optimization and extensive design space exploration. A more detailed description of both solver methods and the differences between them is offered in Chapter 2.

Additionally, the possibility for future scaling integration was considered in the development process (see Chapter 4). This refers to the ability to scale the developed model to different anthropometries (like 5th or 95th percentile), so that a wider and more varied spectrum of women can be utilized in future simulations.

Consequently, the objectives for this Master's Thesis were:

1. To develop a Multi-Body Female 50th percentile HBM.
    a. To analyse the physiological differences across male and female anthropometries.
    b. To evaluate the most suitable human anthropometry database from the available ones.
    c. To select the most suitable HBM developing method.
    d. To build up the morphometry-related part of the model.
    e. To elaborate the dynamics-related part of the model.

2. To validate said model.
    a. To analyse possible approaches for the validation of the developed model.
    b. To perform the selected validation method.
    c. To evaluate the results obtained and the necessity for model modifications.

1.3 METHODOLOGY OF WORK

Due to the characteristics of this Master's Thesis, a variation of the Waterfall project management methodology was followed. Thus, the process was divided into 5 steps: research, elaboration process design and model development, model validation, results analysis, and documentation.

First step: research

Comprises Chapter 1, Chapter 2 and Chapter 3, that is, Introduction, Description of Technologies. and State of the Art. Moreover, it includes the problem identification and contextualization, the motivation, mission and vision definition, the objectives description, and the workflow process definition. Second, an overview of the different technologies utilized throughout this Master's Thesis is presented. Lastly, it includes the analysis of the physiological differences across male and female anthropometries, the identification of the existent alternatives (ATD and HBM), the evaluation of the baseline and references for the model development, and the human anthropometry database selection analysis.

Second step: elaboration process design

Covered in Chapter 4, Development of the FAHM (Female Active Human Model, see Chapter 2). In the first subchapter, the most suitable HBM development method is selected, whereas the rest of the chapter contains the model morphometry and model dynamics development.

Third step: model validation

Comprises the first subchapters of Chapter 4 5, FAHM Validation, where the most suitable approach for validation was evaluated and selected, and where the different validation tests were performed.

Fourth step: results analysis

Covers the final subchapter of Chapter 5, FAHM Validation. In this step, the overall behaviour of the developed model was examined, and the necessity for additional modifications on the model's morphometry or dynamics was evaluated.

Fifth step: documentation

In this last step, several intermediate reports performed throughout the work process, as well as the redaction of this Master's Thesis are included.

Chapter 2. DESCRIPTION OF TECHNOLOGIES

As explained in Chapter 1, the aim of this Master Thesis was to develop a 50th percentile female MB HBM. To this end, several technologies were needed. This chapter aims to overview said technologies, in terms of their purpose in the context of this work, as well as their main characteristics and elements. In the first subchapter, Multi-Body Dynamics (MBD) is presented, alongside with Siemens Simcenter Madymo, the main software employed throughout this work. Afterwards, the baseline HBM of this study (see Chapter 3), the Madymo Active Human 50th percentile Facet Q Model v3.3 (segmented version) is described. The third subchapter presents the Finite-Element (FE) Method Dynamics, together with a small comparison against MBD. Finally, Altair HyperMesh software is introduced.

2.1 MULTI-BODY DYNAMICS & SIEMENS SIMCENTER MADYMO

Multi-Body Dynamics is a type of numerical simulation solution method that considers all elements within a system as rigid bodies, and consequently calculates the kinematics and dynamics of said system. Typically, simplest elements such as free particles can be calculated following Newton's laws. However, if force interactions exist between bodies, Euler equations are needed. Finally, for more complex systems, with multiple articulated bodies, contact forces and restraints, Lagrange's equations are used, as per stated in [13]. These equations are originated from D'Alembert's principle which is, at the same time, derived from the principle of virtual work. In order to include Multi-Body dynamics in the solution of numerical simulations of complex systems, several approaches exist, although the basic behaviour of the solvers follow the abovementioned equations.

Siemens Simcenter Madymo (Mathematical Dynamic Model) is one of the most used software worldwide regarding MBD, although it also includes FEM (see Finite Element Method Dynamics subchapter) and fluid dynamics. This non-linear solver software is

specialized in the analysis of occupant safety and occupant safety systems (such as seat belts, airbags, or tyre modelling) in a wide range of vehicles (from cars and bicycles to airplanes and trains), as well as in the analysis of pedestrian protection. It is also compatible with sensor and control functionality, and with coupling simulations with MATLAB and FEM solvers. The following diagram present in Madymo's Theory manual [14] shows how this software is structured:

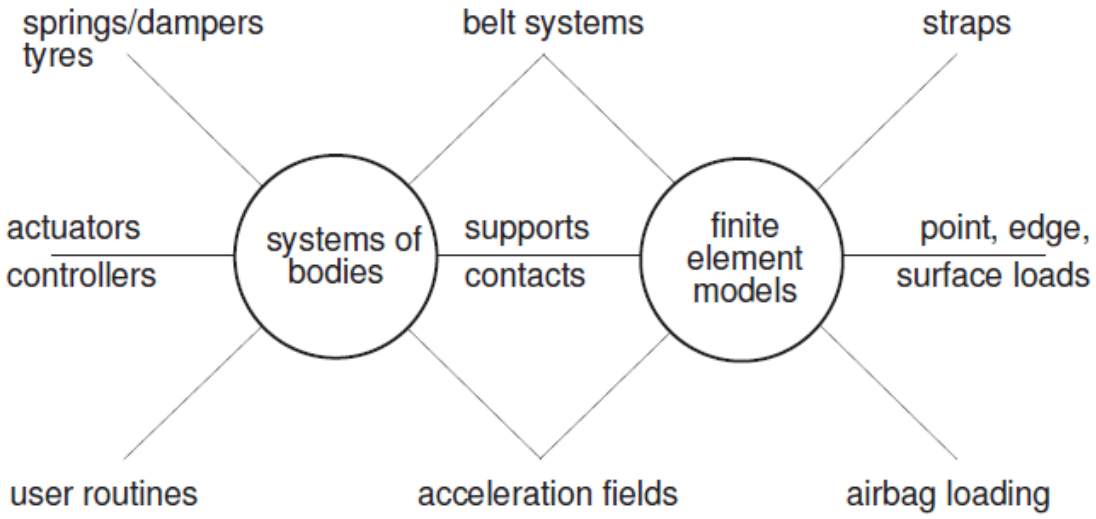

Fig. 5.Madymo Structure [14]

A brief explanation of the most important elements from the previous diagram is offered below:

Multi-body systems

Regarding multi-body systems, Madymo's efficient algorithm generates, in an explicit form, the second time derivative of the different degrees of freedom of the system, solving the kinematics of the bodies in said system. Additionally, different geometries (such as planes, ellipsoids, and cylinders) can be defined for these bodies, so that their shape is represented.

Contacts between these geometries are usually defined as elastic non-linear force-dependent interactions, although other options are possible (such as stress-dependent). This translates in the displacement due to rigid body motion together with the displacement due

to deformation being substituted by an equivalent penetration between bodies (as shown in Fig. 6). Hence, the MB-MB contact characteristic is defined as a function of force vs element penetration (N vs m), distinguishing both loading and unloading conditions under different hysteresis models, and with the possibility of elastic limit definition. Such contact definitions can also consider damping effects, using either a coefficient or a penetration-velocity-dependent function (N vs m/s). A force-dependent amplification function (amplification function vs N) can be applied to either of these cases. An example for a standard MB-MB contact definition (with hysteresis model 2 and elastic limit) extracted from [14] is offered in Fig. 7.

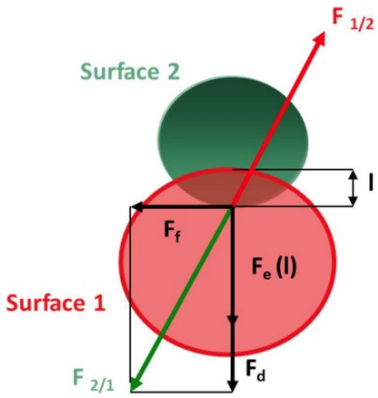

Fig. 6. Force diagram of penetration-based contact definitions [14]

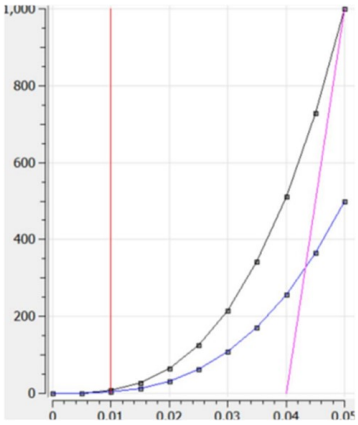

Fig. 7. Example of an MB-MB force-penetration-dependent contact in Madymo [14]

Joint definition allows to create kinematic chains between bodies, either open or closed ones. There are up to 18 different types of joints available in Madymo, although the most common ones are bracket joints (0 degrees of freedom), revolute and translational joints (1 degree of freedom), universal joints (2 degrees of freedom), universal-translational joints (3 degrees of freedom, see Fig. 8), free joints (6 degrees of freedom, see Fig. 9), and used defined. Joint restraints work similarly to that of a contact characteristic definition for each degree of freedom of said joint, although the penetration between surfaces is substituted by the displacement of the joint (Nm vs angle or N vs m, depending on the type of joint and degree of freedom).

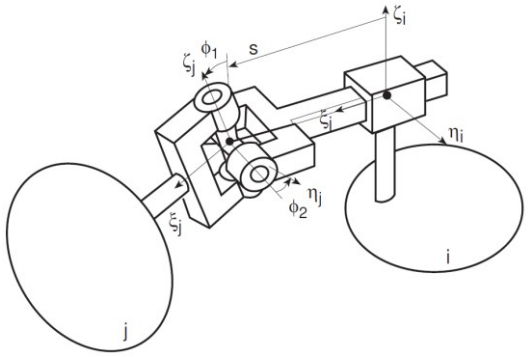

Fig. 8. Universal-translational joint definition [14]

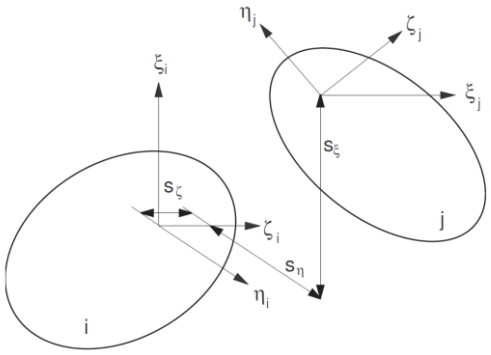

Fig. 9. Free joint definition [14]

Other restraints not related with joints can be defined between bodies or with the reference space. Kelvin restraints (parallel spring and damper system), maxwell restraints (serial spring and damper system), point restraints (equivalent to three orthogonal kelvin restraints

with constant damping), and cardan and flexion-torsion restraints are among the most used ones.

Finite-element systems

Finite-element systems are less common in Madymo simulations, except for seatbelts, airbags, and facet components. This section focuses on the latter since finite elements and their behaviour are explained with more detail in the Finite Element Method Dynamics section. Facet components are not true FE parts, since they have a rigidified structure that act as one when a support is defined in them. Hence, the abstract concept behind facet FE-MB or facet FE-facet FE contacts stays the same as described for MB-MB, although the actual equations to solve do vary.

HBMs and virtual ATDs

Madymo software has a wide range of virtual ATDs (or crash dummies) and Human Body Models, since it is specialized on vehicle occupant and pedestrian safety. Virtual ATDs include frontal, side and rear impact dummies, child dummies, pedestrian dummies and subsystem impactors, motorcycle and aviation dummies, and scalable dummy models, among others. HBM include adult and child models, occupant and pedestrian models, scalable human models, and the AHM. There are certain elements from the diagram of Fig. 7 that grow importance in this section, especially regarding HBM:

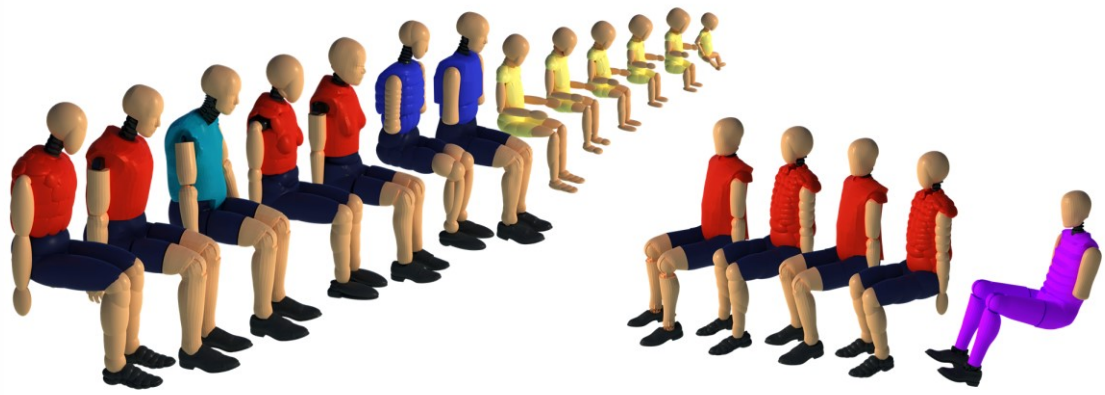

Fig. 10. Representation of some of the virtual ATDs of Siemens Simcenter Madymo Software

- Muscle models: there are uni-axial elements with two anchor points, and passive and active characteristic forces based on Hill type equations.
- Belt systems: not only for interaction of the model with the vehicle, but also some human ligaments are defined using this belt elements.
- Actuators and controllers: they are in charge of the muscle activation and replace in some cases explicit muscle modelling in models such as the AHM (see next subchapter).
- Injury prediction: Madymo includes several injury criteria related to head, neck, thoracic, femur or tibia injuries, among others.
- Deformable bodies: models such as the AHM, are made mainly of facet surfaces connected by facet buffer elements, so that movement is allowed between different components of the model (such as the neck or the extremities). However, to be able to properly address thoracic and abdominal deformations, deformable bodies are needed. These are defined following the assumed-modes method, with complex constrained equations for the relative motion of interconnected bodies, and the mean displacements selected to be equal to zero, to reduce significantly computational cost and high frequencies, as per described in [15]. Hence, different prescribed deformation fields modes are defined for each set of deformable bodies on the same transversal plane of a model. This method is only applicable to regularly shaped geometries, as those present in HBM thorax and abdomen body parts. A more visual approach to this concept is offered in the next subchapter.

Simcenter Madymo Scaler and Siemens Jack Scaling

There are several built-in tools in Madymo software. Nevertheless, the two that give name to this section were particularly important throughout this Master`s Thesis. The Scaler tool was conceived to cover necessities regarding accident reconstruction, diverse anthropometry study, and human variability study and parametrization [16]. It allows for scaling some of the virtual ATDs and HBMs that are specifically made for this purpose.

The Scaler tools uses different local scaling factors to build the required model, given the reference one. This scaling factors can be directly or indirectly defined in 3 ways:

- Madymo Scaler population: the user selects sex (or child), height, and weight (and age if it is a child), and the system automatically calculates the 35 body dimensions (and consequently, all the local scaling factors).
- Fixed scaling factors: the user defines manually 4 scaling factors for each of the 14 body parts.
- Siemens Jack Scaling: the user selects anthropometric database, sex, and population percentile, and the system automatically calculates all the local scaling factors needed.

It is not recommended for the user to mix gender, or adult/child options when selecting the reference model. For instance, the user should not choose a female 5th percentile HBM to scale it to a 13-year-old child, but rather to a 50th percentile female. Additionally, extreme scaling (such as 5th percentile female to 95th percentile female) is not endorsed since anthropometric accuracy could be compromised.

Delving into the anthropometric databases mentioned in Siemens Jack Scaling, there are 12 different adult databases available [16]. Since this tool was key on the firsts steps of the 50th percentile female MB HBM development process, a brief explanation on these databases is provided below:

1. Anthropometric survey of US army personnel (two versions from 1988 and 2012).
2. Anthropometric data from the National Health and Nutrition Examination Survey (from now on, NHANES). Two versions, 1990, and 2011-2014.
3. Anthropometric data of Latin-American population (ages 18 to 65). Guadalajara University 1993-1999.
4. Anthropometric data from the Canadian Land Forces. 1997.
5. Anthropometric data of North American automotive working population.

6. Anthropometric data of Chinese population (age 18 to 60 for males and 18 to 55 for females). 1989.
7. Anthropometric data of Indian population for ergonomic design practice. National Institute of Design (Ahmedabad).1997.
8. Anthropometric data of German population. DIN 33402: German Industry Standard. March 2008.
9. Anthropometric data of Japanese population. Basic human body measurements for technological design Part 1 and Part 2. ISO7250-1 (2008) and ISO7250-2 (2010). 2006.
10. Anthropometric data of Korean population. Basic human body measurements for technological design Part 1 and Part 2. ISO7250-1 (2008) and ISO7250-2 (2010). 2003.

A proper analysis regarding the most suitable database for this project's morphometric reference is carried out in Chapter 3.

2.2 ACTIVE HUMAN 50TH FACET Q MODEL V3.3 - SEGMENTED

Inside Madymo software, the most complex model (both HBM and virtual ATD) is the Active Human Model (from now on, AHM), which is an MB-HBM with facet components, representing a 50th percentile male. The adjective "segmented" from this chapter's title, refers to a specific version of the AHM that is divided by body part regions, making it easier for maintenance and development purposes. This model is only available internally for Madymo's developers.

In order to fulfil the vision and mission of this Master's Thesis, the abovementioned AHM (Fig. 11) has been selected as the male equivalent of the Female 50th percentile MB-HBM (from now on Female Active Human Model or simply, FAHM). Thus, the developed FAHM needed to have the same structure as the AHM. Hence, the importance of understanding and evaluating its origin, complexity, characteristics, biofidelity, and anatomy.

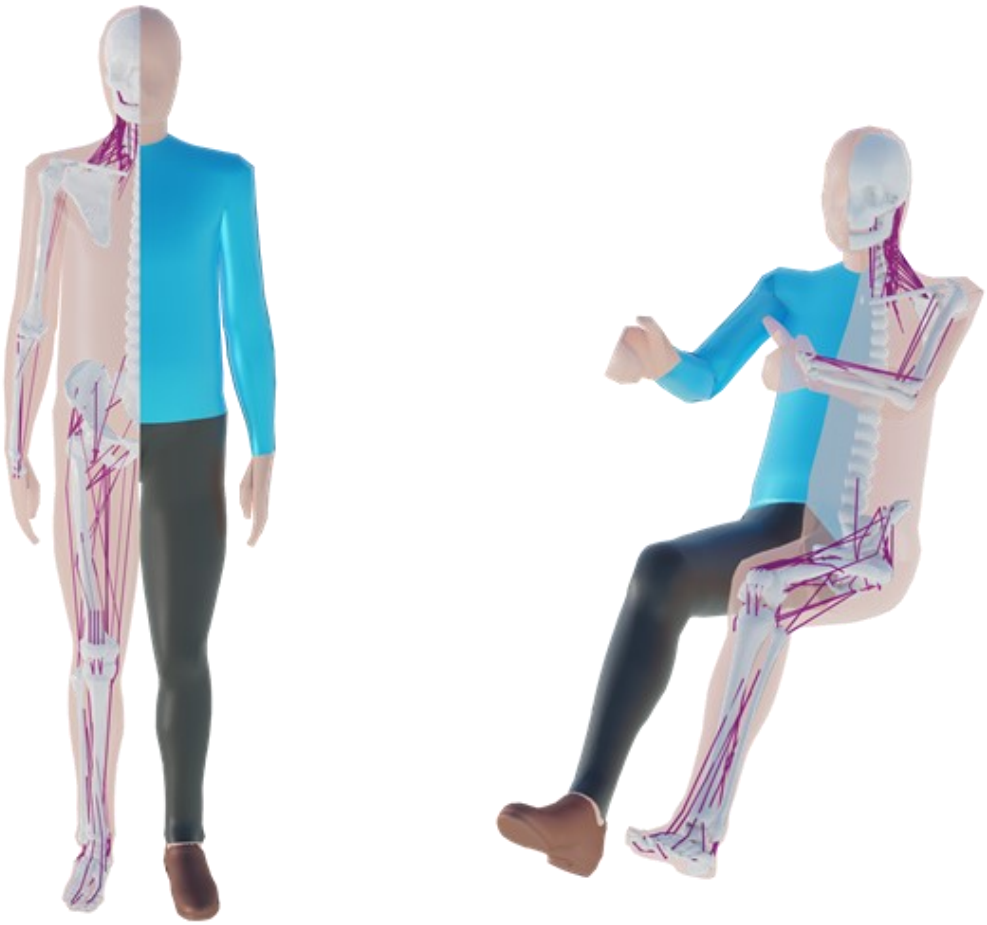

Fig. 11. Active Human Model

Madymo's AHM [17], mimics the passive and active human anthropometry. On the one side, the passive part of the model includes facet skin and bones, kinematic model for core skeleton, flexible bodies for the ribcage and torso, bracket joints for leg fracture, skeleton joint stiffness, torso deformation stiffness, bone bending stiffness, and passive muscle and ligament definitions (belts and restraints).

On the other side, active response includes joint actuators (thoracic and lumbar spine joints and shoulder joints) and muscle actuators (neck co-contraction, muscle strength for different body parts, reaction time, target head facing direction, and target body posture). So as to understand the true complexity of this model, the following element table is provided (only the most relevant components from the passive part are shown):

	Head and Neck	Right and Left Arms	Thorax and Pelvis	Right and Left Legs
Rigid bodies	17	34	61	70
Deformable bodies	-	-	8	-
Joints	17	34	69	70
Muscle elements	136	26	-	86
Belt elements	4	-	-	22
Restraint definitions	231	78	64	50
Injury load cells	72	-	136	-
Ellipsoids	4	-	16	-
Deformable modes	-	-	24	-
Skin parts	8	18	10	52
Bone parts	15	8	6	54

Table 1. Passive elements of the AHM

In total, there are 182 rigid bodies, 8 deformable bodies, 190 joints, 248 muscle elements, 26 belt elements (which account for a part of all the defined ligaments in the model), 423 restraint definitions, 208 injury load cells, 20 ellipsoids, 24 deformable modes, 88 skin parts, and 83 bone parts, among others; and over 150,000 code lines.

In the next sections, the different model elements and their original development processes are described, in accordance with the information presented on [19]. The references mentioned below corresponding to the sources used in the development of the AHM can be found in [18] and [19].

Anthropometry of the AHM

This model is available as vehicle occupant (seating position) and as pedestrian (standing position). The anthropometric dimensions of this model correspond to the 1984 Western Europe population aged 18 to 70 years old (RAMSIS software package), as per [18]. This translates in, among others, a standing height of 1.76m, a sitting height of 0.92m, a weight of 75.3kg, and therefore, a Body Mass Index (from now on BMI) of around 24. Mass distribution also come from this source, obtaining the rotational inertias by integrating volumes for a constant density value. Skin and bone facets are defined by triangular and quadrilateral elements. Internal and external contacts are also defined.

Head and Neck

Cervical spine and skull facet geometry were obtained from HUMOS European project through 50th percentile Post Mortem Human Subjects (from now on PMHS). Vertebrae joints are modelled with free joints. Cardan and point restraints model the intervertebral discs, with stiffness data from different sources. Internal contacts between vertebrae and between vertebrae and the skull are modelled using different methods (such as compression-only point restraints, MB-FE contacts, or FE-FE stress-based contacts). Ligaments are modelled using kelvin restraints and belt systems. Muscle elements can curve around the vertebrae, thanks to intermediate sliding points.

Spine

The muscular resistance, ligaments and intervertebral discs are modelled by rigid bodies (representing each vertebra) connected by free joints with lumped restraint models in all 6 degrees of freedom. The morphometry of the vertebrae is represented by ellipsoids, and the muscles from the thoracic and lumbar spine are modelled using actuators that apply loads to the different joints.

Thorax and abdomen

The most important component in the thorax and abdomen of the AHM is the flexible bodies. Flexible bodies, as explained in the previous subchapter, allow for the model to have accurate deformations in these body parts, although additional point restraints are also

needed. Following the aforementioned assumed-modes method, deformations are defined by deformable bodies and deformable modes, so that the model can address properly thoracic and abdominal deflections. As shown in Fig. 12, there are 8 flexible bodies (also called deformable bodies) that follow the AHM torso proximal to distal, each one corresponding to all nodes present in the thorax facet surface in one transversal plane (forming node rings).

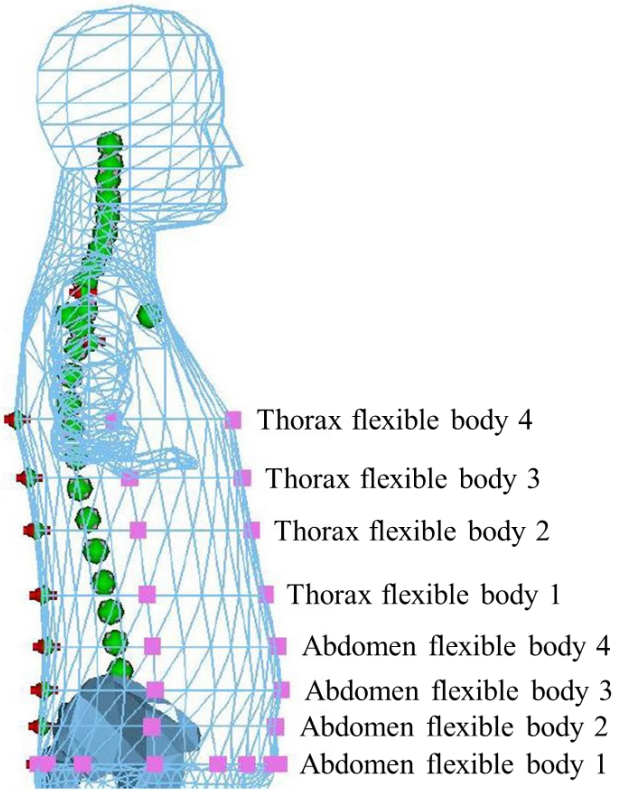

Fig. 12. Flexible bodies in the AHM [18]

Associated to each flexible body, 3 deformation modes are defined (making a total of 24 deformation modes). These 3 deformation modes predefine the field of displacements and deflections of a single node ring in different directions. The first deformation modes correspond to impacts normal to the coronal plane, whereas the second and third deformation modes correspond to impacts normal to the sagittal plane from both sides. Fig. 13, Fig. 14, and Fig. 15 show a top view of these deformation modes on all the flexible bodies of the AHM. In all cases, the blue cloud point represents the original geometry and the orange cloud point the deformed geometry.

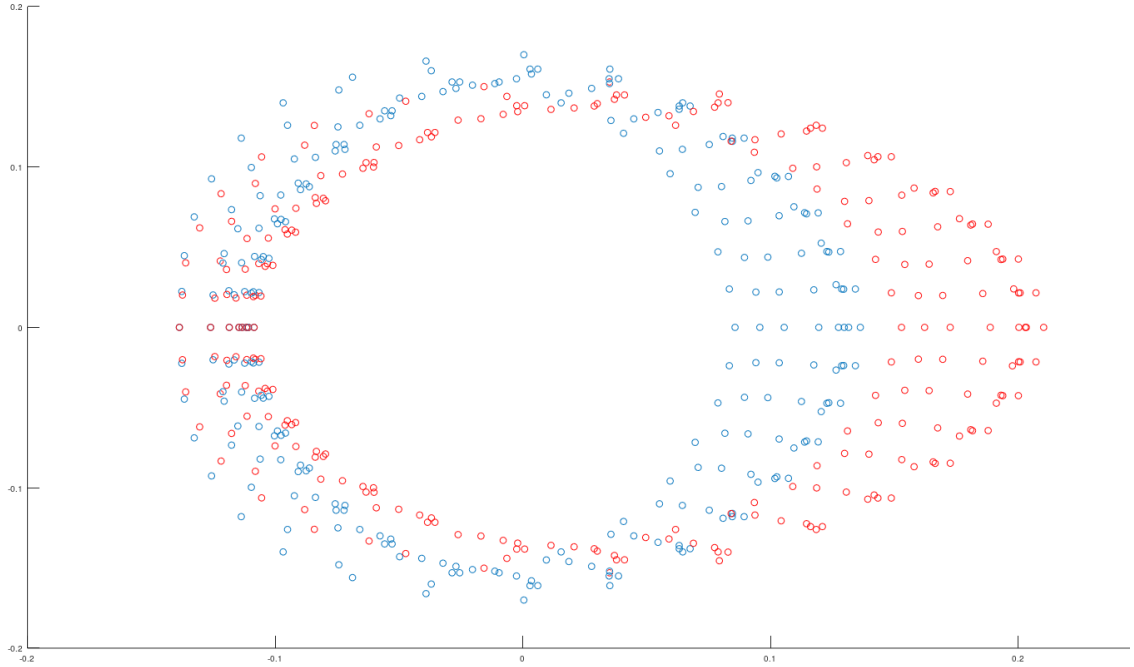

Fig. 13. Deformable mode 1 in all flexible bodies (ring nodes). Top view

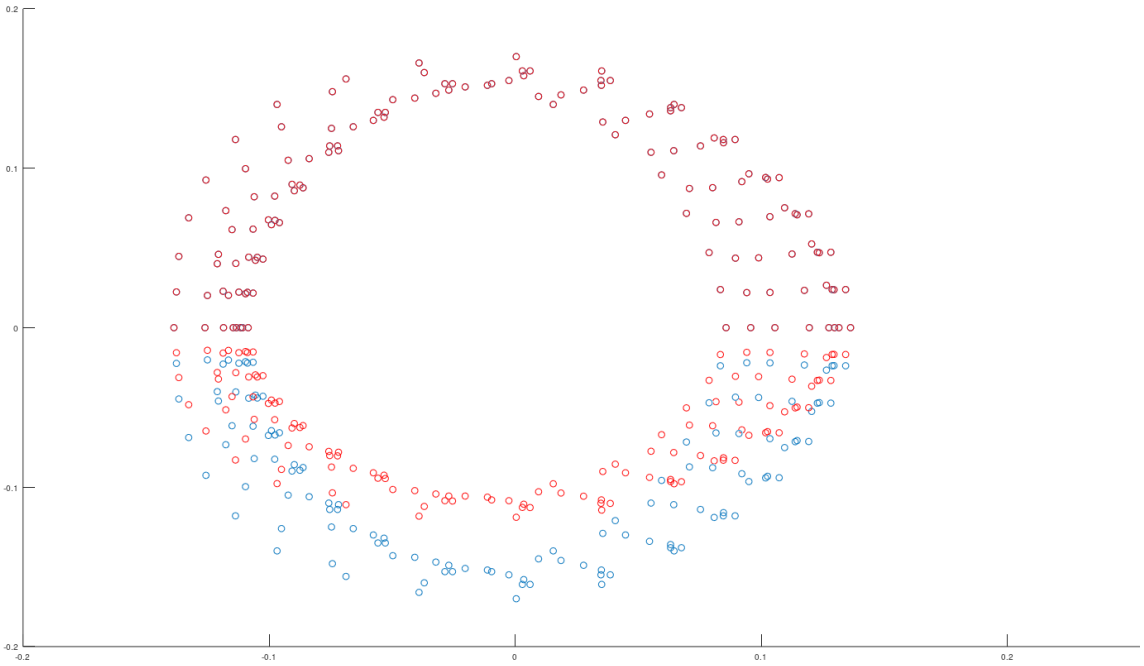

Fig. 14. Deformable mode 2 in all flexible bodies (ring nodes). Top view

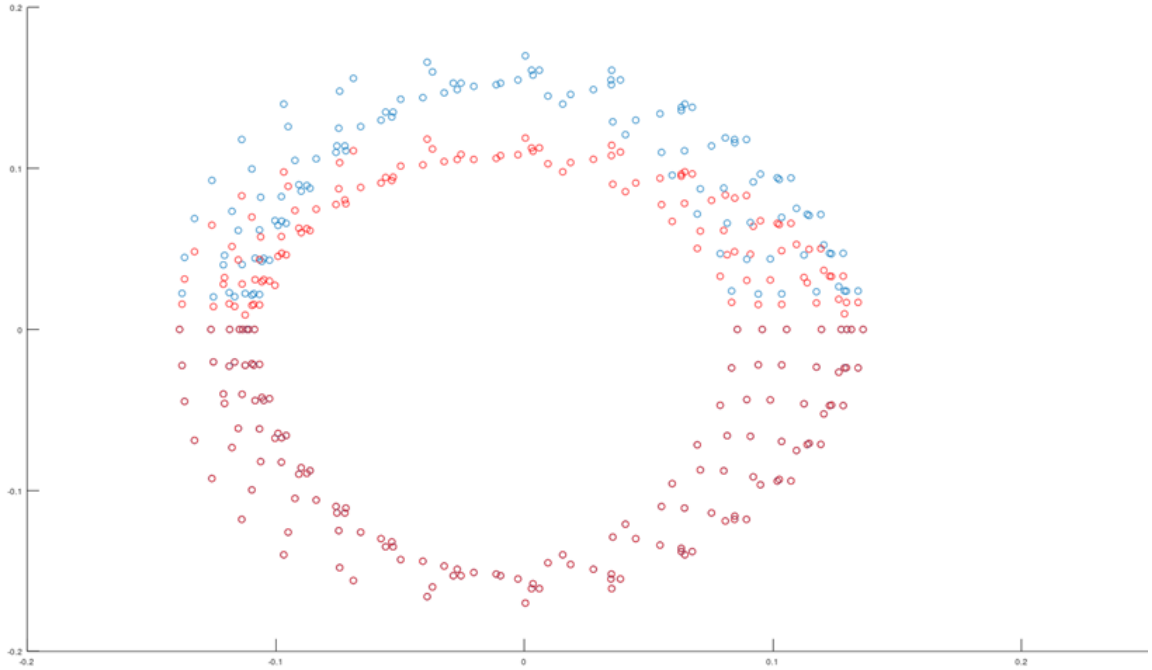

Fig. 15. Deformable mode 3 in all flexible bodies (ring nodes). Top view

Shoulder and arms

Several joints (spherical, revolution, free, and universal types) are defined for the shoulder-arm subsystem, including the acromioclavicular and glenohumeral joints (both spherical types). Restraint definitions are used to define motion range and resistance, and the interaction between this system and the thorax. Humerus, radius, ulna, several hand bones, clavicle, and scapula are defined. Main muscles with passive and active response are also present in this subsystem.

Legs

Similar to the previous subsystem, legs are defined by several joints with cardan and point restraints. Feet bones and skin facets are modelled in detail. Bending and fracture are also considered in the leg bones, capturing stiffness with cardan restraints, and adding a fracture joint in the femur, and three fracture joints for each tibia and fibula bones. These fracture triggers are calibrated using the 50% injury risk for AIS 2+ injuries but can be adapted to

other levels. Muscles and ligaments are also included. Shoes are also present in the AHM, allowing relative movement of the feet with respect to the shoes.

AHM Validation

An overview is offered in this chapter, since the most relevant elements of this topic are extensively described and analysed in Chapter 5.

Two different type of tests can be distinguished related to the AHM validation with regards to type of subject, as per described in [19]. These are volunteer tests and PMHS tests. On the other hand, in relation to boundary conditions, 3 test types can be found: Blunt and segment impact tests, sled and vehicle tests, and vibration tests. All tests come from external literature, and their references can be found in [19] and in [17]. Evidently, PMHS testing was benchmarked against passive AHM response while volunteer testing was benchmarked against active AHM response.

Blunt and segment tests are in all cases localized impact tests with PMHS reference data. Hence, these tests focus on local validation, rather than a global validation, with objective parameters like impactor force, local deformations or local displacements or accelerations. Impactor velocities range from 2.0 to 9.9 m/s. The body parts that suffer the impact include head, shoulder, thorax, abdomen, and pelvis. These are the tests more relevant to this Master's Thesis, as per explained in Chapter 5.

Sled and vehicle tests comprise both PMHS and volunteer testing in rigid seats and vehicles. They were used for global validation purposes, therefore they focused on global kinematics and dynamics. Volunteer testing peak g-force ranges from 0.4 to 15. In the case of PMHS testing, one of the tests was performed at 13.97 g-force peak, while the others were velocity-based tests, ranging from 22.68 to 39.00 kph.

Vibration tests are usually performed for comfort purposes, although in this case the volunteer study with 0.5 to 15 Hz and 0.4 g-force peak was used for full body behaviour validation, similar to that of the sled and vehicle tests.

A summary of these tests is offered below, in Table 2.

Body part/Direction	Type	Subject	Characteristics
Blunt and segment impact tests			
Head	2 frontal impact	PMHS	2.0 & 5.5 m/s
Shoulder	2 lateral impact	PMHS	4.5 & 5.5 m/s
Thorax	7 frontal impact	PMHS	3.4 to 9.9 m/s
	2 lateral impact	PMHS	3.3 & 5.9 m/s
Abdomen	2 frontal impact	PMHS	6.9 & 9.4 m/s
	2 drop tests	PMHS	4.4 & 6.3 m/s
Pelvis	2 lateral impact	PMHS	3.5 & 6.7 m/s
Sled and vehicle tests			
Frontal	sled w/ rigid seat	PMHS	13.97 g-force peak
	sled w/ rigid seat	Volunteer	3.87 g-force peak
	sled w/ rigid seat	Volunteer	15.00 g-force peak
	car w/ 3 seats	Volunteer	0.40 to 1.00 g-force peak
Lateral	sled w/ 2 rigid seats	PMHS	6.3 & 9.1 m/s
	3 pedestrian impacts	PMHS	25 to 39 kph
	sled w/ rigid seat	Volunteer	7.00 g-force peak
	2 test vehicles	Volunteer	0.50 g-force peak
Rear	sled w/ rigid seat	Volunteer	3.60 g-force peak
Vertical	sled w/ 2 rigid seats	Volunteer	6.00 & 10.00 g-force peak
Vibration tests			
Vertical	sled w/ rigid seat	Volunteer	0.5 to 15 Hz, 0.40 g-force peak

Table 2. Summary of AHM validation tests

2.3 FINITE ELEMENT METHOD DYNAMICS

As previously described, the FEM or Finite Element Method is an alternative to MBD (Multi-Body Dynamics) when it comes to solving numerical engineering problems that cannot be calculated analytically, such as when the system is too complex or solid geometries are irregular. Even though this Master's Thesis focuses on developing an MB FAHM, it is important to address its differences with respect to FE HBM. Moreover, and as it is described in Chapter 3 and Chapter 5, the developed model was benchmarked against an FE 50th percentile female HBM that was tested in a coupled simulation environment (Madymo MB solver with LS-Dyna FE solver), emphasizing the necessity to comprehend the implications of Finite Element Dynamics.

The Finite Element Method is commonly used in strength of materials calculations and biomechanical problems. Each object of the considered system is divided into discrete regions, called finite elements, whose most common form is the triangle in two-dimensional problems or the tetrahedron in three-dimensional problems. The set of finite elements of an object of system is known as the mesh. The FEM allows the different differential equations present in said system as a result of physical phenomena to be verified on each finite element at every time step in an average sense. The use of triangles and tetrahedra makes it possible to approximate objects of complex and irregular shapes. This method generates a system of algebraic equations that can be solved by matrix inversion, among others.

There are two types of simulations in FEM, depending on the application and purpose of it. On the one hand, the implicit method is used for long duration simulations or static events and follows the iterative approach. Geometry details can be captured but time steps are computationally very expensive, and wave propagation events are not feasible. Additionally, the simulation behaves as stable, although contact interactions tend to be unstable, and a convergence process is always necessary. On the other hand, explicit method is used for wave propagation and highly non-linear, short transient events, and directly calculates the system solution at each time step. Smaller time steps are needed, although they are less

expensive in terms of computation than the implicit method. Moreover, contact definitions need to be treated with precision, and system instability is frequent.

Biomechanical simulations as the ones present in this Master's Thesis can only use the explicit FEM, via software such as LS-Dyna, Radioss, or Abaqus. Thus, from now on, explicit FEM is referred in this work to as just FEM.

Due to the nature of FEM, displacements due to motion fields and displacements due to deformations are calculated separately, not needing force-penetration based characteristic contacts in the system, as there are no penetrations, but rather the deformations per se (Fig. 16).

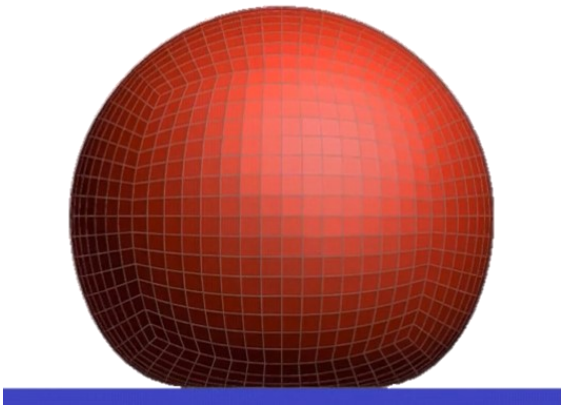

Fig. 16. Example of contact deformations in FEM [20]

The main differences between MBD and FEM besides the mathematical and physical approach to problem solving, in the context of vehicle occupant and pedestrian safety are:

- Computational cost: due to the nature of both methods, Multi-Body Dynamics has a significantly lower computational cost, allowing for extensive design space exploration, Design of Experiments (DOE) and optimization. This gives MBD an advantage over FEM when it comes to vehicle virtual design and testing, and human variability studies.
- Numerical stability: FEM simulations are usually much more instable than MBD simulations, needing of significantly smaller time steps to control the simulation.

There are other elements that can cause problems in this matter, such as the appearance of negative volumes or hourglass values. None of this is present in MBD.

- Accuracy: as FEM is capable of precise definitions for deformations (MBD is also capable, but give some extra implications as described previously with deformable bodies) and for contact interactions (point of application of load or relative motion while in contact, among others), FEM HBM models tend to be much more detailed, and so the accuracy of a simulation is reduced to how the different characteristics are defined. On the other hand, MBD considers in most cases, deformation together with kinematic displacement, and so MB HBM uses mechanical equivalences to reproduce human response, making the improving of the accuracy of a simulation more abstract and conceptual. A similar problem can be found in this context in physical or virtual ATDs (or dummies), where for instance, mechanical joints are used for human joints and body parts are build-up of artificial materials, causing the improvement of these dummies to be more abstract and complex.
- Level of detail: continuing the previous point, soft tissue modelling (such as internal organs or body fat), and therefore soft tissue-related injury criteria assessment, can be defined in FEM as any other element of the HBM (with the appropriate input data). However, on MBD this is a challenge yet in development.
- Optimal mesh size and sensibility analysis: Mesh size is an added variable to deal with in all FEM simulations. If the finite element division is too coarse, its corresponding discretization error can be substantial. The discretization error is the error produced by the discretization of a continuous problem (as previously described, FEM uses an average approach, that is, it simplifies differential equations into algebraic equations, a simplification that only works properly for sufficiently small elements). On the other side, if the mesh is too refined, its respective rounding error can be significant. Rounding errors appear when the computer in charge of the simulation rounds-up the decimals of intermediate

calculations. The sum of both numerical errors is known as the total error. Consequently, a mesh sensitivity analysis is needed in FEM simulations, to address the optimal mesh size, that is, the sufficiently small (and sufficiently big) element size that gives the same results as a smaller element size within an established error margin. A graphical representation of the abovementioned is offered in Fig. 17. In MBD, mesh size (or facet element size) can also be important for contact numerical stability and contact calculation accuracy, although significant differences in mesh sizes are needed to encounter these problems. This topic is briefly addressed in Chapter 4, under the pelvis morphometry modification.

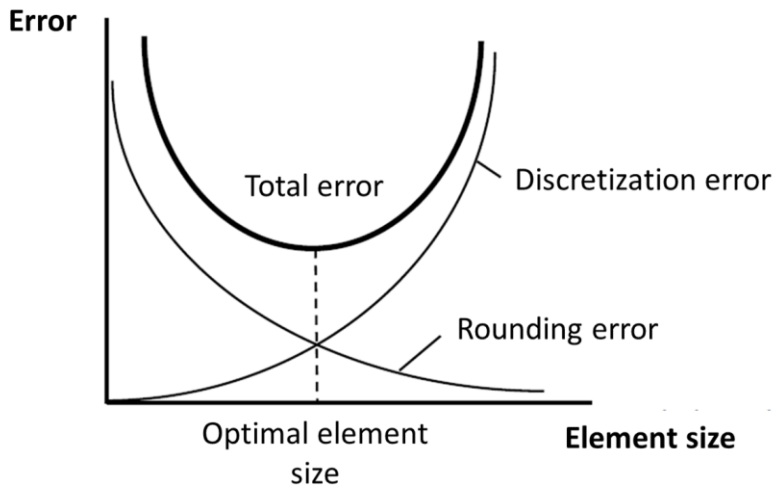

Fig. 17. FEM numerical errors and mesh optimal size

- Development and validation input data: in the same line as the previous points of accuracy and level of detail, FE HBMs being closer to actual human anthropometry can benefit more from medical and anthropometric studies present in literature. The conceptual approach of MB HBMs (mainly materialized in the general lack of deformable components) makes the use of the aforementioned data a challenge.

One of the main software used worldwide regarding FE simulations is LS-Dyna. This software was also used in this Master's Thesis for Madymo with LS-Dyna mpp coupled simulations (see next section).

Coupled simulations: Madymo with LS-Dyna. Massively Parallel Processing (mpp)

Coupled simulations of Madymo with LS-Dyna mpp were needed to simulate an FE HBM in a Madymo environment. Hence, it is convenient to overview this matter in the current section, and particularly, due to its relevance with respect to this Master's Thesis Madymo with LS-Dyna coupled simulations, as described in Chapter 5.

Coupled simulations between Madymo and other software partners can be done using Shared Memory Parallel computations (SMP) or Massively Parallel Processing (MPP) [21]. In the first case, the communication protocol used is the socket, while in the second case, the communication protocol used is the Message Passing Interface (MPI). MPI is a higher communication level than socket and allows direct data transfer between both software sides. Each of the two software involved in the simulation can use internally SMP or MPP. The different options are explained below focusing on Madymo with LS-Dyna coupled simulations.

On the LS-Dyna side, SMP runs the whole system simulation on different computers with the same number of Central Processing Units (also known as CPUs, cores, or processors) and communication is done via shared data bus. It is scalable to around 8 cores, and repeatable under the definition of a specific control flag. However, MPP divides the system in sub-domains, and distributes them among the different CPUs. Communication is done, as previously described, via MPI. It is scalable from 16 cores onwards, and simulations are repeatable. Additionally, using too many processors may result in a negative performance, due to excessive data exchange between them. This limit depends on the dimension order and complexity of the system. Therefore, MPP is the best approach for the simulations needed in this work.

On the Madymo side, MB calculations are always processed serially, whereas FE calculations are scalable and can use either SMP or MPP. SMP in FE Madymo is repeatable. MPP in FE Madymo is faster than SMP, but not repeatable. However, this unrepeatability is typically negligible in most cases, except for highly unstable systems (such as for example a ball falling onto a pointy object).

Furthermore, it is recommended to use the same approach for both software, either SMP, or MPP in both sides. Consequently, the simulations on this Master's Thesis (Chapter 5), were simulated using MPP in both sides.

2.4 ALTAIR HYPERMESH

Altair HyperMesh is a software focused on pre and post processing of Finite Element Solvers. In engineering, it is generally used in mesh optimization and quality, mesh morphing and surface generation. It is also fairly compatible with Madymo simulation files and their structure, being able to import and export them.

Therefore, this software was used in the development phase of the FAHM (Female 50th percentile Active Human Model), taking advantage of its mesh morphing capabilities. Essentially, MB HBM facet elements can be considered as a mesh, and therefore can be modified using this software. In particular, this software was widely used for the modification of the pelvis and thorax morphometry, among others (see Chapter 4).

Chapter 3. STATE OF THE ART

This chapter describes the State of the Art from three different perspectives, and consequently is divided into three subchapters. First, a literature review on female anthropometry and key physiological differences with males is presented, alongside an analysis of ease of implementation of said differences and anthropometric characteristics in Multi-Body Dynamics. Second, a breakdown on other existent technological approaches to female HBM modelling, virtual ATD modelling, and physical ATDs development is offered, together with a discussion on adequate baseline models and main references for the FAHM development. Finally, an anthropometric database analysis is performed, to select from the available databases, the one aligning most with this Master's Thesis aim.

3.1 FEMALE ANTHROPOMETRY ANALYSIS

This subchapter focuses on the key anthropometric differences between adult males and females from a biomechanical point of view, within the scope relevant for vehicle occupant and pedestrian safety. This includes morphometry and structural and mechanical behaviour, considering one male and one female with the same age, height, weight, and behaviour. Additionally, each difference is discussed, in terms of its applicability to MB HBMs.

For future reference, cervical, thoracic, and lumbar spine vertebrae are addressed using the standard designations. Cervical spine vertebrae are numbered C1 to C7, while thoracic spine vertebrae are numbered T1 to T12, and lumbar spine vertebrae L1 to L5, as shown in Fig. 18 (below). Additionally, there are some anthropometric definitions that need to be presented:

- Lean mass: measure that excludes fat, and only considers organs, bones, muscles, and blood. Usually in relative percentage.
- Cortical and trabecular bone: these are the two materials with structural function in bones. Trabecular bone (or spongy bone) has a lesser density (is a porous

material) that can be found in the epiphysis of long bones (see Fig. 19 for a visual representation of bone parts) or between the outer layers of other bones such as the pelvis or skull. One of its main functions is to produce red blood cells, although also provides with certain mechanical properties, that can vary also depending on the body (for instance, load transfer from joints to cortical bone in long bones). On the other hand, cortical bone (or compact bone) has a higher density and can be found for instance on the diaphysis of long bones. It is the one in charge of bearing high mechanical loading. Fig. 20 shows a clarification of these two materials.

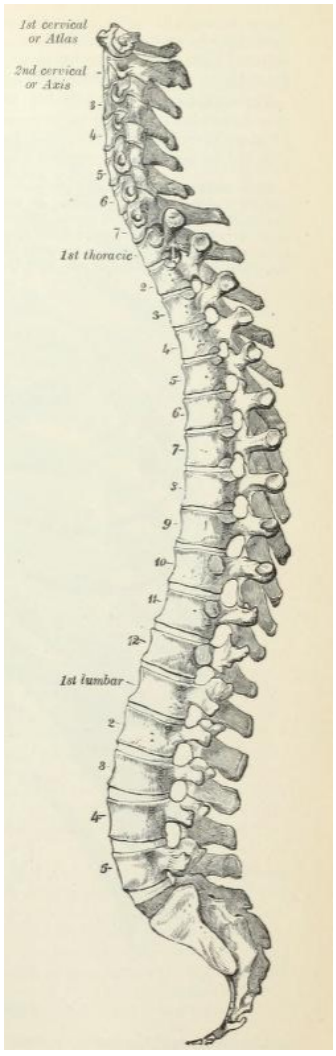

Fig. 18. Spine vertebrae designation [22]

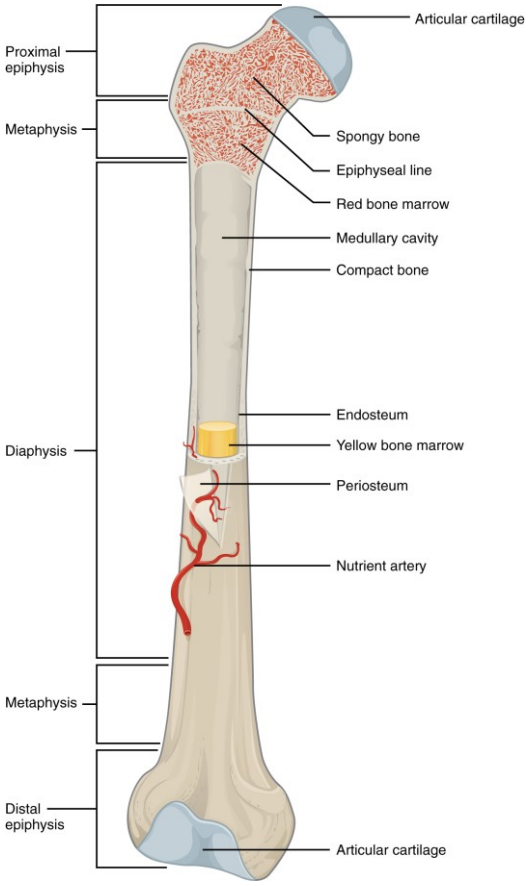

Fig. 19. Anatomy of the long bone [23]

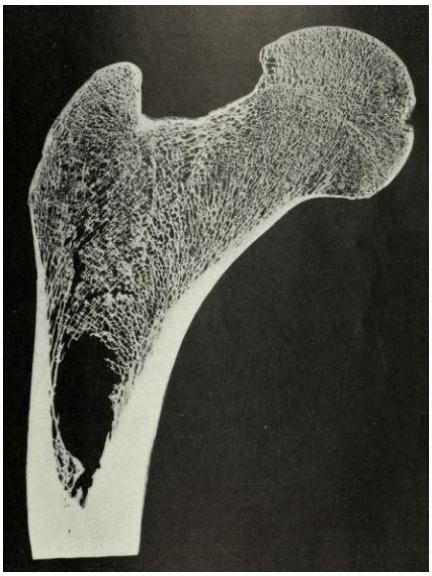

Fig. 20. Cortical and trabecular bone detail [22]

- BA: Bone Area
- BMD: Bone Mineral Density, is the most common parameter for measuring bone density, as inorganic mineral composition in bones is proportional to bone strength.
- BMC: Bone Mineral Content, is obtained by summing the BMD over a projected area (BMD/width of scanned plane line). Therefore, is measured in g/cm.

The analysis is structured from most to least specific, starting with general anthropometric properties such as body fat distribution, lean mass, muscle development and strength, and bone characteristics; and ending up with studies focused on different body parts:

Females have higher estrogen hormone levels, which causes, among others, an increase of adipose tissue (body fat) in thighs, buttocks, and breasts with respect to males, as per described in [24], [25], and [26]. However, according to these same sources, it also decreases abdominal and visceral fat, and consequently, increases the probability and severity of abdominal injuries. Furthermore, it helps increasing muscle strength and bone density, but with less effect than androgen hormones (see next point). Regarding MB HBMs modelling, soft tissues are still a challenge (Chapter 2), and therefore only outer morphometry can be taken into consideration.

Continuing with estrogen effects, collagen levels in ligaments and tendons are also higher in women, which causes a reduction in their stiffness [27]. However, and as stated in [28], ligament stiffness variability among females is significant and further research is still needed to properly address changes in injury prediction metrics. Ligament stiffness can be adjusted in MB HBMs modelling.

On the other hand, males have higher androgen hormone levels that increase muscle mass and strength, which at the same time increases the load on the skeletal system. Subsequently, an activation of bone formation and osteocytes stimulation is produced. Thus, greater osteogenic and muscular response is present on males, as stated in [29], although a general conclusion like this needs further input data for the development of HBMs.

Delving into bone properties and geometry, there are several points that need consideration:

According to [30], 79% of 18 year old females' total body mass is lean mass, whereas in males is a 92%. Besides women having more adipose tissue (as previously explained), and assuming organs and blood account for a similar percentage of lean mass in both cases, the mass of the muscles and bones can explain the observed difference. In particular, the skeletal system has more influence on this parameter since its overall density (considering both trabecular and cortical bone materials) is higher than muscle density. [30] states that spine vertebrae have similar height and BMC in males and females, although the BA is bigger in males. With respect to the femur, males also have higher BMC and BA than females. Similarly, male tibias are greater in BMC, cortical area, and volumetric BMD; and male pelvises have greater BMC and BMD, but similar BA. Consequently, men have a higher mass percentage of skeletal system than women, and therefore, stronger mechanical properties. [31] reaches a similar conclusion, although results do not show significant differences in BMD between both sexes.

Regarding the ease of application in MB HBMs modelling of the differences found in bone BA, BMC, and BMD, BA (that is geometry related) can be considered with an adequate input data. Differences in BMD have been concluded to be neglectable (or at least with respect to Multi-Body Dynamics) and so, related masses do not need to be modified in a relative sense (meaning that if the femur for instance is smaller because the total height of the average female anthropometry is also smaller, its respective masses also need to be smaller in proportion, but no further than that, as density remains constant). BMC differences can only be considered if cortical and trabecular bone materials can be defined. However, this bone material distinction falls out of the current Multi-Body Dynamics capabilities and purpose.

In relation to the cervical spine, [32] concludes that C3 and C7 are similar in males and females in the direction medial-lateral but smaller for females in the direction anterior-posterior. According to [33], female areal and linear cervical spine dimensions are smaller

than those in males, even for matched height population. Moreover, [34] states that females have more curvature (lordosis angle) in the upper cervical spine than males, but less curvature in the lower cervical spine. Similar to the previous case (specifically in the case of BA), with the appropriate input data, the observations made in this case can be incorporated to the FAHM development.

In terms of the tibia, [35] performed a study where cortical bone parameters were measured in several tibia (both male and female) and a set of impact tests was carried out. The study concluded that measured peak impact forces were similar across sexes although males have more cortical bone and greater cross-sectional morphometric values (which aligns with the aforementioned study of bone BA, BMC, and BMD).

In relation to the radius bone, [36] concludes that cortical parameters with respect to morphometry are significantly smaller in females, excluding bone geometry and mineralisation. Additionally, some of these parameters tend to increase with age in males, whereas in females bone quantity and mineral content decreases.

As previously explained, cortical and trabecular bone materials cannot be distinguished in the current state of Multi-Body Dynamics.

Regarding female pelvis morphometry and variability, there are several studies and data sources from literature to take into consideration.

- [37] used 77 female and 39 male subjects to create two parametric pelvis models (male and female, with 31 anatomic reference points and 16 additional calculated ones each) based on sex, age, BMI (Body Mass Index) and bispinous breadth (distance between the anterior superior iliac landmarks, also called anterior spinal distance, see Fig. 21) using PCAR technique (Principal Component Analysis and Regression). Average R-squared values for male model is 0.15 and for female model 0.18 (that is 15% and 18% of the male/female human variability is represented respectively with these two models).

- On the other hand, [38] using also a multivariate linear regression but with sex, age, height, and BMI and the Sparse Principal Component Analysis technique (SPCA) accomplished a single pelvis model (no distinction between males and females) that represents 29% of human pelvis variability. 75 females and 57 males' pelvis were used as reference in this study.
- [39] offers a set of key parameter differences between the average male and female pelvis morphometry. Overall, female pelvis has a "*relatively larger and rounder pelvic cavity, a shorter and more posteriorly projecting sacrum, a wider subpubic angle, and smaller acetabula with a larger distance between them*", although variability in population is high (as previously seen). These key measurements are shown in Fig. 21 and Fig. 22.

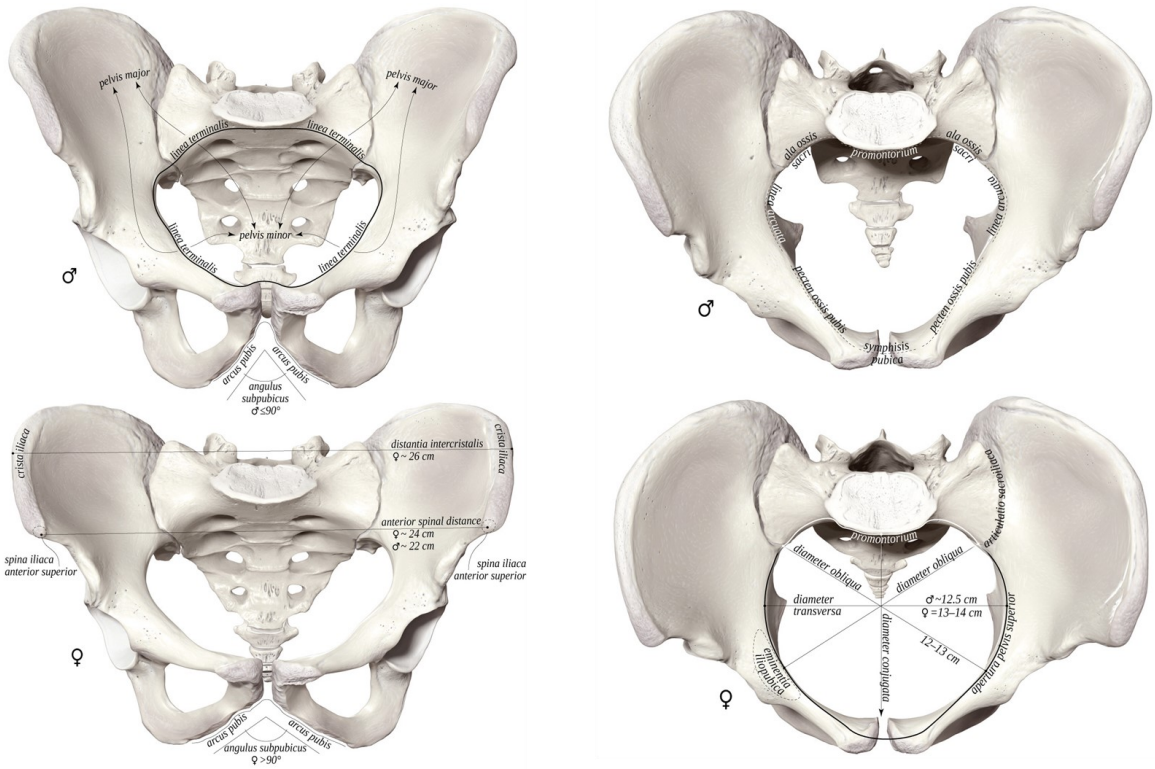

Fig. 21. Average pelvis morphometry. Front view (left) and top view (right). [39]

The first two studies focus on modelling into a singular pelvis model (whether for only one of the sexes or both simultaneously) all anthropometric variability. However, this is not

the aim of this work, but to develop a Female 50th percentile AHM. In the context of the pelvis, this translates to the development of a pelvis morphometry that correctly represents the average pelvis from the group of 50th percentile females. Therefore, the third study provides valuable 2-D input data for this Master's Thesis. The main geometric source (3-D) is presented in the next subchapter as it is part of another existent available technological approach to Human Body Modelling.

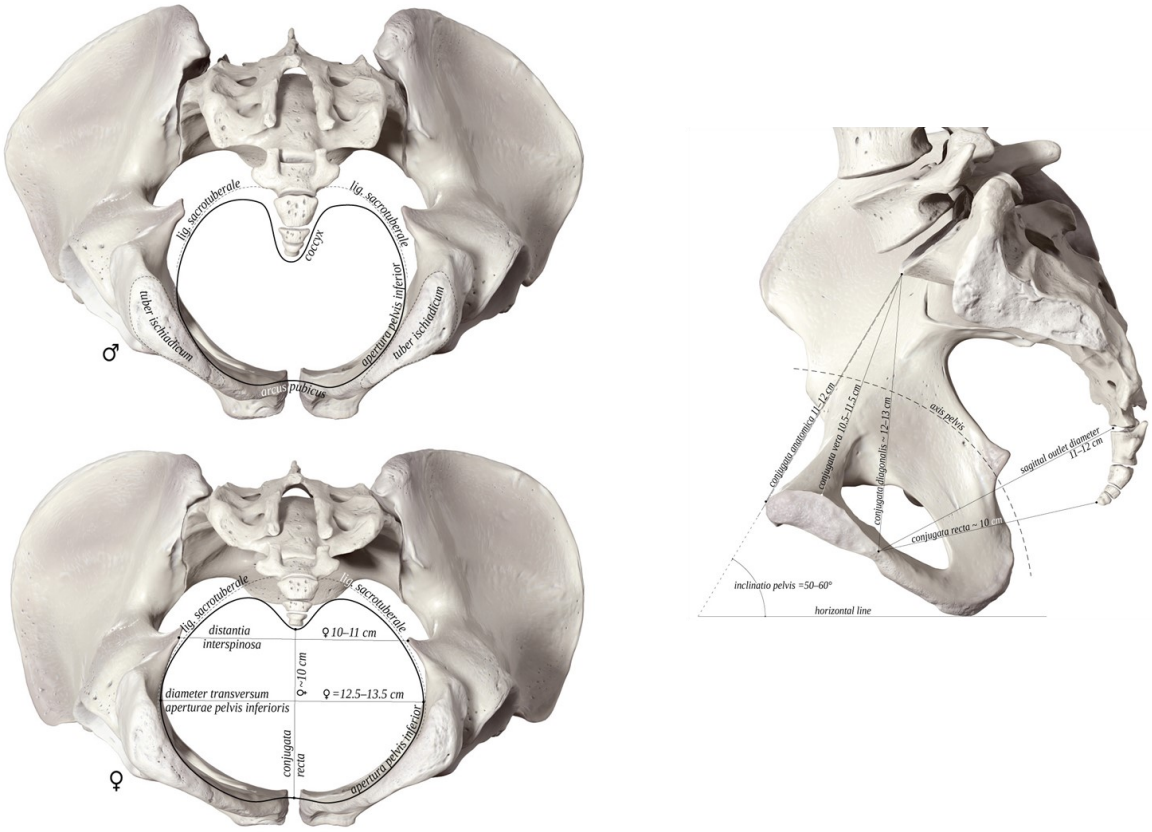

Fig. 22. Average pelvis morphometry. Bottom view (left) and side view (right). [39]

Moving to the head-neck system, [40] states that females have a 9-16% smaller neck (referring to most of the studied anthropometric measures) than males, although only 3-6% smaller heads. In a ratio of head mass/neck muscle area, females have a 33% higher measure than males. Moreover, females have a weaker neck than males, specifically 20% in extension and 32% in flexion, explaining part of the observed phenomena regarding WAD from Chapter 1. These results can be applied in MB HBM, as described in the next subchapter.

Regarding lower extremity injuries, and, in particular, ankle injuries, [41] found that the highest difference in AIS 2+ and AIS 3+ injury data between males and females happens on the lower extremities, and specifically in the ankles. [42] studied widely the possible causes behind this phenomena, some of them with similar conclusions with respect to ligament or bone characterization as the previous points in this subchapter; others, significantly more specific regarding mechanical properties of these elements. This latter study concluded, after several PMHS tests regarding ankle inversion and eversion, that specific Injury Risk Functions (IRFs) differentiating males and females are recommended.

A summary of this female anthropometric analysis is offered below, including the topic, whether said topic is similar or different for both sexes (in the context of MBD), its applicability to MB HBMs modelling in general, and their respective references:

Topic	Sex-related	MB HBMs	References
Fat distribution	Different	Partial	[24], [25] & [26]
Ligaments and tendons strength	Different	Limited	[27] & [28]
General biomechanical properties	Different	N/A	[29]
Bone BMC, BMD & BA	Varies	Limited	[30] & [31]
Cervical spine morphometry	Different	Yes w/ ref. data	[32], [33] & [34]
Tibia cortical bone	Different	No	[35]
Radius anthropometric measures	Different	No	[36]
Pelvis morphometry	Different	Yes w/ ref. data	[37], [38] & [39]
Neck muscle/behaviour and head mass	Different	Yes w/ ref. data	[40]
Ankle behaviour and IRFs	Different	Limited	[41] & [42]

Table 3. Summary of the female anthropometric analysis regarding MB HBMs modelling

In the previous table, partial means that part of the data or conclusions from that study can be applied to MB HBMs modelling, limited is that a very small part can be applied, N/A

is not applicable for analysis (since for that case it was a general conclusion more than specific data results), and yes with reference data meaning that it can be applied with extra input data that has been found (see next subchapter).

How these observations were used in the development of the female 50th percentile Active Human Model (FAHM) are explained in detail in Chapters 3.2 and 4.1.

3.2 BASELINE MODEL AND REFERENCES

In this subchapter, an analysis of the other existent technological approaches to female HBM modelling, virtual ATDs modelling, and physical ATDs development is provided, together with a discussion on the baseline model and main references needed for the FAHM development.

Other existent technological approaches to female 50th models

As briefly mentioned in Chapter 1, 5th percentile female HBMs and virtual and physical ATDs are far more common than their corresponding 50th percentile female versions, as the first ones are (limitedly) used and requested in the automotive sector, such as in type approval and consumer testing, and the second ones are almost not present anywhere. 5th percentile is considered a minimum or low-end case for vehicle occupant and pedestrian safety, whereas the 50th female percentile is assumed to be covered by the 50th percentile male solutions available, situation that this Master's Thesis aims to change.

Among the female 5th percentile HBMs, the Toyota THUMS v6.1 (Total Human Model for Safety version 6) FE AF05 [43], the GHBMC (Global Human Body Models Consortium) FE F05-O [44] and F05-OS (detailed and simplified respectively), and the Simcenter Madymo's h_occ05fc have been developed. On 5th percentile virtual ATDs, the Humanetics THOR 5F FE [45], Hybrid III 5F FE, WorldSID-5F, and SID-IIs (as well as their respective physical ATDs versions), and the Simcenter Madymo's Hybrid III 5th percentile Q dummy, can be found.

In relation to 50th percentile female models, there are only two available solutions (to the knowledge of this Master's Thesis):

Humanetics EvaRID FE virtual ATD (Fig. 23). It is a rear-end testing dummy made from the equivalent male version, the Humanetics BioRID-II FE, via scaling process (see Chapter 4), as per described in their development study [46]. Additionally, a study on WAD for this model was performed [47].

Fig. 23. Humanetics EvaRID FE virtual ATD

ViVA+ 50th FE Female Occupant HBM v0.3.2 (Fig. 24). This model is an evolution of the ViVA version, that started in 2015 under the OpenHBM project, carried out by Chalmers University, and in the context of the ViVA (Virtual Vehicle-safety Assessment: Open Source Human Body Models addressing gender diversity) Swedish project. This model is used as a comparison in Chapter 6, so the origin, development and validation of it was analysed. There is also a standing version of this model.

The original model versions from ViVA, focused mainly on the cervical spine definition, and were developed and validated through different studies: regarding cervical spine [48],

integration of said system in the whole model [49], validation of head-neck system in rear impacts [50], whole model validation with PMHS frontal and rear impacts, and rollover tests [51], and active response of the neck [52].

Afterwards, with the change to ViVA+, sex-specific differences were added, which include head inertia and mass properties, density value for soft tissues, and unstretched length for knee ligaments and quadriceps muscle. Publications involving this model include: a presentation of the new model [53], and a femur model development study [54], although a full set of publications regarding its development and validation is set to be published in the short term. The last published version of this model as of July 2022 is the v0.3.2 (16th May 2022).

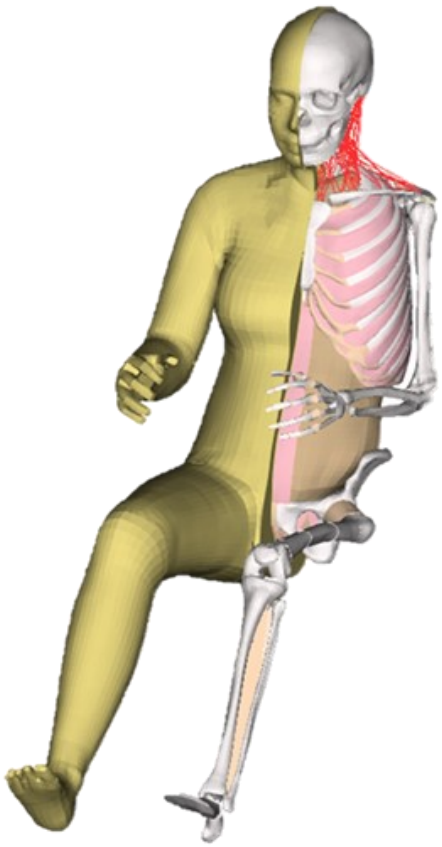

Fig. 24. ViVA+ 50th FE Female Occupant HBM v0.3.2

Therefore, and as of this last version, this model has gone through a head-neck system validation in rear impacts, a femur validation, and a global kinematics validation in a set of frontal and rear impacts, and rollover.

Baseline model for the development of the Madymo Female 50th AHM

The main objective of this Master's Thesis is to generate a female version of the most complex and complete Madymo HBM (and for that matter also more complex than other virtual ATDs). Therefore, the baseline model was the Active Human Model (AHM, Fig. 25), which was already presented in Chapter 2.

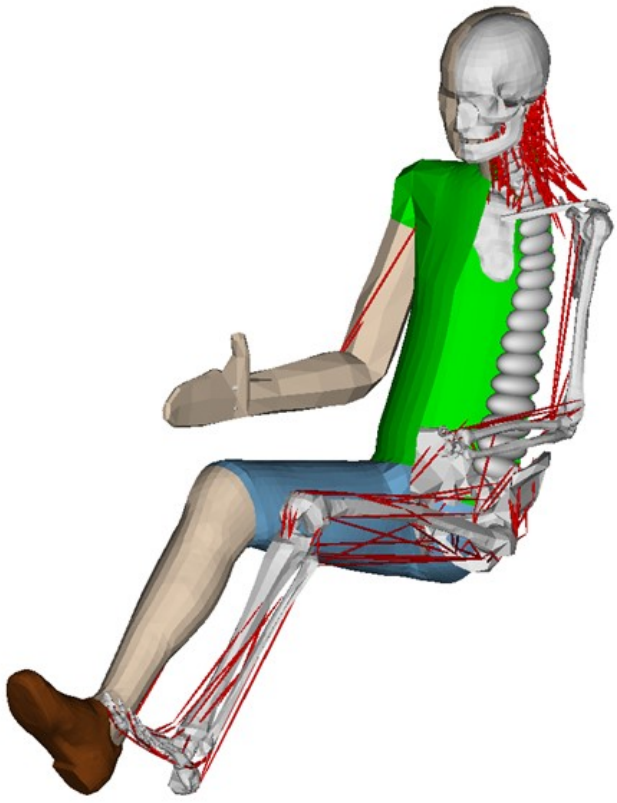

Fig. 25. Madymo Active Human Model (AHM)

The term baseline model used here refers to the structure of said model. That is, for the development of the FAHM, the same structure as the AHM was utilized.

Main reference 1. Female 50th percentile neck model

In a previous internal project of Madymo developer team, [55] developed a female 50th percentile neck model (Fig. 26). After a thoughtful review at the start of this Master's Thesis, this model was included in the FAHM. A discussion on the development and validation process of this subsystem model is offered below.

Fig. 26. Neck model developed in a previous internal study [55]

The neck model study focused on three main differences between male and female physiology regarding this body part. These 3 differences were also identified by the Female Anthropometry Analysis (subchapter 3.1): lower vertebral length to width ratio in female's cervical spine, 33% more head mass to neck muscle area ratio, and more curvature in the upper part of the cervical spine and less curvature in the lower cervical spine than males.

For the development process of this neck model study, the AHM neck subsystem was used. Changes regarding geometry, centre of gravity (COG), masses, lumped masses, joint positioning, restraints, muscles, and belts were implemented (Fig. 27).

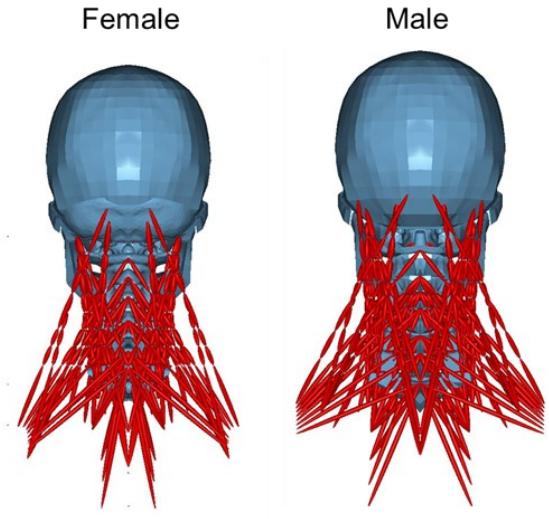

Fig. 27. Comparison of the AHM neck (right) and the female neck (left) [55]

The validation process of this neck study involved the simulation and result comparison of Post Mortem Human Subject (PMHS) data based on Stemper, B. D. studies, 2003, 2004a, and 2004b (these studies as referenced in [55]). The setup of the original PMHS tests is shown in Fig. 28.

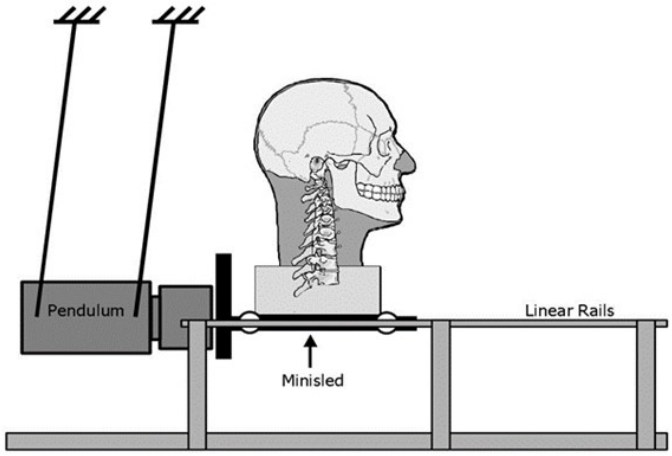

Fig. 28. PMHS tests used as reference for the female neck validation [55]

Results showed that the cervical spine curvature and the head relative to T1 angulation time were within the experimental corridors. However, head relative to T1 shear force (in the rearward direction) were found slightly overestimated the corridors.

The implementation of this model on the FAHM is explained in Chapter 4.

Main reference 2. Facet female 5th percentile scalable model

Inside Madymo scaler tool (see Chapter 2), scalable models can be used. Among them, the facet female 5th percentile scalable model can be found. This model (Fig. 29) is a simplified HBM with facet skin, facet pelvis, simplified facet scapula, ellipsoid-based clavicle, no explicit muscle definitions or muscle activation, and an ellipsoid-based cervical spine. Reference values for this model are 1.5 m height and 50.2 kg of mass. However, it can be scalable using the different methods presented in Chapter 2.

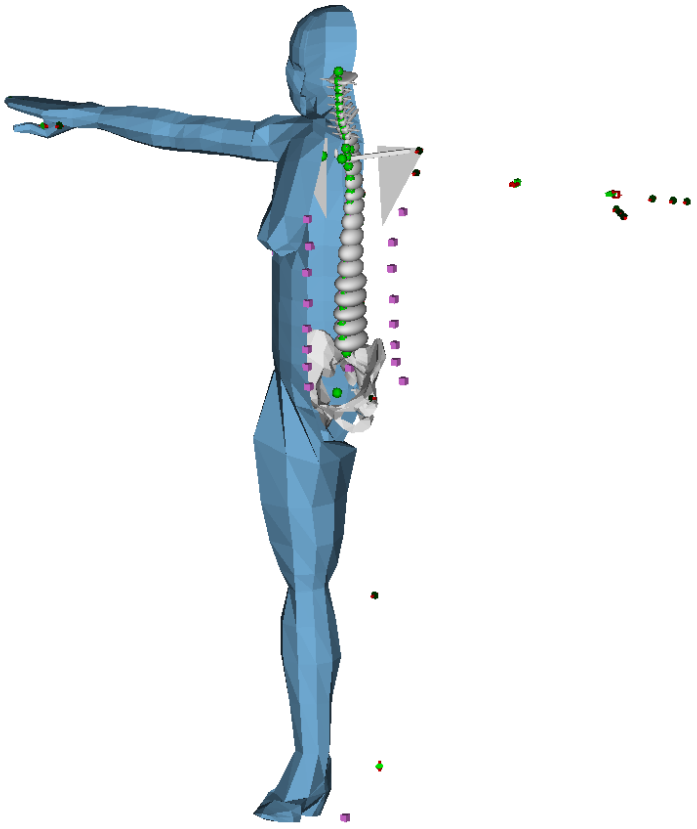

Fig. 29. Facet female 5th percentile scalable model

The method selected for scaling this model was the Siemens Jack scaling, since it contains a wide set of databases to accurately represent different populations (in this case different female 50th percentile populations). This model was used as a pure geometric reference for the body part dimensions and facet skin morphometry. More details are provided in Chapter 4.

3.3 SIEMENS JACK DATABASE ANALYSIS

Evidently, to use as a geometric reference the facet female 5th percentile scalable model, it has to be previously scaled to a female 50th percentile anthropometry by selecting one of the Siemens Jack databases. Hence, this subchapter provides an analysis on which of the presented databases from Jack scaling (Chapter 2) is the most adequate for this Master's Thesis. A summary of the databases explained in Chapter 2 is offered below (Table 4). Additionally, their respective references can be found in [16].

Database name	Population	Relevant info.	Year
ANSUR	USA population	Army personnel	1988
ANSUR II	USA population	Army personnel	2012
NHANES	USA population	NHANES	1990
NHANES 2011-2014	USA population	NHANES	2011-2014
Mexican Jalisco	Latin-American	18 to 65 years-old	1993-1999
CDN LF 97	Canadian	Land forces	1997
NA Auto	North American	Automotive workers	-
Chinese	Chinese	18 to 55 years-old	1989
Asian Indian NID97	Indian	Ergonomic design focused	1997
German	German	DIN 33402	2008
Japanese 2006	Japanese	ISO7250-1/2	2006
Korean 2003	Korean	ISO7250-1/2	2003

Table 4. Summary on anthropometric databases in Siemens Jack

Based on the information present on the previous Table, a preselection of databases can be made. First, military and other force corps members do not represent average anthropometry as they tend to be much fitter. Hence, both USA army personnel studies alongside with the Canadian land forces study can be discarded. Moreover, as there is an updated version of the National Health and Nutrition Examination Survey (NHANES) study, the older version can also be discarded. Likewise, the north American automotive workers can be considered less representative than said NHANES database. Finally, this FAHM is aimed for major OEMs and assessment programmes (both type approval and consumer testing), with a focus on Europe and North America. Consequently, the two preselected databases were NHANES from 2011-2014 and the German database from 2008.

After the preselection, a more technical analysis was performed. In the case of this Master's Thesis, an adequate anthropometric database should comply with the following:

- Because the objective was to develop the female counterpart of the AHM, the database selected must allow for a coherence in the underlaying databases. As explained in Chapter 2, the AHM uses a database from RAMSIS software which was not available to this work. Thus, the male part of the selected database must have a similar anthropometric distribution as the Active Human Model.
- The facet female 5^{th} percentile scalable model scaled to a 50^{th} percentile anthropometry using the selected database must have a similar anthropometric distribution as the ViVA+ 50th FE Female Occupant HBM v0.3.2. In Chapter 5 the FAHM and the ViVA+ model are simulated over a set of validation tests (details on these matter, including reasons and considerations can be found in said Chapter). Thus, in order to allow for a controlled comparison, both models must be similar in the anthropometry. Evidently, this study assumes that the ViVA+ model is an adequate representation of an average female population. Nevertheless, this work needs to be independent with respect to the anthropometric sources, to allow HBM diversity and prevent replicating any possible underlying problems.

The analysis was divided in several parts. From now on, the USA NHANES database 2011 to 2014, is referred to as simply NHANES database. Similarly, the German 2008 is designated as German database. Finally, the AHM original database is referred to as RAMSIS database.

First, a comparison between male NHANES and RAMSIS and male German and RAMSIS was performed. Next, female NHANEs and female German are compared. Finally, a comparison between the female NHANES and ViVA+ and between female German and ViVA+ was performed.

Male NHANES/German against RAMSIS

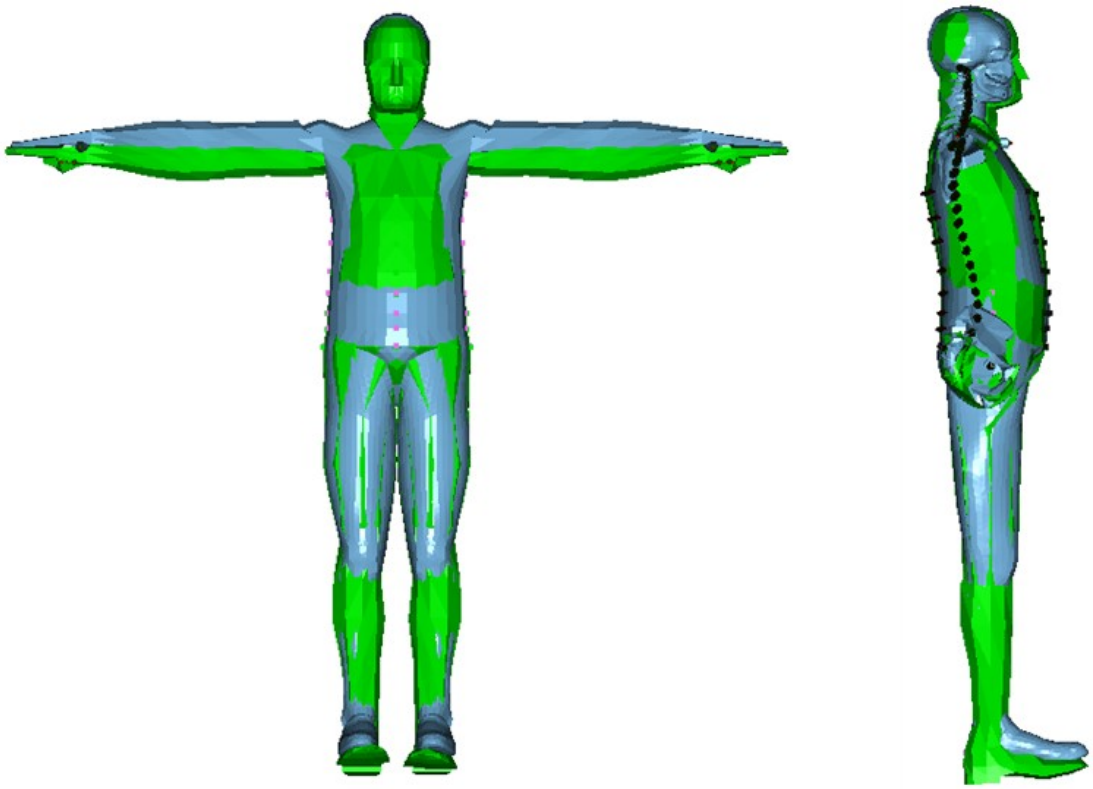

Fig. 30. Male NHANES (green) and RAMSIS (blue)

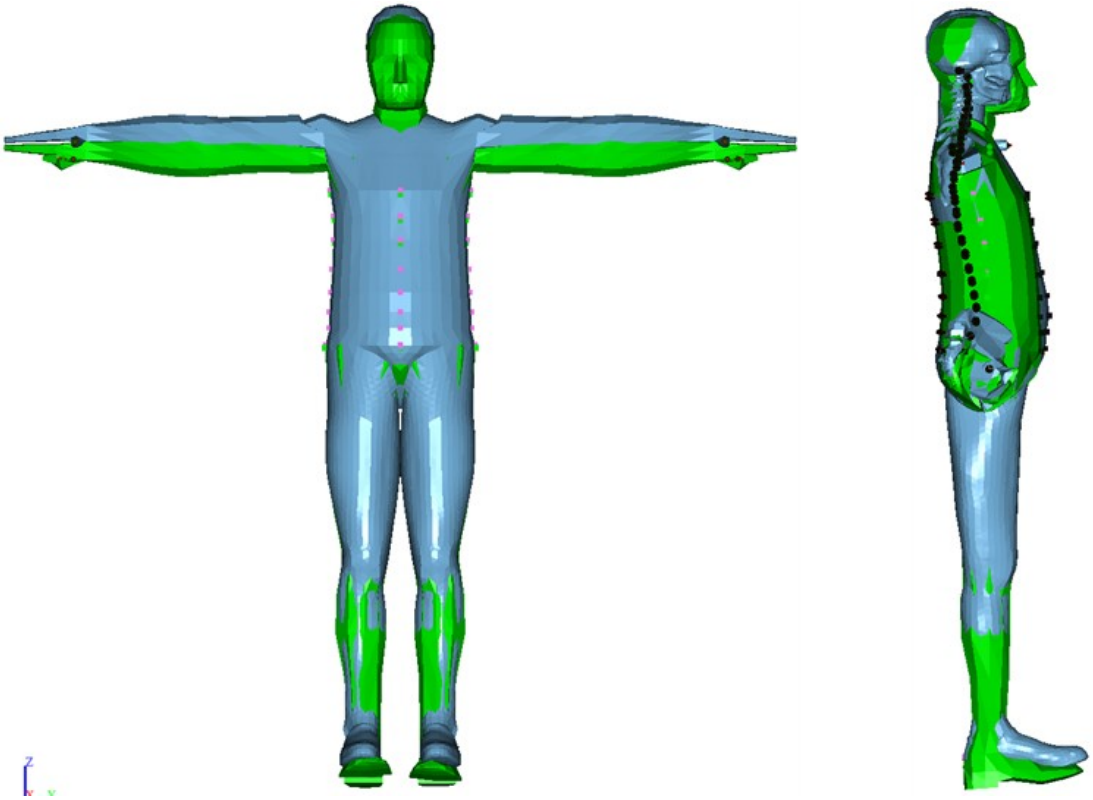

Fig. 31. Male German (green) and RAMSIS (blue)

Fig. 30 and Fig. 31 show frontal and side (with a sagittal cut) views of the male NHANES and male German databases against the RAMSIS database. Both databases present larger legs and a shorter thorax in comparison to the AHM. German head is slightly bigger than the AHM while the NAHNES head is almost identical.

Male NHANES against male German

Fig. 32 shows frontal and side (with a sagittal cut) views of the male NHANES against the male German databases. NHANES has a longer thorax (also is taller). German's thorax is slimmer while its head is bigger.

With respect to the male databases, the NHANES database is closer in anthropometric distribution to the RAMSIS database (AHM).

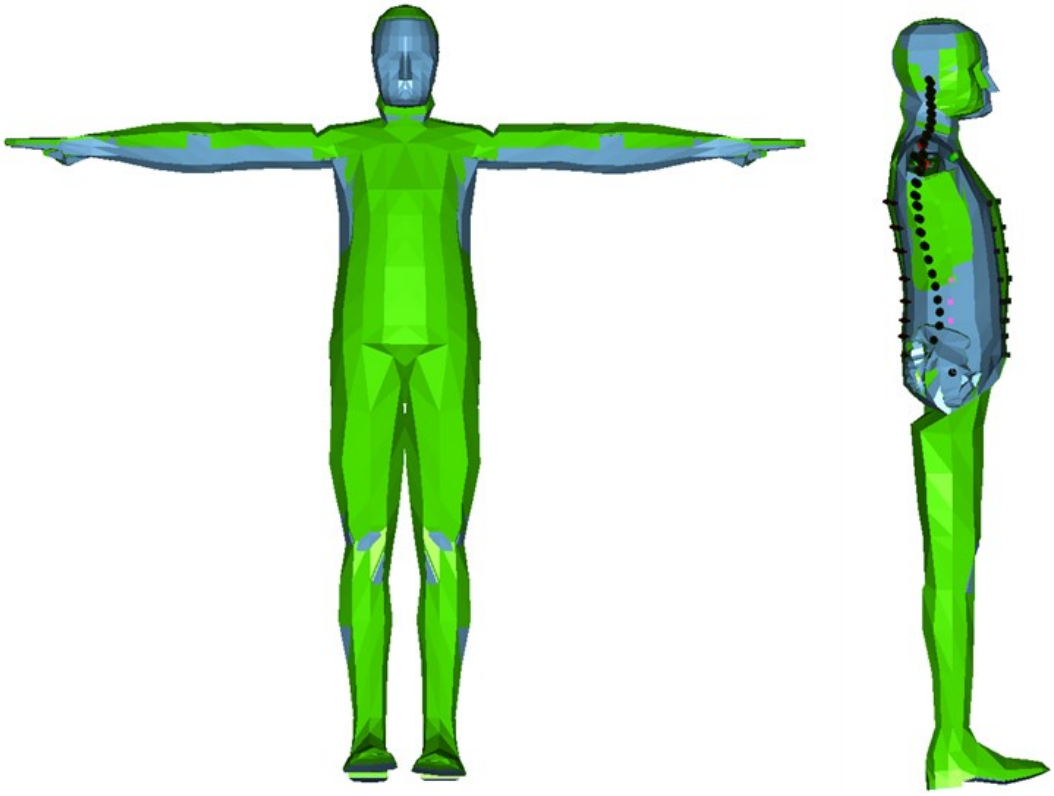

Fig. 32. Male NHANES (green) and male German (blue)

Female NHANES against female German

Fig. 33 and Fig. 34 show the female NHANES and the female German. The first figure correspond to frontal and side (with a sagittal cut) views. The second figure corresponds to a side view of the occupant positioning. NHANES has a shorter thorax (in opposition to the case with the male anthropometric databases). NHANES upper leg is shorter. German's thorax is slimmer while its head is bigger.

Female NHANES/German against ViVA+

Fig. 35 and Fig. 36 show frontal, sagittal cut side, and side view for occupant positioning comparing the female NHANES and the female German with the ViVA+ model (see Chapter 5 for HBM occupant positioning). NHANES database adjusts better to the ViVA+ model's thorax, upper leg length, head size and overall BMI. German's thorax is slimmer while its head is bigger.

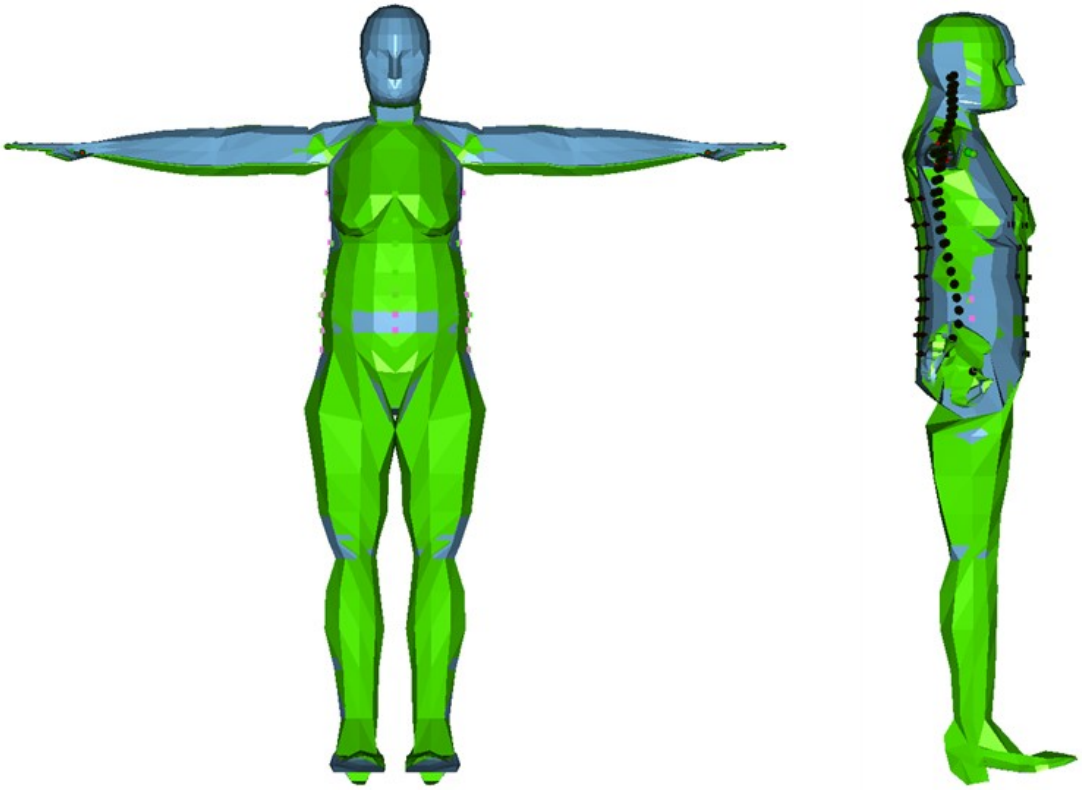

Fig. 33. Female NHANES (green) and female German (blue)

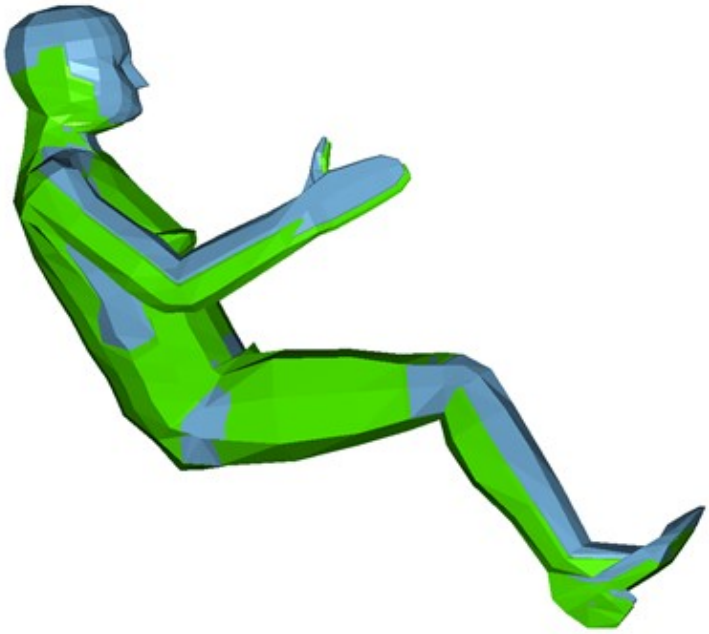

Fig. 34. Female NHANES (green) and female German (blue). Occupant positioning.

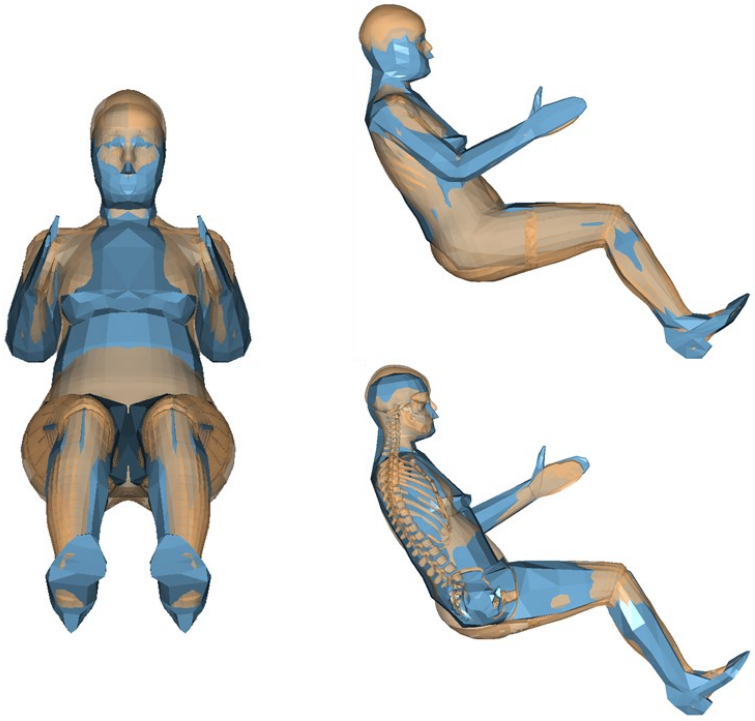

Fig. 35. Female NHANES (blue) against ViVA+ (orange)

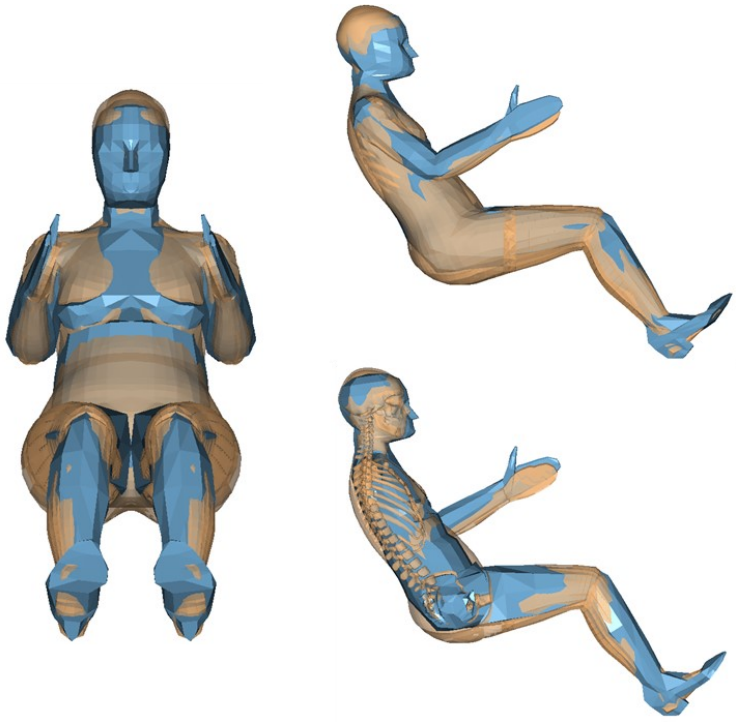

Fig. 36. Female German (blue) against ViVA+ (orange)

To summarize, male NHANES adjust better to the underlaying AHM anthropometric database, although legs are slightly larger, and the thorax is slightly shorter (but the total height is undistinguishable). Likewise, female NHANES adjusts adequately to ViVA+ anthropometric distribution, even though some differences can be addressed, regarding seated height (due to a shorter thorax), and BMI (NHANES is slightly slimmer than the ViVA+, especially in the thighs and buttocks). The final morphometric dimensions of the FAHM were not identical to that of the female NHANES database, due to some considerations that are properly addressed in Chapter 4. Hence, a final anthropometric distribution comparison between the developed FAHM and the ViVA+ model is offered in the aforementioned Chapter.

Chapter 4. DEVELOPMENT OF THE FAHM

The previous three chapters of this Master's Thesis correspond to the first step of the work methodology presented in Chapter 1, research. This Chapter links with the second step, the elaboration on process design, key in the context of this study. In this Chapter, a discussion on the most adequate approach to the FAHM development is offered, alongside with a detailed description of said development, including its morphometry and model dynamics.

4.1 MODEL DEVELOPMENT APPROACH

In subchapter 3.1, the physiological differences between males and females (from a biomechanical point of view) were analysed. From there, a discussion on which of said differences were coherent to include in Multi-Body Dynamics Human Body Model development process was offered.

In this subchapter, the conclusions that were drawn there are contextualized with respect to Madymo, and to the FAHM (and in consequence, also to the male AHM). That is, a discussion on how the gathered input data (both qualitative and quantitative) align with the aim of this work, and which modelling approach allows for an effective and efficient application of these data.

Typically, the approach of FE HBM modelling is reduced to the implementation of detailed input morphometric information, such as Computerised Tomography (CT) data, and to the definition and characterization of materials via gathered literature. On the other hand, MB HMB modelling, as described in Chapter 2, is a much more abstract process. In most cases, body part explicit deformation is not possible, and most elements are either defined implicitly or substituted by engineering equivalencies. A good example of this is spine musculature in the AHM, which is defined by actuators that apply loads on the different vertebrae joints. Hence, direct material definition and characterization is usually not

possible, and this part of the input data is often completed with biomechanical tests on different subsystems, mixing the development with the validation process.

Topic	Suff. Input data	Implicit/Explicit	FAHM dev.
Fat distribution	Partial	Both	Partial
Ligaments and tendons strength	No	Both	No
General biomechanical response	No	-	N/A
Bone BMC, BMD & BA	No	Implicit	No
Cervical spine morphometry	Yes*	Explicit	Yes*
Tibia cortical bone	No	Implicit	No
Radius anthropometric measures	No	Implicit	No
Pelvis morphometry	Yes	Explicit	Yes
Neck muscle/behaviour and head mass	Yes*	Mainly explicit	Yes*
Ankle behaviour	No	Both	No
IRFs	No	-	No

Table 5. Anthropometry analysis application on FAHM development

Table 5 offers a summary on the application of the different topics examined in the Female Anthropometry Analysis to the development of the FAHM model. The column 'sufficient input data' refers to whether the gathered quantitative information from literature (their respective references can be found in Chapter 3) was considered sufficient to correctly include it in the FAHM development process. The column 'Implicit/Explicit' informs if said topic is present implicitly or explicitly in the male AHM, and therefore, also in the FAHM (as explained in Chapter 3, the AHM was also the baseline model, hence, no additional explicit elements were included in its respective female equivalent, the developed FAHM). The 'FAHM development' column states whether that topic was introduced in the modelling

process. The asterisk signs are used for topics that form part of the neck-head subsystem, and that are already included by Main Reference 1 (from now on MR1, see Chapter 3).

First, an explanation on the reasons and considerations behind Table 5 together with further information regarding each topic is presented below. After, the most appropriate approach to the FAHM development based on Table 5 is analysed.

- Fat distribution: as expressed before, adipose tissue is yet a challenge to model in MBD, and additionally, is not present in the AHM. Nevertheless, this topic has a direct effect on skin morphometry, which was considered in the FAHM development using as input data mostly Main Reference 2 (from now on MR2, see Chapter 3).
- Ligaments and tendons: present both explicitly and implicitly in the AHM. However, there is not enough quantitative data to implement a sex-dependent difference in their strength.
- General biomechanical response: this topic refers to males having greater muscular and osteogenic response, as a results of higher androgen levels. This topic was fully qualitative, and therefore, was not implemented in the model development.
- Bone BMC, BMD & BA: BMC and BMD can only be implemented indirectly via biomechanical tests, mixing development with validation, since bone properties are defined implicitly in the AHM. No study was found in literature regarding BMC and BMD and compatible with Multi-Body Dynamics nature. On the other hand, this study considers that not enough input data was found in relation to BA differences.
- Cervical spine morphometry: this topic was implemented in MR1, the female neck model, and the used input data are referenced in [55].
- Tibia cortical bone: identical case to Bone BMC & BMD.
- Radius anthropometric measures: idem.
- Pelvis morphometry: as expressed in Chapter 3, the third study of the Female Anthropometry Analysis regarding this topic was used as a 2D source for the

FAHM pelvis morphometry modelling. Moreover, the ViVA+ pelvis was used as a 3D geometric reference (see next subchapter).

- Neck muscle and biomechanical behaviour and head mass: implemented in the female neck model study [55].
- Ankle behaviour and its respective Injury Risk Function (IRF): a sex specific IRF has yet to be defined by literature (additionally, the AHM lacks an ankle IRF). Also, not sufficient quantitative data (in the context of MBD) has been found regarding physiological differences between males and females in the ankle.

As concluded from the above discussion, there is currently not much quantitative data available regarding anthropometric differences between males and females, and even less for MBD-compatible data. This makes HBM modelling of 50th percentile females challenging, especially for MB HBMs (and consequently, the FAHM). The general lack of studies on this matter can be explained with the same reasoning as in Chapter 1. Since average female anthropometry is considered covered with average male anthropometry by OEMs and vehicle safety assessment programmes, no sufficient investment in research has been put on this topic. Therefore, the weight is being carried mainly by universities, with lower resources, and so, fewer studies can be published.

Considering all the aforementioned, there is currently only one approach possible for the development of the FAHM. This approach is scaling, similar to that of the EvaRID presented in Chapter 3, but with a different mathematical background and with some exceptions. The manual scaling process followed was identical to that of the Madymo scaling tool, and almost completely parametrized. This allows for future use of the FAHM in Madymo Scaler Tool, and consequently, future studies on human variability and creation of a wide range of female AHM models, not only following anthropometric percentiles, but also introducing randomized algorithms locally.

There are diverse mathematical backgrounds for model scaling available in literature. As previously mentioned EvaRID uses a different method focusing on mass ratio, and scale factor length. Among other methods, Mertz 1989 [56] is widely used, especially for response

scaling, as per described in Chapter 5. However, Madymo Scaler tool [16] uses a different scaling method, that was made specifically for Madymo, and that considers the abstract nature of MBD (see Chapter 2). Depending on the application, this method uses both isometric and non-isometric scaling. A detailed description, justification, and considerations of all the mathematical background used in the FAHM development process is offered throughout the next two subchapters.

Lastly, exceptions to this scaling approach were mentioned before. Said exceptions include pelvis morphometry (as already explained) and several elements of the facet skin parts (as a consequence from adipose tissue distribution, such as thorax and breasts, or upper leg geometry).

The FAHM development process per se is detailed in the next 2 subchapters. Subchapter 4.2 focuses on morphometry, entailing centre of gravity (COG) of bodies, joint positioning, ellipsoids and facet elements positioning and sizing (including the aforementioned pelvis and thorax morphometric development), muscle, restraint and belt attachments, deformable bodies modes, and other elements such as sensors or outputs positioning. The following subchapter (4.3) focuses on the model dynamics, which includes masses, inertias, and load and contact characteristics (load characteristics are applied to joints and restraints).

4.2 MODEL MORPHOMETRY

As explained before, this subchapter focuses on the model morphometric development, which is divided into three different sections. The first two present the process of morphing the pelvis, and thorax (including breasts) respectively, using the references described in Chapter 3. The third section delves into the morphometry-related part of the scaling development process, alongside with other minor morphing modifications, such as that of the upper leg geometry.

4.2.1 PELVIS MORPHOMETRY

The pelvis is one of the most important body parts regarding vehicle occupant safety. Its function in the context of this field of study is to bear the load of the lap belt, as a result of accelerations transmitted from the vehicle, while avoiding it to slide under the belt in the iliac crest area (Fig. 37), preventing the phenomena called submarining. In a submarining event, the lap belt pressures the abdominal area. Said area only contains soft tissue, and therefore, this phenomena usually causes severe internal organ injuries.

Fig. 37. Iliac crest representation [57]

Moreover, and from a more mechanical point of view, the seat belt (that is, shoulder belt and lap belt) has a critical role in controlling the acceleration that is transmitted to the occupant from the vehicle, and so the kinematics and dynamics of the system are very sensitive to this safety element. Hence, the contact definition and behaviour between the seatbelt and the pelvis has to be as stable and robust as possible (apart from accurate), to be able to capture adequately the system response. Fig. 38 shows the interaction (skin facet geometry has been hidden for an appropriate visualization of said interaction) between the seatbelt and the pelvis of the FAHM in Simcenter Madymo environment.

As explained before, the approach to the development of a female pelvis in this study follows, together with the thorax skin and other minor cases, takes a different path to that of the rest of the model. There is no scaling involved in the listed elements, but rather a

morphing of the male corresponding geometry using a 3D reference (and, in this particular case, also a 2D reference).

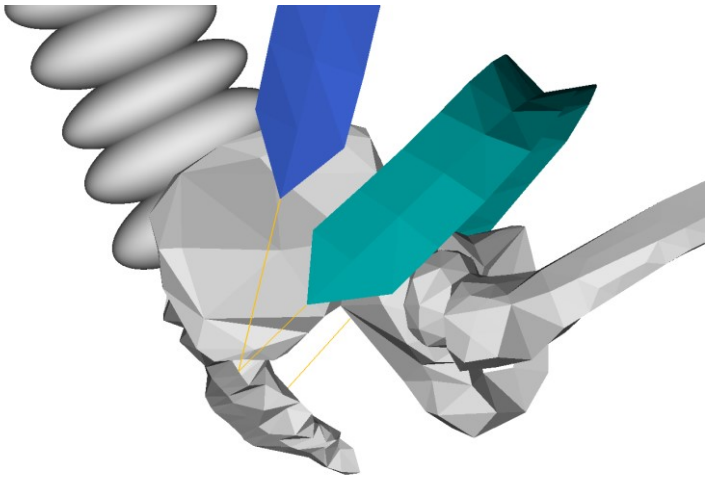

Fig. 38. Seatbelt-pelvis interaction

As previously described, HyperMesh software was used for said morphing. This process involved the utilization of different tools, although the main ones were 'map to geometry' and manual morphing. Map to geometry allows to set a target element shell (ViVA+ pelvis) for the defined handles (morphing points) inside the geometric domain established (that is, the baseline geometry, the male AHM pelvis). Manual morphing allows to adjust the geometry by dragging handles. This last tool was used after the map to geometry tool to correct defects on the geometry such as dissymmetry or negative volumes. Many iterations were performed in order to achieve an adequate result. Fig. 39 shows the final FAHM pelvis, whereas Fig. 40 and Fig. 41 offer a visual comparison between the developed pelvis and the abovementioned target element shell, the ViVA+ pelvis.

There is one main reason to explain why the FAHM pelvis (and, for that matter, also the male AHM pelvis) has a coarser element mesh than the ViVA+ pelvis. From the point of view of MBD, and in particular of Simcenter Madymo, bone characteristics are defined mostly implicitly. However, the outer geometry is defined explicitly, using a shell of facet elements, whose purpose is solely for contact interactions. The mathematical approach to said FE interactions can be challenging, as explained in Chapter 2. Thus, the mesh size of

both the male AHM and the FAHM pelvis represent the optimal balance between morphometric accuracy and contact stability and robustness.

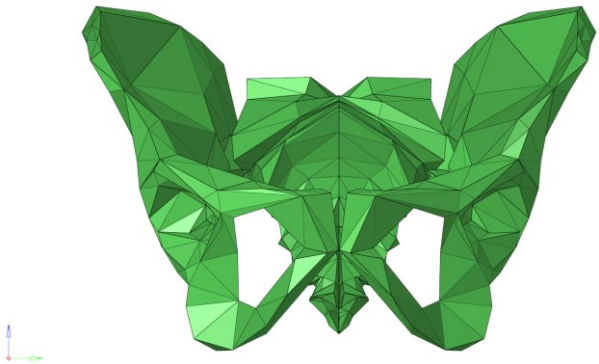

Fig. 39. FAHM pelvis

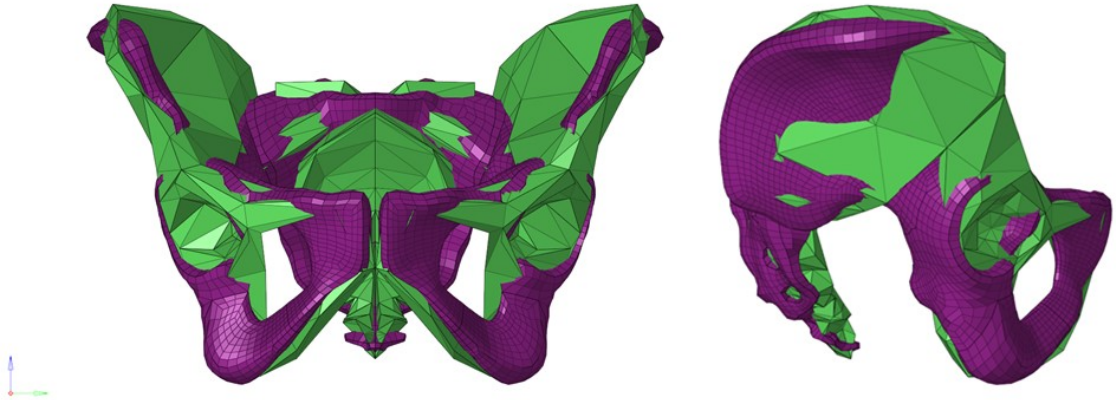

Fig. 40. Comparison between FAHM (green) and ViVA+(purple) pelvis. Front and side view

Fig. 41. Comparison between FAHM (green) and ViVA+(purple) pelvis. Back and top view

Additionally, Fig. 42 offers a comparison between the male AHM pelvis and the FAHM pelvis. The male pelvis is bigger than the female one as the average female is smaller than the average male. Furthermore, the characteristic differences described in Chapter 3 (especially from the 2D reference), were found between these two pelvises.

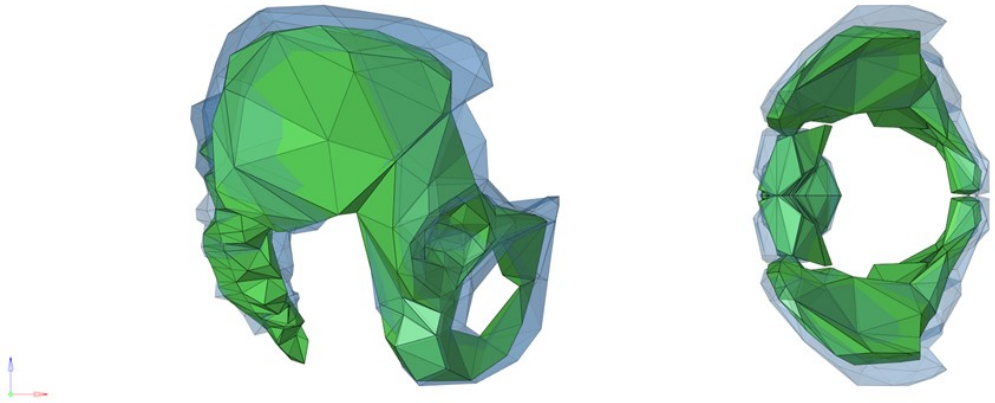

Fig. 42. Comparison between FAHM (green) and AHM (blue) pelvis. Side and top view

After the morphing of the pelvis using a 3D reference, several landmark distances were measured and compared with the input data from the 2D reference [39]. Regarding the front view image reference (Fig. 43), all FAHM pelvis measures were found inside the given interval or very similar to the average value.

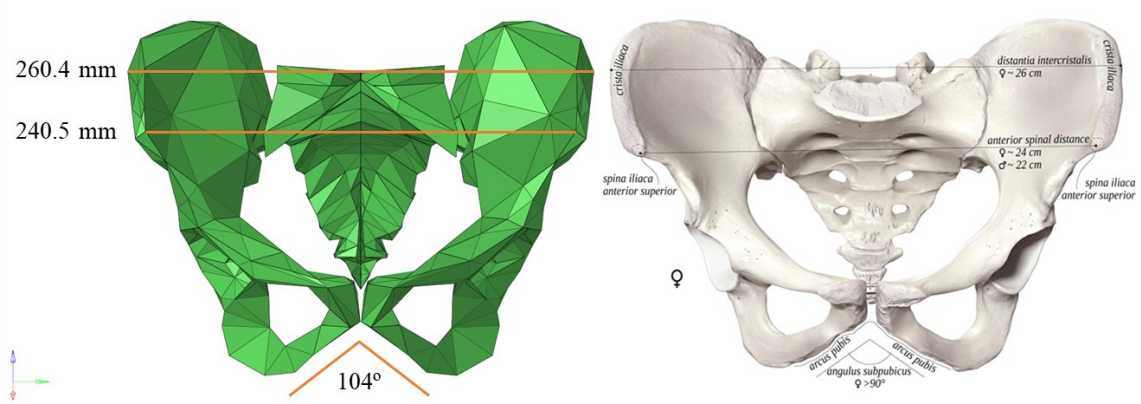

Fig. 43. Landmark measures comparison with [39]. Front view

Similarly, reference intervals were met for the top view reference image, in Fig. 44, and the bottom view reference image, in Fig. 45.

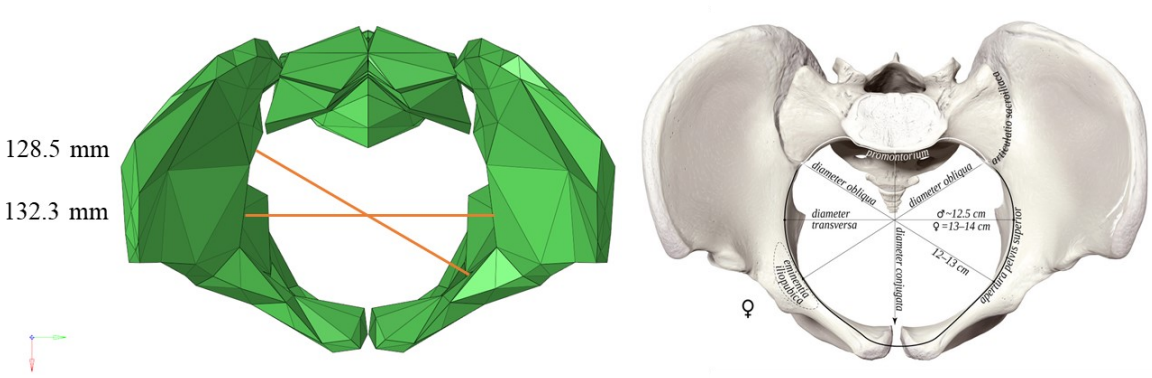

Fig. 44. Landmark measures comparison with [39]. Top view

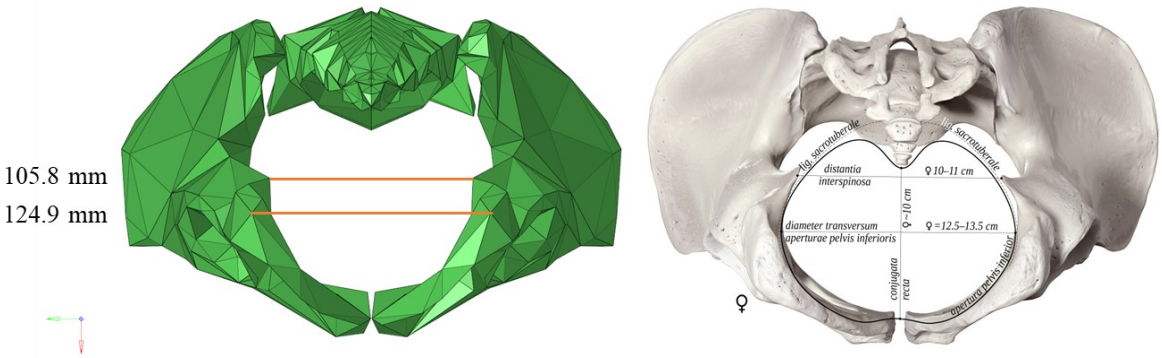

Fig. 45. Landmark measures comparison with [39]. Bottom view

Lastly, the side view Fig. 46, also give values inside the given reference intervals, except for the 110.5 mm measurement that was found slightly over the average value given (100 mm).

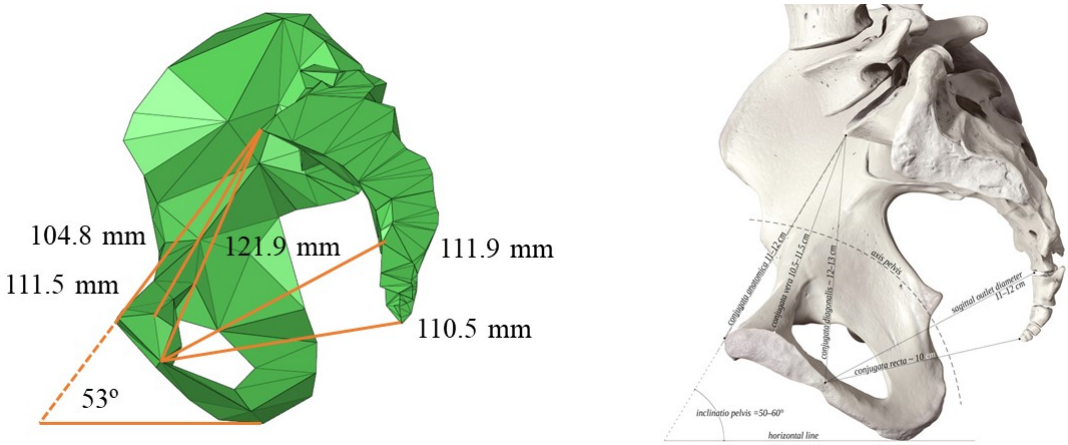

Fig. 46. Landmark measures comparison with [39]. Side view (cut)

Table 6 shows a summary of the abovementioned landmark measures including the target value from the 2-D reference and the obtained value.

Landmark measure	Target	Obtained value
Distantia intercristalis	~26 cm	26.04 cm
Anterior spinal distance	~24 cm	24.05 cm
Angulus subpubicus	>90°	104°
Diameter obliqua	12-13 cm	12.85 cm
Diameter transversa	13-14 cm	13.23 cm
Diameter interspinosa	10-11 cm	10.58 cm
Aperturae pelvis inferioris	12.5-13.5 cm	12.49 cm
Conjugata anatomica	11-12 cm	11.15 cm
Conjugata vera	10.5-11.5 cm	10.48 cm
Conjugata diagonalis	12-13 cm	12.19 cm
Sagittal outlet diameter	11-12 cm	11.19 cm
Conjugata recta	~10 cm	11.05 cm
Inclinatio pelvis	50°-60°	53°

Table 6. Summary of the landmark measures in the developed female pelvis

Consequently, the developed pelvis for the FAHM can be considered representative of the average female pelvis morphometry.

4.2.2 THORAX MORPHOMETRY

The thorax facet skin definition is also a very important part of occupant vehicle safety in the context of Simcenter Madymo. The shoulder belt applies pressure directly on the thorax, affecting significantly the kinematics and dynamics of the system. This section focuses exclusively on the facet skin definition of the thorax. Deformable bodies and other topics are treated in the next section of this subchapter.

The female thorax morphometric development was similar to that of the female pelvis, although more challenges were faced.

First, Altair HyperMesh is only compatible with older versions of Madymo, and therefore keywords such as MODE are not recognised by this software. This particular keyword is directly related to the deformable bodies of the thorax (in fact, these are the deformable modes), and without it, thorax geometry cannot be imported correctly in some cases (depending on how the facet elements were defined originally). Consequently, the female anthropometry of the 5th percentile scalable model scaled to a 50th percentile female (that is, MR 2 of Chapter 3), could not be used as 3D reference via map to geometry tool (but only for visual comparison back in Madymo environment). However, the male AHM thorax could still be used as the baseline geometry, as it was not affected by this problem due to the original definition of its facet surface. Moreover, at the time of this female thorax development, a standing version of the ViVA+ model was not available publicly. Subsequently, said model was also not used as a 3D reference. To solve this problem, the THUMS AF05 Pedestrian Model Version 4.02 was used for the breast area, performing a previous manual scaling to a female 50th percentile anthropometry.

Second, the number of facet skin elements present on the superior anterior part of the male AHM thorax were insufficient to morph towards the breast geometry from the THUMS 3D reference. Thus, new facets were created, attending to element numbering, part numbering and orientation of the element's normal (to avoid negative penetration forces in future contact interactions).

After solving the aforementioned problems, the process carried out was similar to that of the pelvis morphometry section. That is, multiple iterations with map to geometry and manual morphing with symmetry tools. In this case, the manual morphing served also for small modifications, after comparing the new geometry to the MR2 thorax on Madymo environment.

Fig. 47 compares the developed FAHM thorax with the THUMS manually scaled thorax. In the FAHM models, the shoulders are part of the thorax, whereas in the THUMS (and ViVA+) models, the shoulders are part of the upper arm subsystem (and therefore, not present in their respective figures). As shown in said figure, both geometries are similar, with small differences in the abdomen and breast regions, due to later modifications to better resemble the MR2.

Fig. 47. FAHM (blue) vs scaled THUMS F05 (purple) thorax. Front and side (cut) views

Fig. 48 compares the FAHM thorax with the MR2. It is concluded that the female FAHM serves as a middle ground between both THUMS and MR2 references.

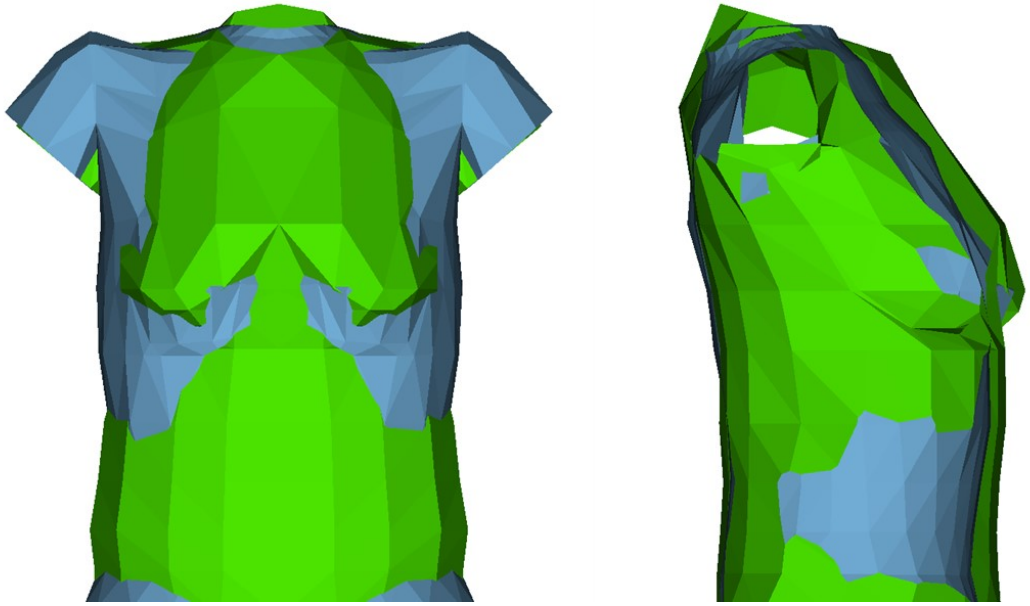

Fig. 48. FAHM (blue) vs MR2 (green) thorax. Front and side (cut) views

Additionally, a comparison between the FAHM thorax and the ViVA+ thorax is offered in Fig. 49, to check that both models are similar enough to assume a coherent comparison on the validation phase described in Chapter 5.

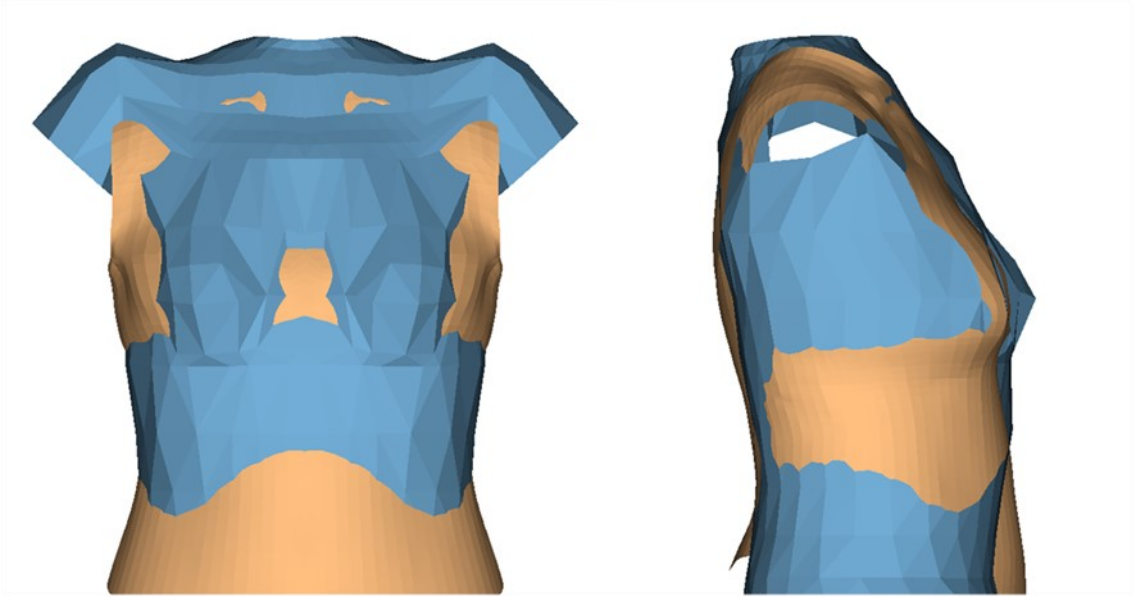

Fig. 49. FAHM (blue) vs ViVA+ (brown) thorax. Front and side (cut) views

Consequently, the developed thorax for the FAHM can be considered representative of the average female thorax morphometry.

4.2.3 MODEL BUILD-UP

This section details the model morphometric build-up, that is, the modification of the male AHM geometry to obtain the corresponding FAHM geometry mainly via scaling approach, and implementation of the developed pelvis and thorax.

As previously explained, the scaling methodology used in this study is identical to that of the Madymo Scaler tool. This method uses a non-isometric scaling distinguishing body parts and absolute axes. Hence the equations used in this section were:

$$\lambda_x = \frac{l_{female_x}}{l_{male_x}}$$

$$\lambda_y = \frac{l_{female_y}}{l_{male_y}}$$

$$\lambda_z = \frac{l_{female_z}}{l_{male_z}}$$

Where female refers to Main Reference 2 (Chapter 3), and male refers to the baseline model, the male AHM.

These equations were used in all elements that have any relation with the model morphometry. Said elements include the centre of gravity (from now on COG) of rigid and deformable bodies, the relative positioning of the joints, the positioning and size of ellipsoids and facet elements, the muscle, restraint, and belt attachment points' relative positioning, the deformation modes' table values, and other elements (such as sensors and outputs' relative positioning).

By convention, the so-called H-point is used in vehicle design to define the position of a vehicle occupant relative to the interior and the origin of all models, and corresponds to the midpoint of the line that joins the centre of the left and right acetabula of the pelvis.

The process was divided into body part subsystems, taking advantage of the AHM segmented structure (described in Chapter 2). A breakdown of the process, the different scaling parameters, and other modifications made is offered below.

Arms subsystem

This subsystem was the first one to be developed. The process established here was followed afterwards in the rest of subsystems, with some exceptions that needed extra steps. The general process focused first on rigid bodies and joints' relative positioning, to set the 'location' scaling factors. After, these scaling factors were applied to muscle, restraint, and belt attachment points' relative positioning, and on sensor and outputs definitions. Later, manual scaling factors for the facet bone elements were created, since not just the positioning but also the facet element size was scaled, and so, the 'location' scaling factors were not adequate. Thus, this scaling factors do not follow the scaling methodology described before. Finally, manual scaling factors for the facet skin elements were also defined, not only for the same reasons as facet bone scaling, but also for addressing independent adipose tissue distribution and for control of the buffer facet skin elements' positioning.

In the case of the arm subsystem, three different areas were considered: upper arm, lower arm, and hand, making a total of 27 morphometric scaling factors. In all cases, the length scaling factor was equal for location, facet skin, and facet bones. Moreover, HyperMesh was used to adjust the upper arm geometry on the more distal facet elements, and to modify the 'zeroing' of facet bones. In the original development of the AHM, the absolute coordinate position of certain facet bones was defined following a vehicle driver's position. Thus, in order to scale, re-position and parametrize said facet bones, the absolute coordinate position was changed to the origin.

Fig. 50 shows the resultant FAHM left arm morphometry, including all its elements. Furthermore, Fig. 51 offers a comparison (restraints have been hidden for an easier visualization) between the left arms of the AHM, the FAHM, and the MR2. The AHM arm is not only larger than the others, but also starts more distally, as shoulders are wider for the male. In addition, the simplicity of the system definition on the MR2 with respect to the AHM and FAHM can be observed.

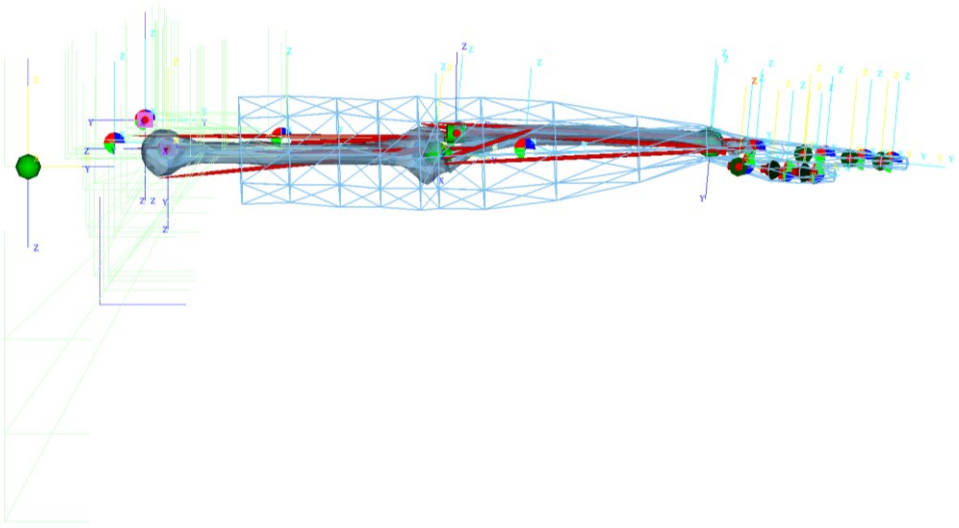

Fig. 50. FAHM left arm subsystem

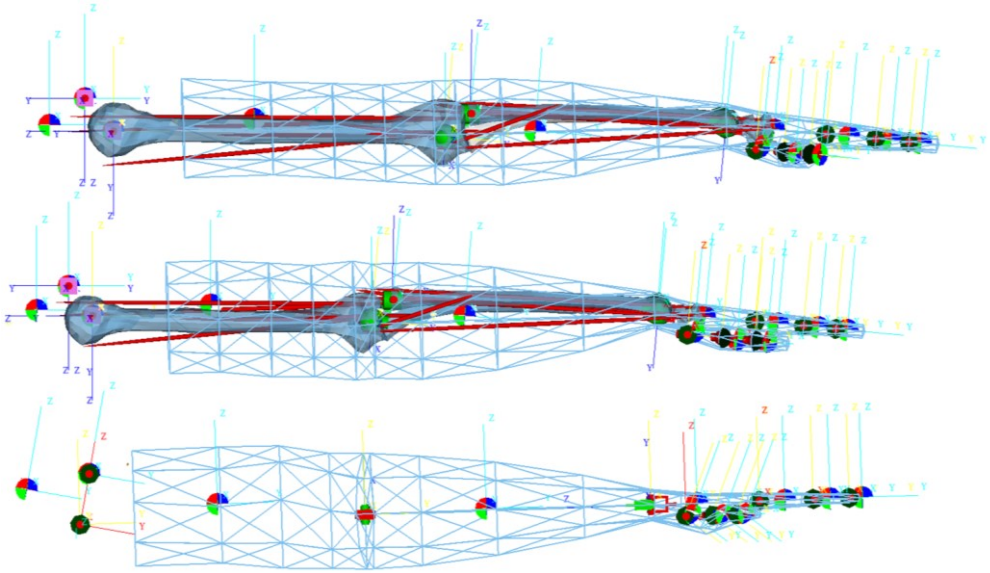

Fig. 51. AHM (first), FAHM (second) and MR2 (third) left arm subsystem (simplified)

Leg subsystem

In the case of the leg subsystem, the different areas considered were upper leg, lower leg, and foot, making a total of 27 morphometric scaling factors. Similar to the arm subsystem, the length scaling factor was equal for location, facet skin, and facet bones, and HyperMesh was used to adjust the upper leg geometry on the more distal facet elements. A 'zeroing' for facet bone elements was only needed for the femur, tibia and fibula since the absolute coordinate location for the foot bones was already the origin. Fig. 52 shows a comparison between the left leg subsystem for the AHM, FAHM, and MR2. In this particular case, the resulting FAHM leg is slightly shorter than MR2 leg, even though the joint positioning is equivalent, due to how the shoe geometry is defined in the MR2 model. Lastly, FAHM leg is shorter than the AHM leg, but unlike the arm, they both start at a similar location. This is explained by both pelvises having similar heights (z axis scaling factor of 1).

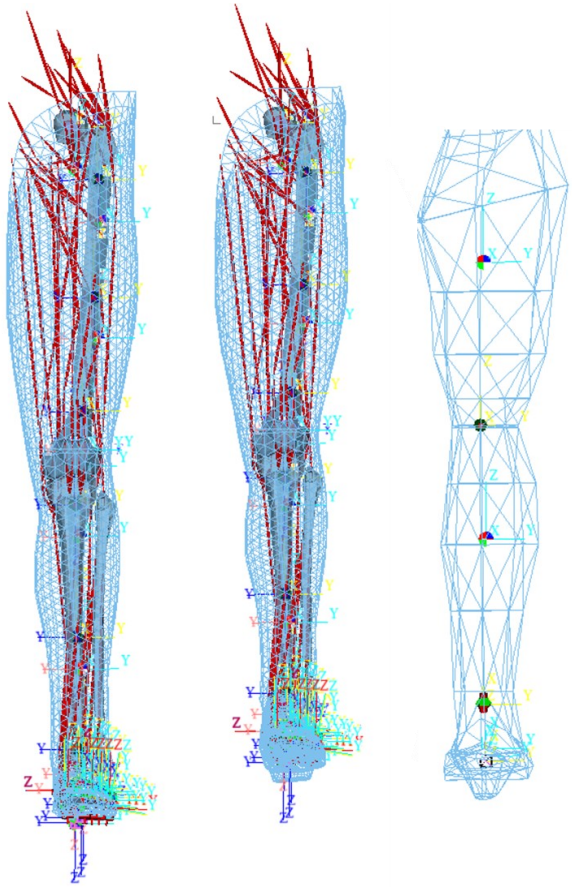

Fig. 52. AHM (left), FAHM (middle) and MR2 (right) left leg subsystem (simplified)

Head-neck subsystem

The head-neck subsystem corresponds to Main Reference 1 (see Chapter 3), and therefore was directly implemented in the new model. The key word structure was updated, as there was a newer version of the segmented AHM. Additionally, some minor scaling was performed to adapt the facet skin of the neck and head to the new subsystem (MR1 focused on the musculoskeletal system development), in certain skull bone facet elements, and in some ellipsoids present in this area. In total, 12 morphometric scaling factors were defined.

Thorax, pelvis and spine subsystems

The first element scaled of this subsystem was the thoracic-lumbar spine (the cervical spine forms part of the head-neck subsystem), with 3 morphometric scaling factors (one for each absolute axis). Fig. 53 shows that MR2 and FAHM thoracic-lumbar spines are almost identical, whereas the AHM is longer, as expected.

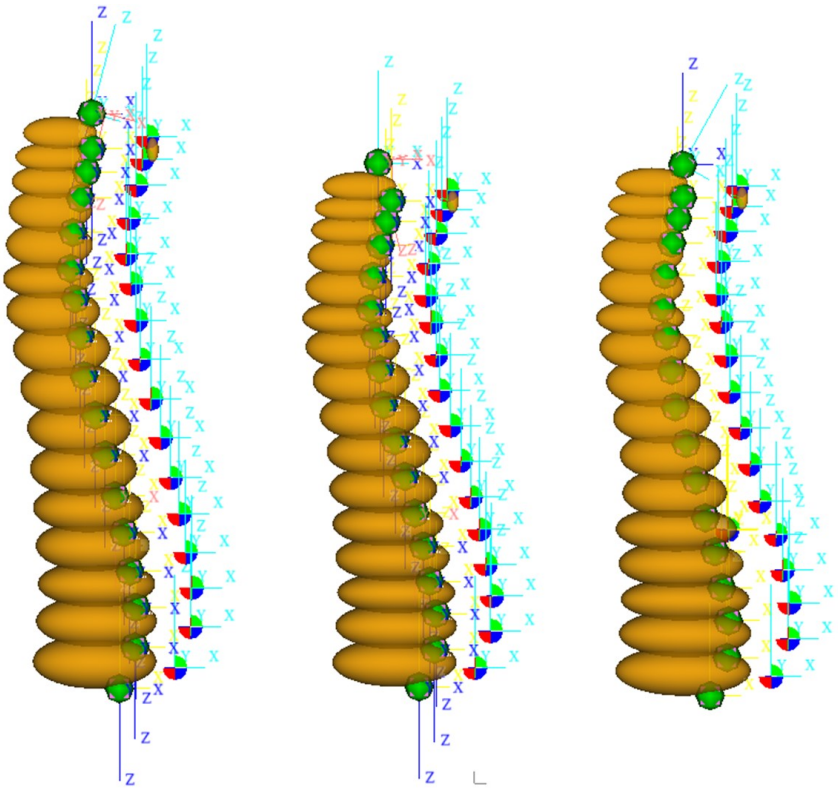

Fig. 53. AHM (left), FAHM (middle) and MR2 (right) spine

The next step was to implement the developed facet pelvis (see section 4.2.1) and to scale the facet skin (3 scaling factors) and other definitions (3 scaling factors) of the pelvis and buttocks area. In total, 6 morphometric scaling factors were used.

Lastly, the thorax subsystem was developed. This subsystem included the clavicle and scapula bones, that were 'zeroed' using HyperMesh software for an adequate scaling. The developed thorax (see section 4.2.2) was implemented, and other definitions were scaled. In total, 6 morphometric scaling factors were used. Moreover, the deformation modes were scaled with 3 of said scaling factors, and a proper explanation of the considerations made is offered below. Fig. 54 shows a comparison (simplified view) between the AHM, the FAHM, and the MR2 thoraxes. Similar to the previous cases, both FAHM and MR2 are equivalent whereas the AHM is larger.

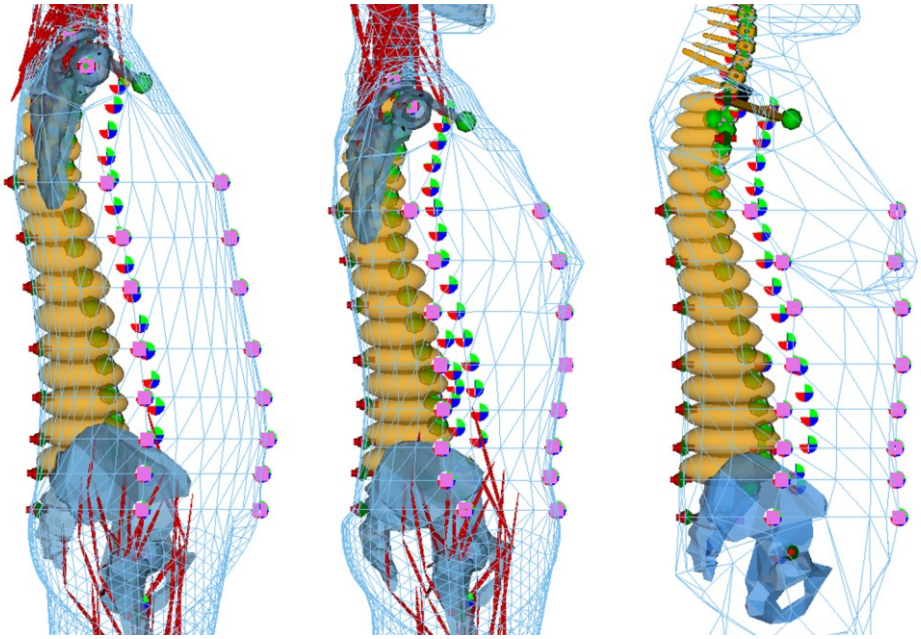

Fig. 54. AHM (left), FAHM (middle) and MR2 (right) thorax, spine and pelvis subsystem (simplified)

Deformation modes are defined in the AHM as distance increments for each node and direction of deformation. As explained in chapter 2, modes are separated by node rings, so all the nodes present in a transversal plane of the thorax go in the same 3 modes of deformation (corresponding to 3 impact directions) and are related to the same deformable

body. Deformation nodes are defined identically in the MR2, although due to differences in the definition of other elements of the model, it was decided not to perform the standard scaling established at the beginning of this section, to avoid facing problems that could only be discovered later on in the validation process (similar to what is explained in the previous section, though the definition incompatibility was discovered early thanks to a different compatibility issue with HyperMesh software). The approach followed on this case consisted in applying the same relative distance increments. That is, if a certain node is set to deform a specific distance in each axis for a specific impact direction (out of 3), the same distance in a relative percentage with respect to the original positioning of said node in said axis is applied on the new model. This method implies two assumptions. First, the relative thorax deformation for a specific impact, is approximately equal on males and females. Second, breast geometry can be modelled with the same material as the rest of the thorax within MBD accuracy levels. This last assumption was also considered in the next subchapter.

Fig. 55, Fig. 56, and Fig. 57 show a top view of the original (blue) and final (orange, refers to maximum deformation possible) thorax geometry for the node ring at the breast height for mode 1 (impact normal to the coronal plane of the model), and modes 2 and 3 (impacts normal to the sagittal plane of the model from both sides), respectively.

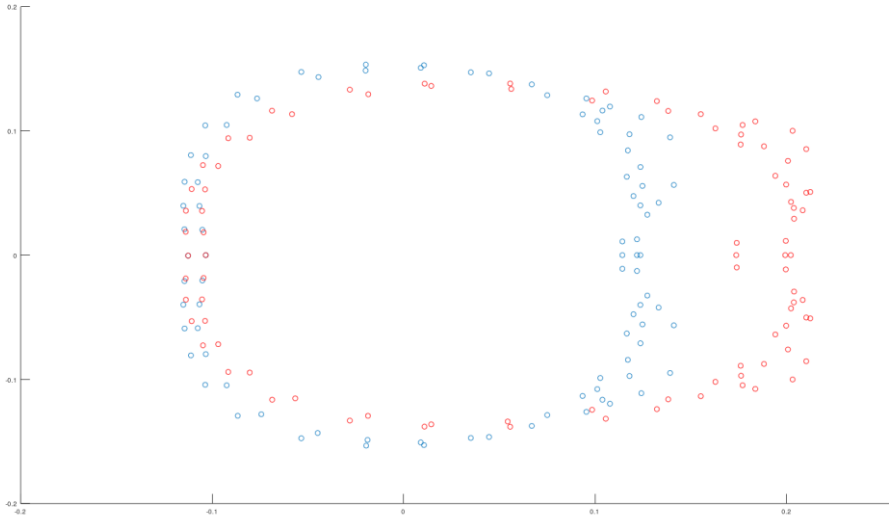

Fig. 55. FAHM deformable mode 1 of the breast ring node

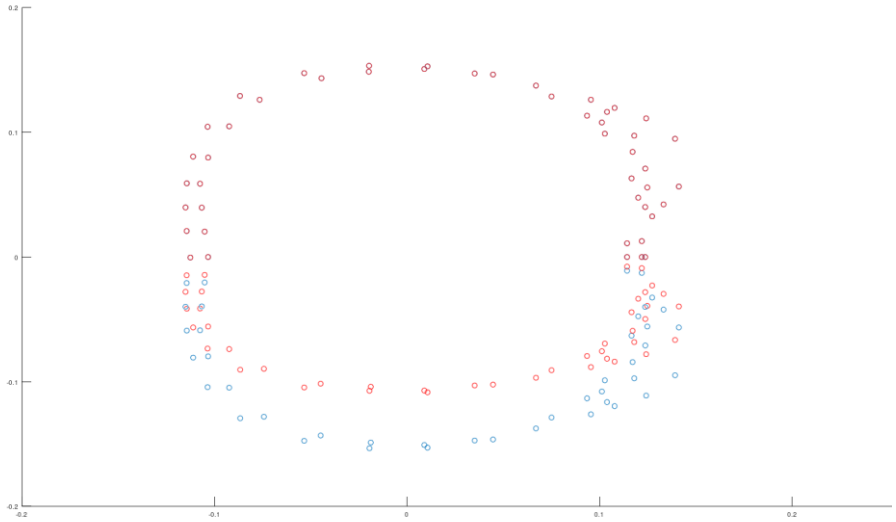

Fig. 56. FAHM deformable mode 2 of the breast ring node

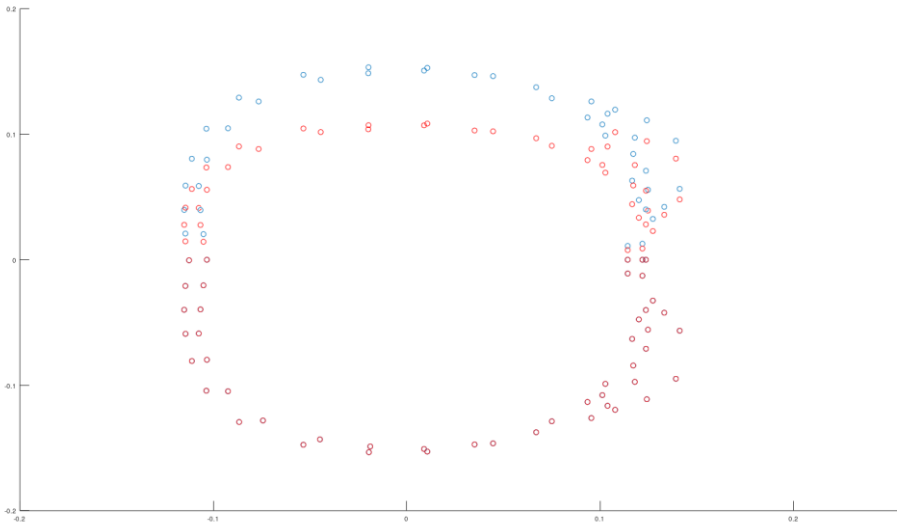

Fig. 57. FAHM deformable mode 3 of the breast ring node

To end this subchapter, Fig. 59 shows the final model (with respect to morphometry) with all the aforementioned modifications implemented. At this point, the model looked consistent, and it was decided to proceed with the model dynamics (next subchapter). Additionally, the final standing height for the developed FAHM was 1.63m almost identical to MR2 standing height, 1.65m (1.23% difference). The difference in 2 cm can be explained with the MR2 shoe geometry.

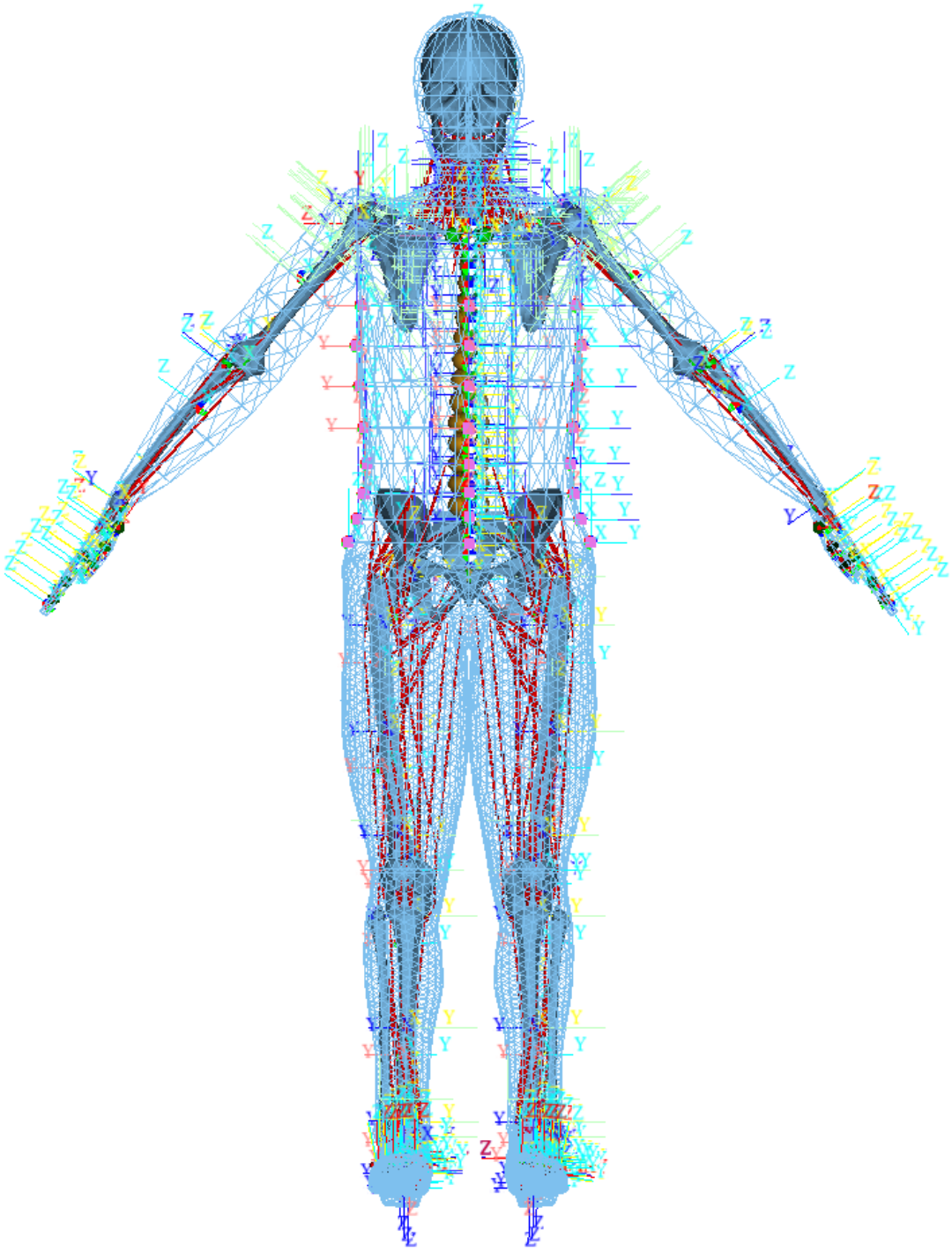

Fig. 58. FAHM morphometry build-up

4.3 MODEL DYNAMICS

This section details the model dynamics definition, that is, the implementation of the response behaviour of the FAHM via scaling the AHM's response. As previously explained, the scaling method used in this Master's Thesis considers isometric and non-isometric approaches to the different elements of the model.

The elements that were scaled in this subchapter were mass, inertia, and load and contact characteristics. The only elements that have not been scaled (or adapted by other methods to an average female anthropometry) in this study are injury criteria, active response-related elements (actuators and muscle definitions), and controllers. Active response falls out of the scope of this study, and with respect to injury criteria, insufficient input data and resources were available.

Masses

Masses were scaled non-isometrically using all three axis scaling factors and a relative density ratio. This ratio was considered equal to 1 since female average body density and male average body density are very similar. Evidently, this was performed for all rigid bodies and lumped masses in the system, and the scaling factors used depended on the body part to which each one of them was associated.

$$\lambda_m = \delta \cdot \lambda_x \lambda_y \lambda_z, \quad \delta = \frac{\rho_{female}}{\rho_{male}} \cong 1$$

Inertia

Inertia scaling also followed a non-isometric approach. To be able to understand the nature of the final equations used here, a mathematical breakdown is offered below:

The main products of inertia can be derived as:

$$I_{xx} = \int (y^2 + z^2)\rho \, dV = \int y^2 \rho \, dV + \int z^2 \rho \, dV = H_{yy} + H_{zz}$$

Thus, the three main products of inertia can be expressed as:

$$\begin{bmatrix} I_{xx} \\ I_{yy} \\ I_{zz} \end{bmatrix} = \begin{bmatrix} 0 & 1 & 1 \\ 1 & 0 & 1 \\ 1 & 1 & 0 \end{bmatrix} \begin{bmatrix} H_{xx} \\ H_{yy} \\ H_{zz} \end{bmatrix}$$

And the H products as:

$$\begin{bmatrix} H_{xx} \\ H_{yy} \\ H_{zz} \end{bmatrix} = \begin{bmatrix} 0 & 1 & 1 \\ 1 & 0 & 1 \\ 1 & 1 & 0 \end{bmatrix}^{-1} \begin{bmatrix} I_{xx} \\ I_{yy} \\ I_{zz} \end{bmatrix} = \frac{1}{2} \begin{bmatrix} -1 & 1 & 1 \\ 1 & -1 & 1 \\ 1 & 1 & -1 \end{bmatrix} \begin{bmatrix} I_{xx} \\ I_{yy} \\ I_{zz} \end{bmatrix}$$

The H products can be scaled with:

$$\frac{H_{xx_{female}}}{H_{xx_{male}}} = \frac{\int x_{female}^2 \rho_{female}\, dV_{female}}{\int x_{male}^2 \rho_{male}\, dV_{male}} = \frac{x_{female}^2 m_{female}}{x_{male}^2 m_{male}} = \lambda_x^2 \lambda_m \cong \lambda_x^3 \lambda_y \lambda_z$$

And therefore, the inertia is scaled with:

$$\frac{I_{xx_{female}}}{I_{xx_{male}}} = \frac{H_{yy_{female}} + H_{zz_{female}}}{H_{yy_{male}} + H_{zz_{male}}} = \frac{\frac{H_{yy_{female}}}{H_{yy_{male}}} + \frac{H_{zz_{female}}}{H_{yy_{male}}}}{1 + \frac{H_{zz_{male}}}{H_{yy_{male}}}} =$$

$$= \frac{\frac{H_{yy_{female}}}{H_{yy_{male}}} \cdot \frac{H_{yy_{male}}}{H_{zz_{male}}} + \frac{H_{zz_{female}}}{H_{yy_{male}}} \cdot \frac{H_{yy_{male}}}{H_{zz_{male}}}}{1 \cdot \frac{H_{yy_{male}}}{H_{zz_{male}}} + \frac{H_{zz_{male}}}{H_{yy_{male}}} \cdot \frac{H_{yy_{male}}}{H_{zz_{male}}}} = \frac{\frac{H_{yy_{female}}}{H_{yy_{male}}} \cdot \frac{H_{yy_{male}}}{H_{zz_{male}}} + \frac{H_{zz_{female}}}{H_{zz_{male}}}}{\frac{H_{yy_{male}}}{H_{zz_{male}}} + 1} =$$

$$\cong \frac{\lambda_x \lambda_y^3 \lambda_z \cdot \frac{H_{yy_{male}}}{H_{zz_{male}}} + \lambda_x \lambda_y \lambda_z^3}{\frac{H_{yy_{male}}}{H_{zz_{male}}} + 1}$$

Lastly, the equations used for scaling the inertias were:

$$\lambda_{Ixx} = \frac{\lambda_x \lambda_y \lambda_z \left(\left(\lambda_y^2 \frac{H_{yy_{male}}}{H_{zz_{male}}} \right) + \lambda_z^2 \right)}{\frac{H_{yy_{male}}}{H_{zz_{male}}} + 1}$$

$$\lambda_{Iyy} = \frac{\lambda_x \lambda_y \lambda_z \left(\left(\lambda_z^2 \frac{H_{zz_{male}}}{H_{xx_{male}}} \right) + \lambda_x^2 \right)}{\frac{H_{zz_{male}}}{H_{xx_{male}}} + 1}$$

$$\lambda_{Izz} = \frac{\lambda_x \lambda_y \lambda_z \left(\left(\lambda_x^2 \frac{H_{xx_{male}}}{H_{yy_{male}}} \right) + \lambda_y^2 \right)}{\frac{H_{xx_{male}}}{H_{yy_{male}}} + 1}$$

With:

$$H_{xx_{male}} = \frac{1}{2}(-I_{xx_{male}} + I_{yy_{male}} + I_{zz_{male}})$$

$$H_{yy_{male}} = \frac{1}{2}(I_{xx_{male}} - I_{yy_{male}} + I_{zz_{male}})$$

$$H_{zz_{male}} = \frac{1}{2}(I_{xx_{male}} + I_{yy_{male}} - I_{zz_{male}})$$

These final equations were applied to all the rigid bodies' inertias of the FAHM, but no extra scaling factors were created (the equations were implemented directly in the definition using the existing scaling factors). The different values of H_{xxmale}, H_{yymale}, and H_{zzmale} were calculated for each rigid body in the AHM. The values of λ_x, λ_y, and λ_z, where varied depending on the body part said rigid body is associated with. There are no rotational inertias nor crossed inertias (such as I_{xy}) in the AHM, and consequently, in the FAHM.

Load and contact characteristics, and other restraint-related elements

As described in Chapter 2, load characteristics are defined for joints and restraints, whereas contact characteristics are defined for facet elements and ellipsoids. Both characteristics are scaled following an isometric scaling.

This is the first and only time in this subchapter that isometric scaling was used. The reason is that load and contact characteristics are applied in all directions, that depend for instance on how much a specific joint rotates or the configuration of the contact interaction

between the model and the environment. Therefore, distinguishing absolute axis is not coherent, and so a resultant scaling factor is calculated with:

$$\lambda_r = \sqrt[3]{\lambda_x \lambda_y \lambda_z}$$

After that, different cases were found including, load characteristics with a torque involved, load characteristics without a torque involved, and contact characteristics.

Load characteristics without torque

Total deformations are derived from a strain integrated over a specific length. If identical strain distribution is assumed, then the deformation will be proportional to the initial length, and therefore:

$$\frac{d_{female}}{d_{male}} = \lambda_r$$

Moreover, and assuming equal material characterization in both models, an identical strain distribution yields an identical stress distribution. Since the integration of stress over a surface results in force, and said stress is assumed to be equally distributed, then:

$$\frac{F_{female}}{F_{male}} = \lambda_r^2$$

Thus, the load and unload functions from (depending on the hysteresis model defined) non-linear stiffness characteristics (that is, the ones here described), were scaled using λ_r for x values and λ_r^2 for y values. In order to maintain the consistency in the loading curves, the hysteresis slope and elastic limit values were scaled with λ_r.

On the other hand, assuming an identical strain-rate distribution allows to scale external deformation velocity as:

$$\frac{v_{female}}{v_{male}} = \lambda_r$$

As linear damping equals force divided by deformation rate:

$$\frac{D_{female}}{D_{male}} = \frac{\lambda_r^2}{\lambda_r} = \lambda_r$$

And the non-linear velocity-dependent damping functions (N vs m/s) can be scaled using λ_r for x values and λ_r^2 for y values.

Load characteristics with torque

Torques are proportional to force and length, hence:

$$\frac{M_{female}}{M_{male}} = \lambda_r^3$$

Rotation angles are dimensionless, and thus, invariant to scaling:

$$\frac{\varphi_{female}}{\varphi_{male}} = 1$$

And consequently, the load and unload functions from (depending on the hysteresis model defined) non-linear stiffness characteristics (that is, the ones here described), were scaled using λ_r^3 for y values. In order to maintain the consistency in the loading curves, the hysteresis slope value was scaled with λ_r^3, and the elastic limit was not scaled.

Linear rotational damping equals torque divided by rotation-rate obtaining:

$$\frac{D_{T_{female}}}{D_{T_{male}}} = \frac{\lambda_r^3}{1} = \lambda_r^3$$

And the non-linear rotation-dependent damping functions (Nm vs rad/s) can be scaled using λ_r^3 for y values.

As previously mentioned, identical stress distribution is assumed, and so:

$$\frac{\sigma_{female}}{\sigma_{male}} = 1$$

And stress-dependent damping factors were not scaled.

Other restraint-related elements

Restraint definitions such as joint restraints, cardan restraints, and flexion torsion restraints can have friction functions associated. In the first case, said functions should be scaled as a force or torque, depending on the type of degree of freedom (displacement or rotation) which

is referring to. In the second and third case, they always refer to torsion, and so they were scaled accordingly.

Contact characteristics

For the AHM 13 different contact interactions are initially defined, including body to head, arms, and legs, between legs, between a leg and the shoe from the other leg, and between shoes.

In all cases, these contact characteristics where stress-based and so the load and unload functions from (depending on the hysteresis model defined) non-linear stiffness characteristics are defined with the units N/m^2 vs unitary penetration. This unitary penetration is dimensionless as the displacement is divided by the thickness of one of the contact surfaces (depending on how it is defined). Nevertheless, this penetration should still be scaled, as the deformation is still proportional to the initial length, and so it was treated as a penetration distance (m) for all cases. Thus, x values were scaled using λr for x values (and stress was not scaled). In order to maintain the consistency in the loading curves, the hysteresis slope and elastic limit values were scaled with λ_r.

Linear damping is scaled as in the case of load characteristic without torque, that is, with λ_r. Moreover, for these type of stress-based contact characteristics, the velocity-dependent damping functions use different units (N/m^2 vs m/s) and subsequently, only x values are scaled with λ_r. Finally, damping amplification factors are defined, in the context of this type of contact, with amplification factor vs N/m^2, and so, no scaling was needed.

The previous explanation could not be followed in all cases. Some of these contact characteristics describe general interactions, such as between bones, and no scaling was considered. In other cases, a resultant scaling factor was calculated for a specific body subsystem. For instance, the resultant scaling factors for upper arm, lower arm, and hand were merged into a single one:

$$\lambda_{r_{arm}} = \sqrt[3]{\lambda_{r_{upper\ arm}} \lambda_{r_{lower\ arm}} \lambda_{r_{hand}}}$$

This allowed for contact definitions such as body to each arm.

In the previous subchapter, a height comparison between the FAHM and the MR2 was offered since it was related to morphometry. Now, mass is related to dynamics, and so the MR2 has a mass of 72.2kg, and the FAHM a mass of 69.3kg (4.02% difference).

In total, 93 scaling factors where defined, and almost the entire model is parametrized (except the part of the head-neck subsystem that was developed in MR1), fulfilling also one of the optional objectives defined at the beginning of this Master's Thesis. Moreover, the FAHM resulted in around 260.000 code lines, a 73% more than in the AHM (see Chapter 2), due mainly to the detailed cervical spine facet mesh implemented in Main Reference 1 (see Chapter 3).

Finally, Fig. 59 shows both, the AHM and the FAHM together, as part of Simcenter Madymo HBMs family.

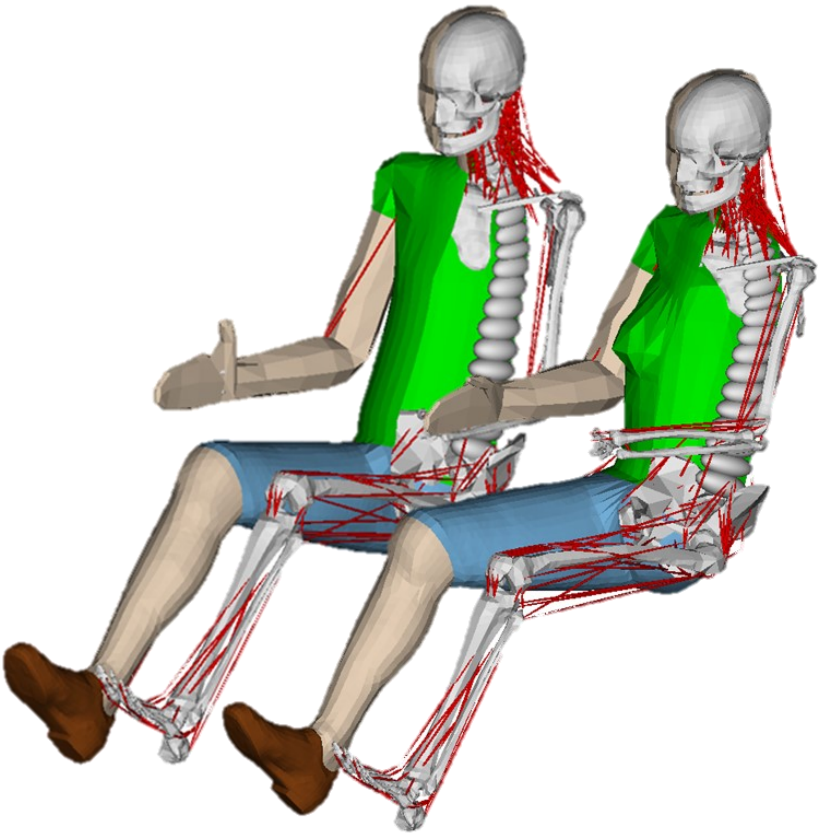

Fig. 59. AHM (left) and FAHM (right)

Chapter 5. FAHM VALIDATION

Once the development of the FAHM was completed, the next step was its validation. This Chapter describes how said validation process was performed, alongside with some considerations, assumptions, and limitations of it. Hence, the first subchapter, overview, offers a discussion on different approaches to MBD models validation, together with a selection of the most suitable one in the context of this study. After, in the second subchapter, a breakdown of the first part of the chosen validation approach is described. In it, the selected tests, together with their results and conclusions are presented. Finally, the third subchapter offers the second part of the validation process, alongside with their results and conclusions.

5.1 OVERVIEW

Validating a model, either a dummy or an HBM, FE or MBD, is to check whether said model behaves, within an established error margin, as the human group (in this case, 50th percentile females worldwide) it is representing would on average, both kinematically and dynamically. At this point, it is important to comprehend first some main considerations and challenges regarding human behaviour characterization in the context of biomechanics and vehicle occupant and pedestrian safety.

First, in order to predict how a human group would behave on average, the behaviour of members of said group has to be measured individually. To this end, volunteer tests or Post Mortem Human Subject (from now on PMHS) tests can be performed. Volunteer testing is often more focused on active response in zero-risk tests, and so, they can be very limited. On the other hand, PMHS testing allows to perform more severe scenarios (useful for injury criteria prediction for instance), but only passive response is measured (although some techniques have been developed to improve the biofidelity of these responses, such as filling the subject's lungs with air, or injecting pressurized blood through the circulatory system).

Ideally, both test types are needed to comprehend and characterize the biomechanics of a specific human group.

Second, the complete characterization of the behaviour of a single individual would imply performing tests in every possible scenario. This is challenging, as infinite tests would be needed. This problem is solved, with the introduction of the terms 'local characterization' and 'global characterization'. Local characterization focuses on different subsystems' response to external work, such as blunt impact tests. This way, precise characterization for each subsystem can be defined. On the other hand, global characterization focuses on specific common scenarios (sled and vehicle tests) and key responses of the whole system (such as seatbelt force, thoracic deflection, or head impact time).

Finally, response normalization is frequently performed for experimental data. Response normalization consists of the standardization of the biomechanical behaviour of the tests' subjects by scaling the different outputs according to their height or mass, among others. Said approach is used particularly when response characterization is studied (and not used when population variability is studied) and helps mitigating three main problems:

- A single individual (either subject or volunteer) can only be part of a very limited number of tests for diverse reasons.
- The optimal sample size for producing statistically significant results is typically high in comparison with the availability of PMHS and with the given resources. Consequently, sample sizes in experimental studies are commonly small, and the anthropometric variability of the subjects high. Thus, response normalization reduces the variability of the subjects and improves the statistical significance of results (even though height and mass are identical now, other elements such as age, sex, musculoskeletal development, or hidden medical conditions, are usually not normalized, therefore still accounting for said variability).
- Even if a high sample size could be achieved, the response corridors (that is the range in which all non-outlier responses fall in) would be significantly wide without normalizing the responses, and any chance of comparison with that study

could compromise biofidelity (in the case of response characterization). To illustrate this problem with an example, if non-normalized responses were used for the validation of a model, and that model happens to have identical anthropometric data as one of the subjects but different response values, but said response is still within the corridors made from all subjects, then, biofidelity might be compromised. However, reducing variability (and subsequently the range of the corridors) via response normalization helps mitigate this problem.

A further discussion on the response normalization method used in this Master's Thesis, is offered in the next subchapter.

Consequently, the validation of HBMs is reduced to replicating, in a software environment the boundary conditions of the selected input normalized data from global and local volunteer or PMHS tests, running the simulations, comparing the results, and if needed and possible, modifying (with coherence and physical sense) the definition of the HBM. This is an iterative process that can only end when the established objectives are met (and so, evidently, the definition of these objectives is key).

Regarding the selection of the input data for the developed FAHM, designing and performing experimental tests would be outside the scope of this study and its corresponding resources available. Therefore, said input data must be gathered in literature. Unfortunately, there is currently a very limited number of studies regarding female response that are compatible with Multi-Body Dynamic's nature (similar to the discussion on FAHM development from Chapter 4). Additionally, more general studies include both male subjects and female subjects, but usually only the response corridors built from all of the normalized responses are provided as data, so extracting the female data is not possible. Furthermore, in the first stage of the validation of the FAHM developed in this study, only PMHS local normalized input data should be considered:

- Volunteer data includes muscle activation which was not scaled or modified in the FAHM as it was outside the scope of this Master's Thesis as established in Chapter 1.

- Skipping local validation and performing global validation directly increases exponentially the number of variables in the system, and so, if the responses were outside corridors for a specific case, it would not be possible to adequately identify the causes of it. On the other hand, local validation reduces the number of variables, easing the identification of possible definition improvements.

Considering the aforementioned, the initial approach for FAHM validation was to study local PMHS tests, as explained throughout the next subchapter. After, the subchapter 5.3 offers a first step towards global validation. Nevertheless, further validation is still needed, as discussed throughout this Chapter, and as detailed in Chapter 7 (Future Work).

5.2 FAHM LOCAL VALIDATION

As abovementioned, the most adequate approach to an initial validation of the developed FAHM was against local PMHS tests. However, there are two elements to take into consideration:

- At this stage of the project, the response behaviour of the FAHM is unknown, both locally and globally. It is expected to be similar to that of the AHM but manifesting overall higher deformations and lower stiffness (proportional to how it was scaled). However, mistakes in the development process could produce uncoherent or even unstable responses, hindering the validation process.
- To the knowledge and resources of this study, there is no input data available regarding specific female response studies in local PMHS testing compatible with Multi-Body Dynamics (with the exception of the head-neck subsystem already performed in MR1).

Consequently, the validation process (and this subchapter) was divided into three sections:

1. Robustness check. The from now on 'standard AHM validation tests' (explained below) were performed for both the AHM and the FAHM. Then, their responses were compared, to check for coherent behaviour and stability. Experimental

corridors were also included, to add contextualization. Additionally, said corridors were normalized with the height and mass of the FAHM.

2. Benchmark. The from now on 'modified AHM validation tests' (see section 2 of this subchapter), were performed for both the FAHM and ViVA+ model. Models were then compared, to check for similarities and differences. Responses were normalized with the height and mass. A discussion on the implications, considerations, and limitations of the abovementioned is offered in its respective section.
3. Analysis. An analysis of the status of the FAHM regarding local validation after sections 1 and 2 was performed.

Standard AHM validation tests

Following the information described in Chapter 2, the AHM was validated against blunt and segment impact tests, sled and vehicle tests, and vibration tests. In the context of this subchapter, 'standard AHM validation tests' refers solely to the blunt and segment impact tests, as the rest correspond to global validation-oriented volunteer and PMHS tests. These were the tests selected for the robustness check, as the experimental data was already processed and normalized, and the corridors were already built (however, an additional normalization was needed, as mentioned above, as detailed in the first section of this subchapter).

The tests included blunt impacts on the most significant subsystems in biomechanical response regarding vehicle occupant and pedestrian safety: frontal impact on the head, lateral impact on the shoulder, frontal and lateral impacts on the thorax, frontal and lateral impacts on the abdomen, and lateral impact on the pelvis.

A summary table with the different tests is provided below, in Table 7, with information regarding the type of test, velocity and mass of the impactor, and its correspondent reference or references.

Moreover, a full explanation on the boundary conditions, or some considerations regarding initial model positioning among others, is offered in the first section of this subchapter.

Test	Velocity (m/s)	Impactor Mass (kg)	Reference
Frontal impact on head	2.0	23.4	[58]
	5.5	23.4	
Lateral impact on shoulder	4.5	23.4	[59]
	5.5	23.4	[60]
Frontal impact on thorax	3.4	23.4	[61]
	5.8	23.4	
	4.9	23.4	[62], [63] & [64]
	6.9	23.4	
	9.9	23.4	
	7.0	10.4	[65] & [66]
	9.9	22.2	
Lateral impact on thorax	3.3	23.4	[61]
	5.9	23.4	
Frontal impact on abdomen	6.9	31.4	[67]
	9.4	63.6	
Lateral impact on abdomen	4.43	N/A	[59]
	6.26	N/A	
Lateral impact on pelvis	3.46	23.4	[61]
	6.66	23.4	

Table 7. Standard AHM validation tests

Response normalization

Throughout this Chapter, three different normalized elements are referred:

1. PMHS data from standard AHM validation tests normalized to build-up response corridors (already processed data, not performed in this Master's Thesis).
2. A new normalization of the previous corridors to adapt them to the FAHM anthropometric distribution (height and mass). An explanation of the implications and limitations of this is offered in the next section.
3. A normalization of the ViVA+ responses for a coherent comparison against the FAHM (see section 2).

Several methods for impact response normalization are used in this field of study, although amongst the most common is the one from Mertz´s study from 1984 [56]. Additionally, this response normalization method is also present in the standard AHM validation tests, so it was considered by this Master's Thesis as the most adequate one.

Mertz observed in his study that PMHS lateral drop tests produced half sine waves on the thorax and pelvis's force-time responses. From there, the drop test was modelled as a simple spring-mass system, obtaining, after an analysis of the motion's differential equations, several normalizing factors and equations. These equations, applied to the second element from the above list, are:

$$Force\colon\ R_F = \frac{F_{FAHM}}{F_{AHM}} = \sqrt{R_m}\ * \sqrt{R_k}$$

$$Deformations\ and\ dislacements\colon\ R_x = \frac{x_{FAHM}}{x_{AHM}} = \frac{\sqrt{R_m}}{\sqrt{R_k}}$$

$$Time\colon\ R_t = \frac{t_{FAHM}}{t_{AHM}} = \frac{\sqrt{R_m}}{\sqrt{R_k}}$$

$$Velocity\colon\ R_v = \frac{v_{FAHM}}{v_{AHM}} = 1$$

$$Acceleration:\ R_a = \frac{a_{FAHM}}{a_{AHM}} = \frac{\sqrt{R_k}}{\sqrt{R_m}}$$

With:

$$R_k = C * L_c \ \rightarrow R_k = L_c = \frac{SH_{FAHM}}{SH_{AHM}}$$

Where k is stiffness, C is a proportional constant, L_c is a characteristic length, and SH is the seated height. C is neglected since it can be considered identical for all PMHS and HBM (is related to the material properties, which are assumed invariant for a same body part). The characteristic length is selected depending on the nature of the performed tests. In this case, all models and PMHS throughout this Chapter are seated, and hence, the seated height was chosen as the characteristic length.

And with:

$$R_m = \frac{m_{FAHM}}{m_{AHM}}$$

Where m is the mass of the model or subject.

These normalizing factors were created from a specific drop test that showed sine-type responses and does not consider sex or age. Therefore, its general applicability to impact response scaling, although widely used in literature, should be seen as an approximation. In particular in this Master's Thesis, sex could be determinant in the normalization process, emphasizing the fact that these new corridors or normalized responses are more an estimation than accurate curves. Further discussion on this topic is offered on the next sections.

5.2.1 AHM COMPARISON ANALYSIS I

As aforementioned, in this subchapter the standard validation tests were performed, comparing the AHM response with that of the FAHM, to check for robustness and numerical and biomechanical stability. The structure of this section is divided in two parts. First, the

boundary conditions for the standard validation tests, together with the equilibrium (also called positioning) simulations are described. After, the results are presented and discussed.

Boundary conditions and initial positioning

These virtual tests were defined for the AHM previous to this Master's Thesis, and so, they were considered as optimal regarding the replication of boundary conditions from their respective experimental tests without any further analysis needed. Said tests were adapted to the FAHM, modifying the initial positioning of the impactor and inertial plane (the latter for initial equilibrium, as explained below). The initial position of the impactor was modified to match the impact area (joint alignment) from the AHM setups.

Nevertheless, it is essential to analyse the implications on biomechanical response of said conditions for each test. Fig. 60 to Fig. 63 show the different configurations for each impactor test, although in all cases (except for the lateral impact on abdomen), the model is seated on an inertial plane with a contact definition. This translates to the kinematic chain being reduced, and so the new first link is the pelvis, whereas the final link (or free end) is maintained as the head.

The kinematic chain definition is key in understanding anthropometric behaviour. Impacts on the final link of the chain can be mostly considered as independent, and so the definition of the subsystem in this part usually does not affect the response of the rest of elements. However, an impact on the following links is each time less independent than the one before, as the previous links are affected by it. Hence, the definition of subsystem from proximal links usually influences the behaviour of the subsystems from more distal links.

Additionally, all tests have the standard gravity field defined, to mimic the boundary conditions of the experimental tests. The possibility for neglecting this additional load on the model's response is analysed in the next section.

Fig. 60 shows the configuration for frontal impact on the head and one of the two tests for lateral impact on the shoulder. The other lateral impact on shoulder test configuration is shown in Fig. 61, and a notable difference in the arms' positioning can be appreciated. Said

difference could produce a modification in the model response, not only because of inertia-related effects but also because of the contact area's geometry, even though the impact velocity of the tests is similar (4.5 and 5.5 m/s respectively).

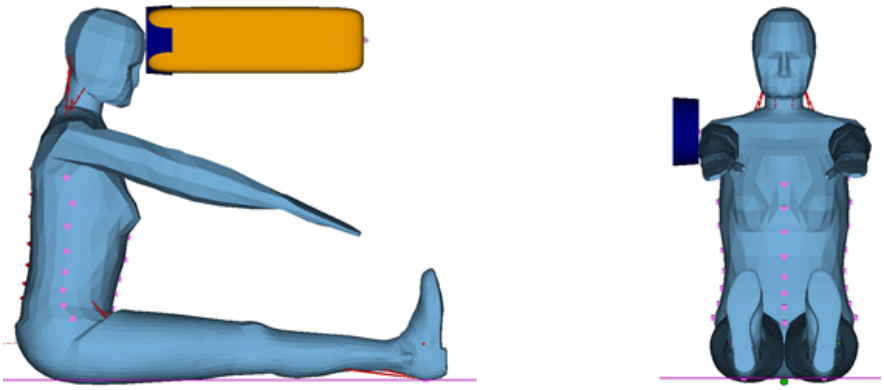

Fig. 60. Standard validation tests. Frontal impact on head and lateral impact on shoulder 1

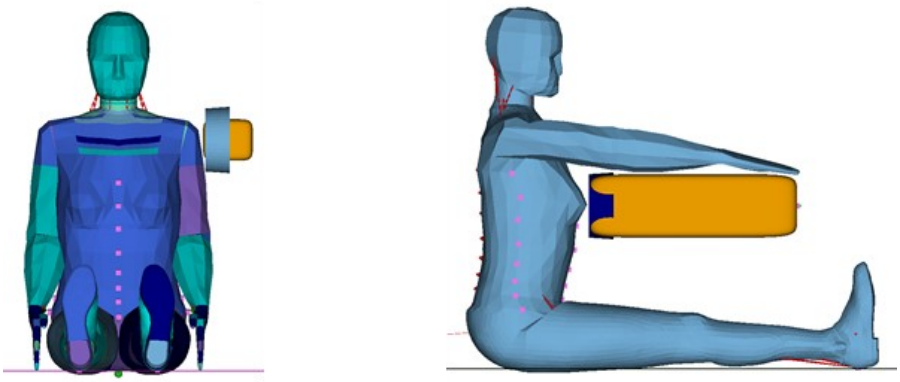

Fig. 61. Standard validation tests. Lateral impact on shoulder 2 and frontal impact on thorax

Fig. 61 also shows the configuration of the frontal impact on thorax, which is identical for the three different studies (see Table 7), and only the impactor's velocity and mass are varied, allowing for a comparison in the thorax behaviour for the different tests.

Fig. 62 offers the boundary conditions for the lateral impact on thorax tests and the frontal impact on abdomen tests. The lateral impact on abdomen tests' boundary conditions are considerably extreme, with impactors ranging from 31.4 to 63.6 kg and initial velocities ranging from 6.9 to 9.4 m/s; and so biomechanical stability issues are frequent in these type of conditions.

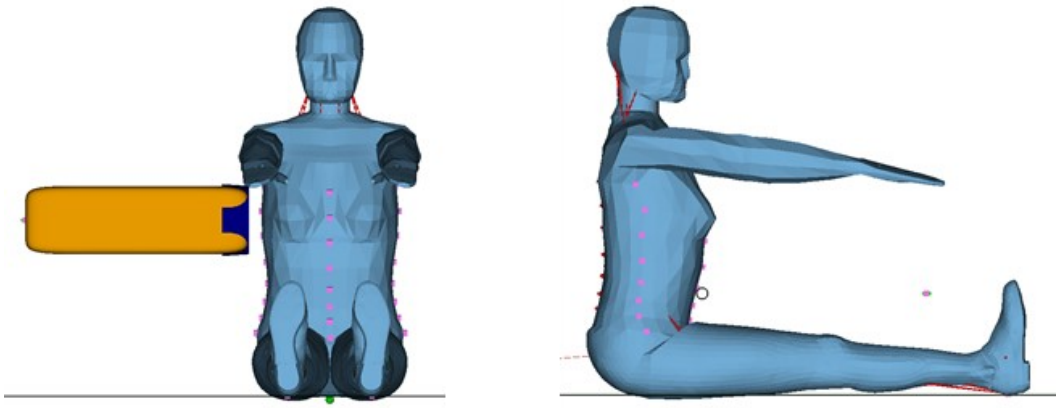

Fig. 62. Standard validation tests. Lateral impact on thorax and frontal impact on abdomen

Fig. 63 shows the boundary conditions for the lateral impact on abdomen tests and for the lateral impact on pelvis tests. The lateral impact on abdomen tests are the only ones in these standard validation tests where the impactor is fixed in space, and so the initial velocity is applied to the model, as the corresponding experimental test was a drop test (in fact, the gravity field in Madymo environment was in this case defined parallel to the model's initial displacement).

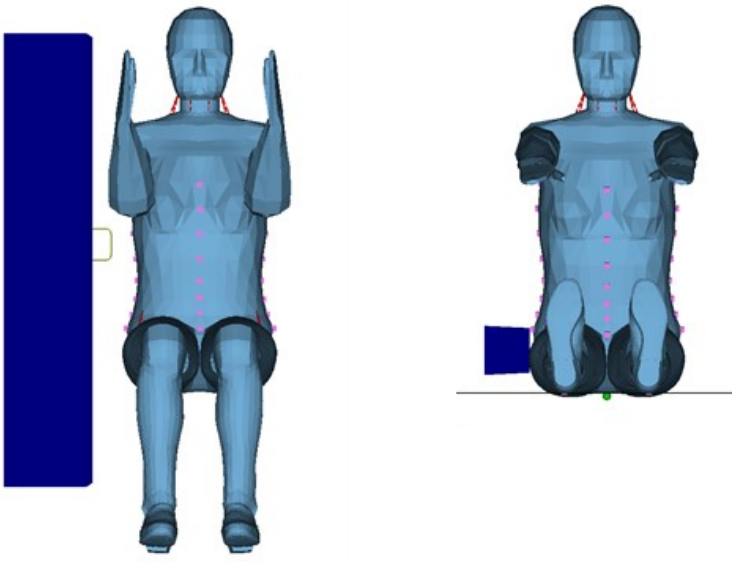

Fig. 63. Standard validation tests. Lateral impact on abdomen and lateral impact on pelvis

As abovementioned, the tests were adapted to the FAHM by means of the modification of the positioning for the initial impactor to match that of the AHM boundary condition, and

with the same purpose, the initial positioning of the whole model (or equivalently the absolute position of the inertial plane) was modified via an equilibrium simulation. An equilibrium simulation seeks physical stability in the contact between the model and the inertial plane (and so this intermediate simulation was not needed in the case of the lateral impact on abdomen tests). In these simulations, all the joints in the FAHM were fixed, except for the H-point joint, origin of positioning of the model (as explained in Chapter 4), and the only load applied to the system is the gravity. When the model stabilizes, the simulation is stopped, and the penetration between the model and the inertial plane is marked as the equilibrium positioning of the model.

A final consideration to point out is simulation time in the standard validation tests. As presented throughout the next part of this section, the impactor force measured by its load cell is an output present in all said tests. Hence, the criteria selected (before this Master's Thesis) for end simulation time was in most cases the impactor force reaching stably the value zero.

Results

This part offers the main results obtained in all tests and compares the biomechanical behaviour of the AHM and FAHM, to check for robustness and numerical and mechanical stability. In all cases, red curves represent the AHM responses, whereas the blue curves represent the FAHM responses. Additionally, experimental corridors are showed in grey.

As previously explained, these corridors were also normalized to match the FAHM mass and height and are showed in the results with dashed lines. That is, AHM response should fall inside solid corridor lines, and FAHM inside dashed corridors lines. However, this latter statement needs further analysis since, for instance, sex is not considered in the normalization process (as abovementioned). A discussion on this topic is offered at the final section of this subchapter.

The normalization factors from the Mertz method for response normalization (as previously explained) used in this case are:

$$R_k = \frac{SH_{FAHM}}{SH_{AHM}} = \frac{0.8153}{0.8639} = 0.9437$$

$$R_m = \frac{m_{FAHM}}{m_{AHM}} = \frac{69.3303}{75.3307} = 0.9203$$

Frontal impact on head (Melvin)

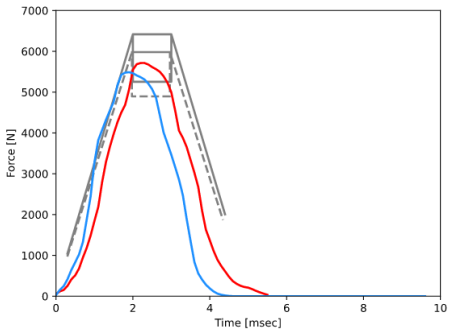

Fig. 64. Impactor force x-axis in test 2.0 m/s.

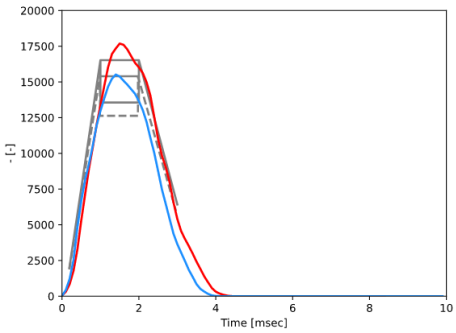

Fig. 65. Impactor force x-axis in test 5.5 m/s.

Fig. 64 and Fig. 65 show the response for the frontal impact on head at 2.0 and 5.5 m/s. The force values recorded by the load cell of the impactor in the FAHM simulations are, as expected, scaled from that of the AHM, mainly in the y values but also in the time values. FAHM force peak values (and overall, FAHM responses) are within corridors for both cases.

Lateral impact on shoulder (ISO, and Meyer)

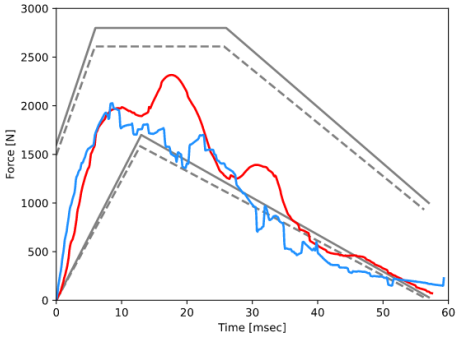

Fig. 66. Impactor force y-axis in test 4.5 m/s.

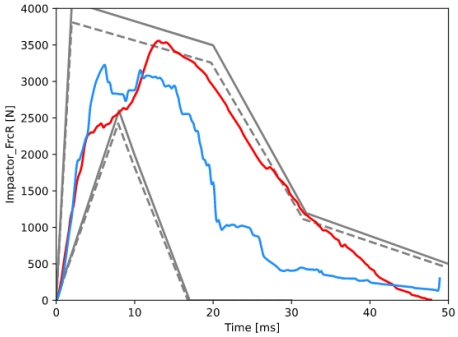

Fig. 67. Impactor force resultant in test 5.5 m/s.

Fig. 66 and Fig. 67 show the impactor forces for the lateral impact on shoulder tests. As aforementioned, both tests have different model positioning. In the first of the cases (Fig.

66) the arms were up, and so a higher instability was observed. However, said instability was considered within the established criteria. The peak force value (and overall, the whole response) for the FAHM was found inside corridors in both tests.

Frontal impact on thorax (Bouquet, Kroell, and Nahum)

Fig. 68 to Fig. 73 offer the results for the first frontal impact on thorax test, with 23.4 kg and 3.4 m/s. Similar to the previous tests, responses are scaled in both axis as expected. Additionally, in these tests, there are other outputs besides impactor force, such as thoracic deflection, impactor displacement or T1 and T12 displacements (all of them in the x-axis direction, which corresponds to the direction of the impactor).

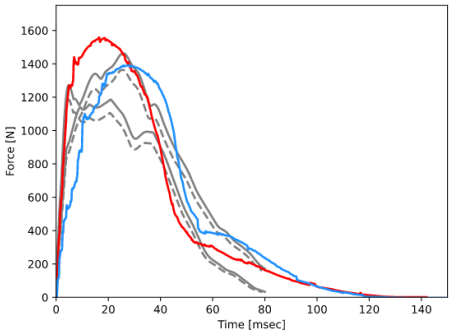

Fig. 68. Impactor force x-axis in test 3.4 m/s.

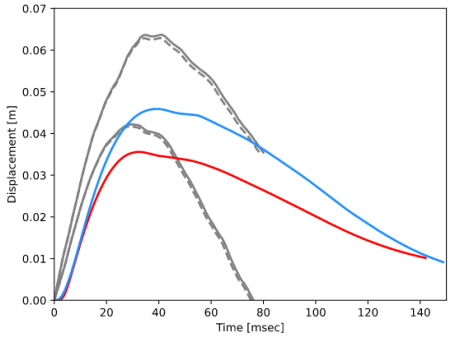

Fig. 69. Frontal thoracic deflection x-axis in test 3.4 m/s.

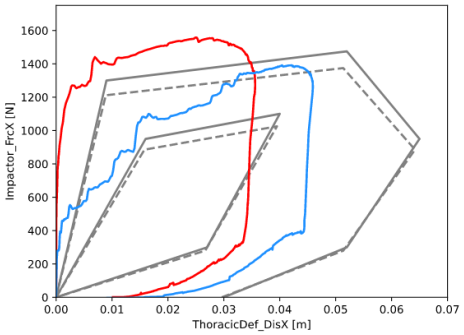

Fig. 70. Impactor force vs frontal thoracic deflection x-axis in test 3.4 m/s.

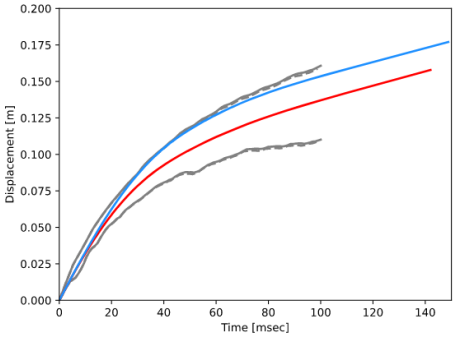

Fig. 71. Impactor displacement x-axis in test 3.4 m/s.

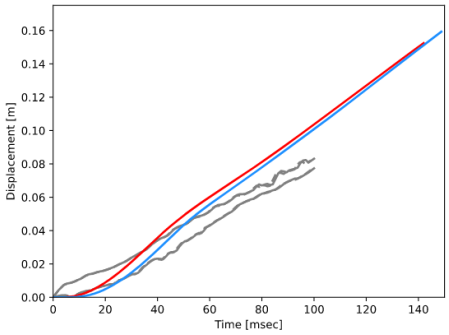

Fig. 72. T12 displacement x-axis in test 3.4 m/s.

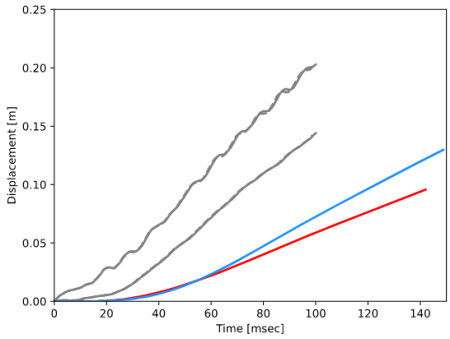

Fig. 73. T1 displacement x-axis in test 3.4 m/s.

In some cases, such as that of Fig. 69 and Fig. 70, the response even seems to have improved in the FAHM with respect to its corridors, although, these corridors should be considered, as explained before, as an approximation (and for this type of impacts, breast area definition could be significant for sex-related normalization). On the other hand, Fig. 72 and Fig. 73 show both models out of corridors. This illustrates what the FAHM development process followed implies, that it has the same characteristics as the AHM. A discussion on this topic is offered at the end of this subchapter.

Fig. 74 to Fig. 79 show the second of these frontal impact on thorax tests and corresponds to the 23.4 kg 5.8 m/s impactor. Similar to the previous case, some responses seem improved from the AHM, and others are out of corridors for both models. However, the difference between the male and female responses is smaller, which could be indicating a proportional relationship with velocity, an observation useful for the next section of this subchapter.

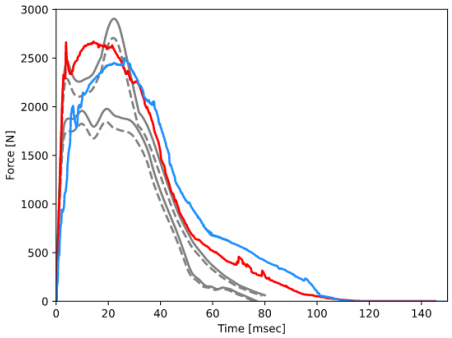

Fig. 74. Impactor force x-axis in test 5.8 m/s.

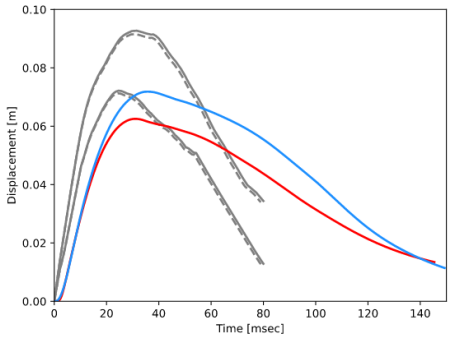

Fig. 75. Frontal thoracic deflection x-axis in test 5.8 m/s.

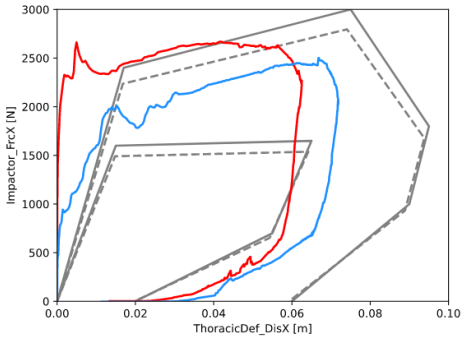

Fig. 76. Impactor force vs frontal thoracic deflection x-axis in test 5.8 m/s.

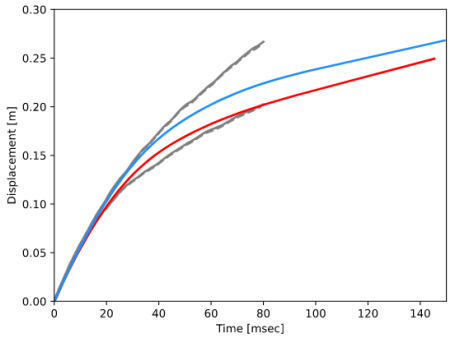

Fig. 77. Impactor displacement x-axis in test 5.8 m/s.

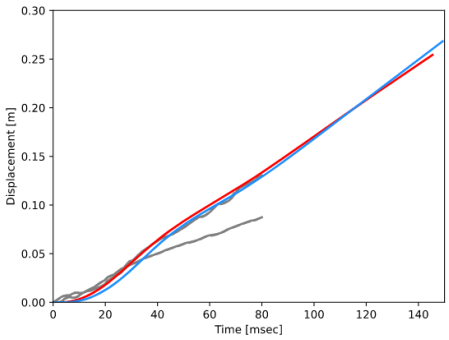

Fig. 78. T12 displacement x-axis in test 5.8 m/s.

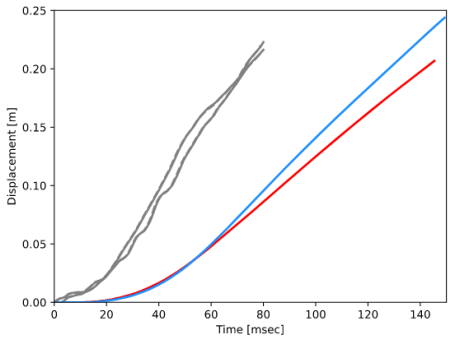

Fig. 79. T1 displacement x-axis in test 5.8 m/s.

Fig. 80 to Fig. 88 form part of a different study, with the same positioning and impactor mass as the previous one but performed at different impactor velocities.

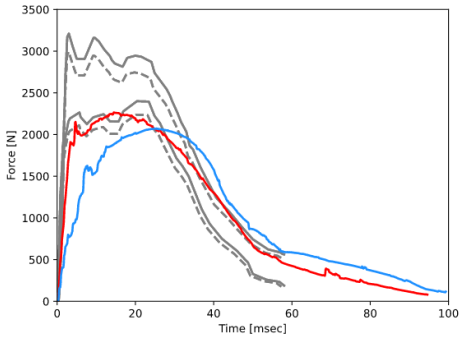

Fig. 80. Impactor force x-axis in test 4.9 m/s.

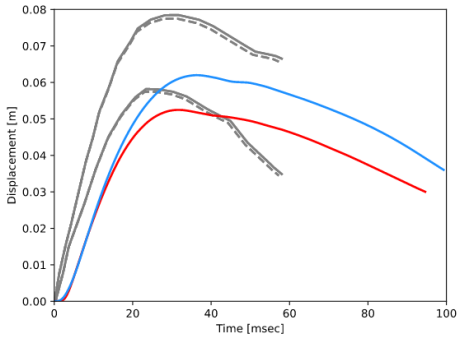

Fig. 81. Frontal thoracic deflection x-axis in test 4.9 m/s.

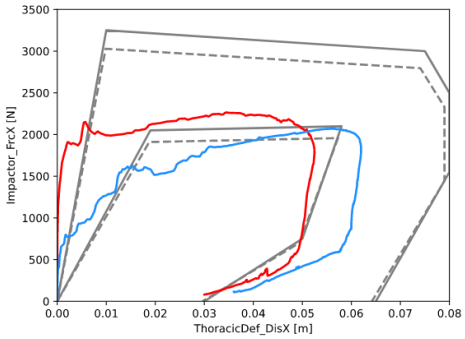

Fig. 82. Impactor force vs frontal thoracic deflection x-axis in test 4.9 m/s.

The conclusions from the previous tests can be applied also to these results, and even the difference between the male and female models' response serves as middle ground, endorsing the previous hypothesis formulated (the proportional relationship with velocity).

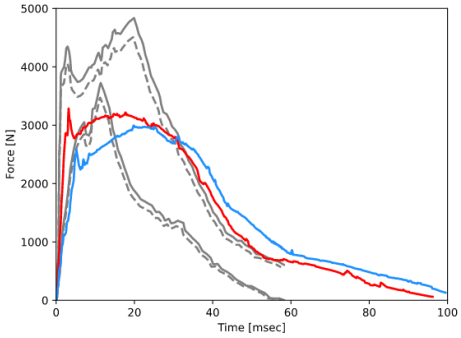

Fig. 83. Impactor force x-axis in test 6.9 m/s.

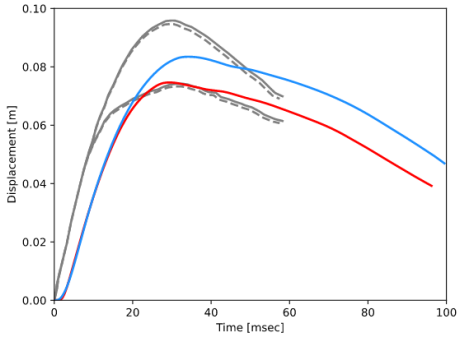

Fig. 84. Frontal thoracic deflection x-axis in test 6.9 m/s.

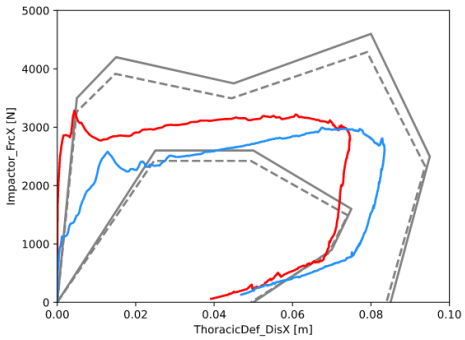

Fig. 85. Impactor force vs frontal thoracic deflection x-axis in test 6.9 m/s.

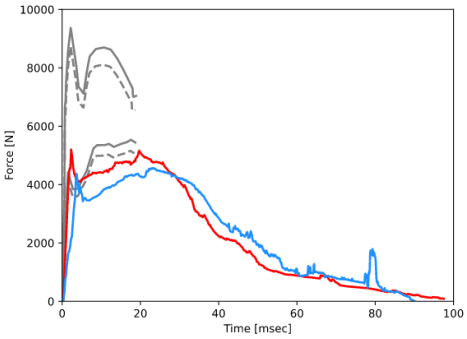

Fig. 86. Impactor force x-axis in test 9.9 m/s.

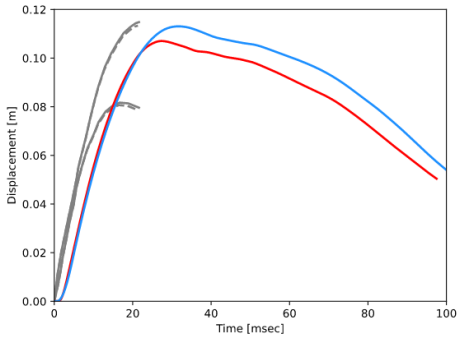

Fig. 87. Frontal thoracic deflection x-axis in test 9.9 m/s.

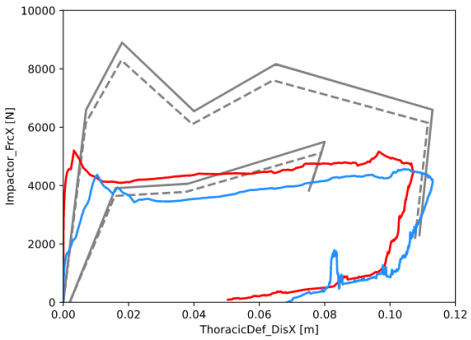

Fig. 88. Impactor force vs frontal thoracic deflection x-axis in test 9.9 m/s.

On this second study inside the frontal impact on thorax tests, the 9.9 m/s impactor velocity test shows a small instability in the unloading part. It was considered within the established criteria and attributed to a partial change in the material of the contact area.

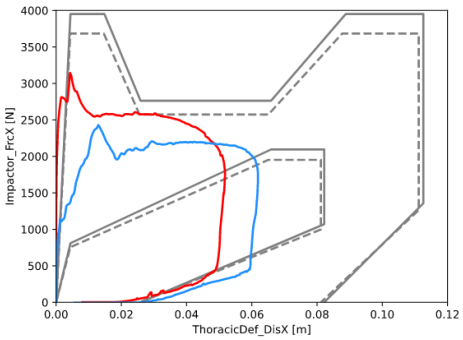

Fig. 89. Impactor force vs frontal thoracic deflection x-axis in test 7.0 m/s.

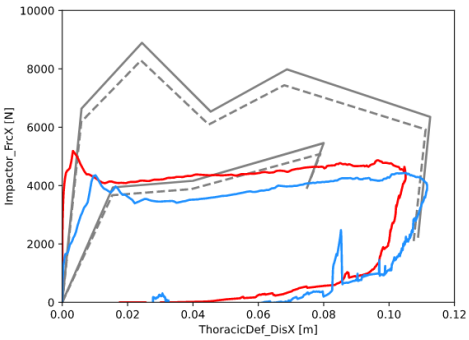

Fig. 90. Impactor force vs frontal thoracic deflection x-axis in test 9.9 m/s.

The last two tests (Fig. 89 and Fig. 90) form part of a third study regarding frontal impact on thorax tests. In these cases, different impactor masses are used (and not only different impactor velocities), and therefore their responses should not be compared with the previous tests. Similar to the last test of the previous study (the one with a higher velocity), Fig. 90 shows again the previously mentioned numerical instability. Hence, said instability seems to be only manifesting at higher velocities, where the partial change in the material of the contact area appears.

Lateral impact on thorax (Bouquet)

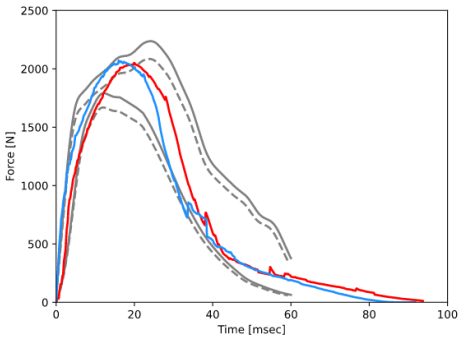

Fig. 91. Impactor force y-axis in test 3.3 m/s.

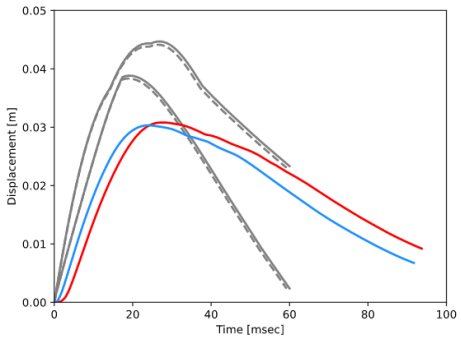

Fig. 92. Lateral thoracic deflection y-axis in test 3.3 m/s.

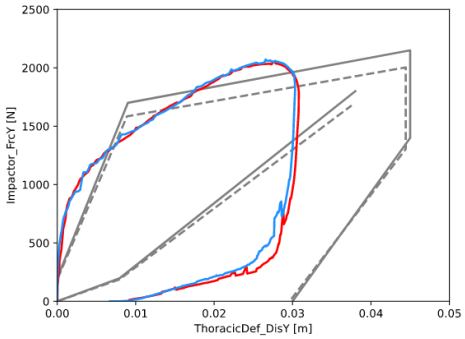

Fig. 93. Impactor force vs lateral thoracic deflection y-axis in test 3.3 m/s.

Fig. 91 to Fig. 93 offers the models' responses to the low velocity test from the lateral impact on thorax set. As shown in said figures, thoracic lateral responses are similar for both models. This is coherent to the FAHM development process followed, as lateral scaling factors were predominantly close to 1.

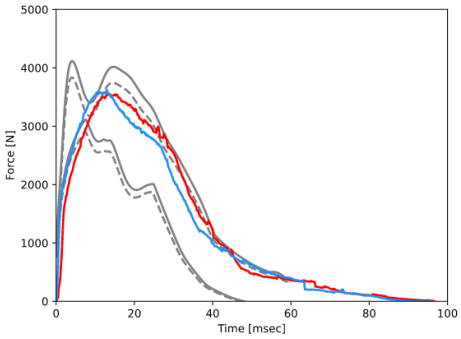

Fig. 94. Impactor force y-axis in test 5.9 m/s.

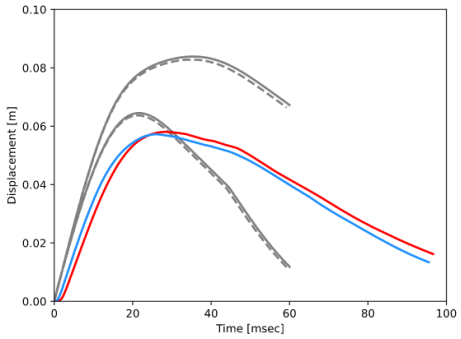

Fig. 95. Lateral thoracic deflection y-axis in test 5.9 m/s.

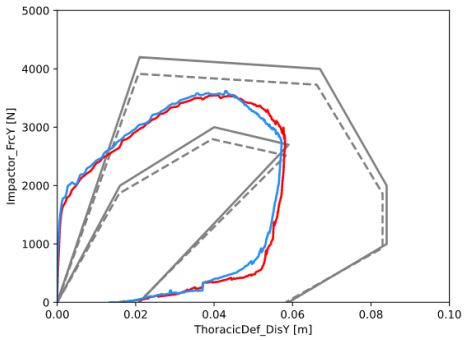

Fig. 96. Impactor force vs lateral thoracic deflection y-axis in test 5.9 m/s.

For the high velocity test of this set (Fig. 94 to Fig. 96), the behaviour is identical to that described in the previous test, although the difference between both models' response is smaller, which could be indicating a proportional relationship with velocity (as in the frontal impact on thorax tests).

Frontal impact on abdomen (Cavanaugh)

Fig. 97 to Fig. 100 show the results for the frontal impact on abdomen tests. As in the rest of the tests, the FAHM response is scaled from that of the AHM. In the case of the low velocity impact, the impactor force recorded against the female model was found outside corridors, whereas in the case of the high velocity impact, the output was found inside corridors. Moreover, no stability issues were found, despite the extreme nature of these tests (due to the mass and velocity of the impactors) as previously mentioned.

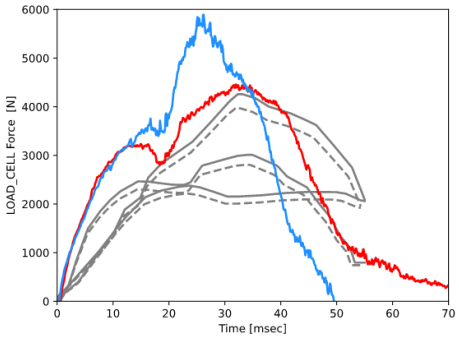

Fig. 97. Impactor force x-axis in test 6.9 m/s.

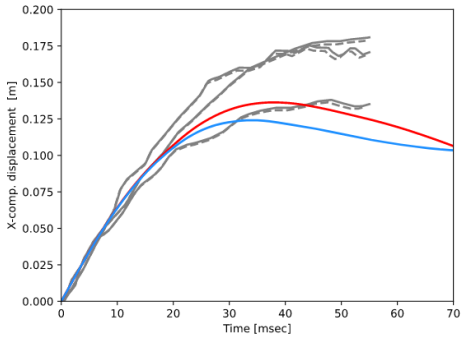

Fig. 98. Frontal abdominal deflection x-axis in test 6.9 m/s.

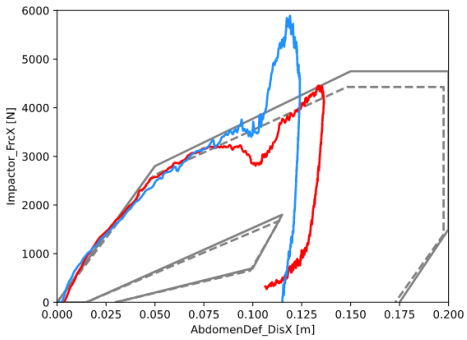

Fig. 99. Impactor force vs frontal abdominal deflection x-axis in test 6.9 m/s.

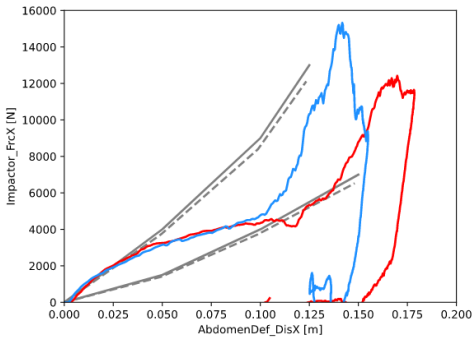

Fig. 100. Impactor force vs frontal abdominal deflection x-axis in test 9.4 m/s.

Lateral impact on abdomen (ISO)

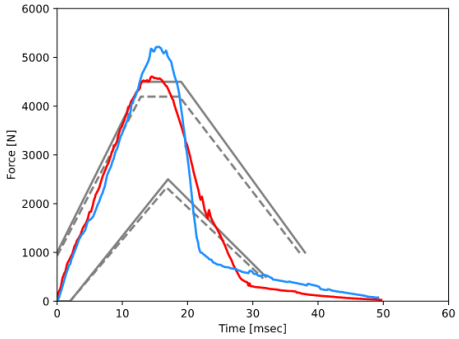

Fig. 101. Impactor force y-axis in test 4.43 m/s.

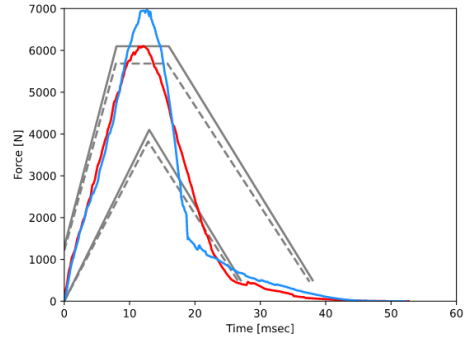

Fig. 102. Impactor force y-axis in test 6.26 m/s

Female peak impactor force value was found over the normalized corridors for the lateral impact on abdomen tests, as shown in Fig. 101 and Fig. 102. Thus, abdomen response seems overall stiffer and less deformable relative to both, the AHM and the PMHS corridors.

Lateral impact on pelvis (Bouquet)

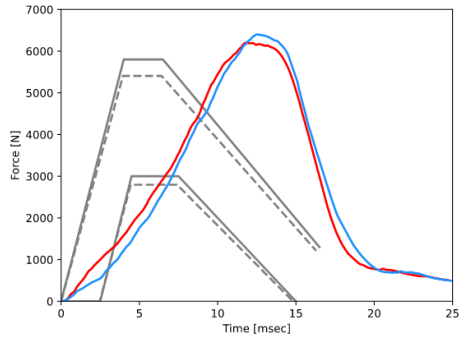

Fig. 103. Impactor force y-axis in test 3.46 m/s.

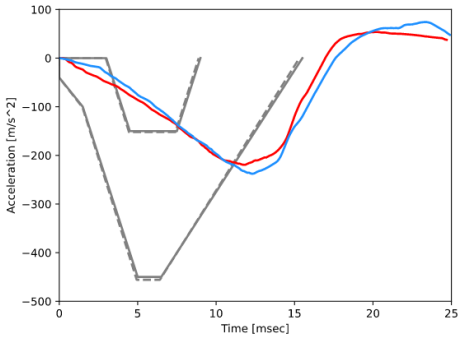

Fig. 104. Sacrum acceleration y-axis test 3.46 m/s

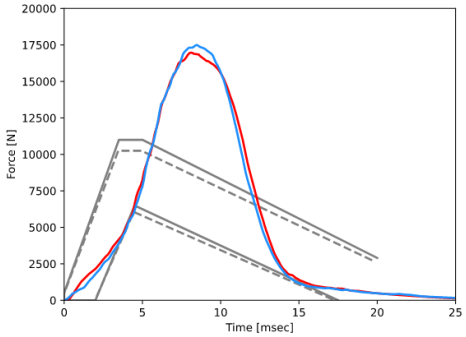

Fig. 105. Impactor force y-axis in test 6.66 m/s.

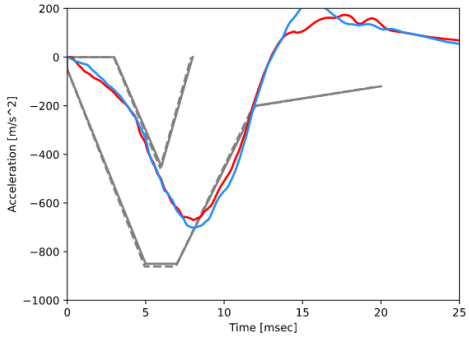

Fig. 106. Sacrum acceleration y-axis test 6.66 m/s

Fig. 103 to Fig. 106 offer the responses for the lateral impact on pelvis test set, with impact velocities of 3.46 and 6.66 m/s. Both male and female responses are almost identical, aligning with the conclusion drawn in the lateral impact on thorax test, which is that overall (with the exception of the lateral abdomen), the lateral behaviour of the FAHM is similar to that of the AHM, as lateral scaling factors were predominantly close to 1.

On the other hand, the kinematic behaviour of the FAHM in the tests of this section is overall scaled from the AHM, confirming that the FAHM has a biomechanical response proportional to that of the AHM, and so, that the FAHM development process was performed adequately.

5.2.2 ViVA+ Model Comparison Analysis

As aforementioned, in this subchapter the modified validation tests were performed, comparing the ViVA+ response with that of the FAHM, to analyse similarities and differences between their biomechanical behaviour. The structure of this section is divided into two parts. First, the boundary conditions for the modified validation tests, together with the positioning simulations are described. After, the results are presented and discussed.

As described in Chapter 3, the ViVA+ model v0.3.2 is a female 50th percentile FE model that currently has only been validated at a local level for the neck subsystem and at a global level. The local validation for the rest of subsystems is being carried out at the same time as this Master´s Thesis, and so, unfortunately, a newer model that includes possible improvements is not available yet.

Consequently, from the comparisons presented in this subchapter, no conclusions can be drawn with respect to model validation. The aim of this subchapter is to point out the similarities and differences between the behaviour of both models, so that future work on this model can focus initially on specific characteristics that need revision.

To be able to compare adequately the response of both, the ViVA+ model and the FAHM, several elements should be considered:

1. Both models have a similar anthropometric distribution.
2. The responses have been normalized.
3. The positioning of both models is identical for all tests.
4. The simulation environment is the same, or sufficient actions to reduce unknown variables associated with different simulation environments have been made.
5. The boundary conditions of the tests for both models are not only identical, but also equivalent (see next section).

Points 1 and 3 to 5 are explained in the first section, whereas point 2 is described in the second section.

Boundary conditions and initial positioning

The ViVA+ model, as already explained, is an FE HBM. These models have usually a specific method for positioning, that involves pre-simulations, as all the different elements of said model have to deform in order to achieve the new position desired. There is currently only one method for doing this positioning in the ViVA+ model, which involves using a specific software called PIPER (software focused on FE model scaling and positioning). On the other hand, HBMs in Simcenter Madymo can be positioned directly using the specific built-in tool, although a small pre-simulation is still needed for stability reasons (see explanation below).

As seen in the standard validation tests, each test required a different model positioning. Pre-simulations for positioning FE models are complex, computationally expensive, and resource consuming, and are not part of the scope of this Master´s Thesis. For this reason, the modified validation tests were designed.

These modified tests maintain the main characteristics and key elements of the standard validation tests but allowed to almost keep the original occupant positioning of the ViVA+ model in all tests (the model was rotated 15 degrees clockwise using LSTC LS-PrePost software to mimic as much as possible the boundary conditions of the standard validation tests without the need of performing FE-positioning pre-simulations).

However, the ViVA+ model's original occupant positioning was not identical to that of the FAHM, and so a small pre-simulation of the FAHM in Simcenter Madymo environment was still needed (much less resource consuming than positioning the ViVA+ model). The positioning pre-simulation of the FAHM was performed in a user-defined seat (a seat specifically built to force the FAHM to match the ViVA+ model positioning). Additionally, neck and spine active behaviour were set to on, and all flexible bodies were set to rigid (evidently, these elements were set back to default for the validation tests). After, the model reached an equilibrium state under a gravity load in said pre-simulation. Finally, the joint positioning was exported, alongside with the final values of the controllers (at the time step were the model reached the equilibrium). This process replicates the initial positioning of

PMHS for experimental testing (the active behaviour and the rigidification of flexible bodies can be considered equivalent to external forces, and in both cases, they are taken out just when the experimental or virtual test starts).

Fig. 107 shows a comparison between the initial positioning of both models, after the FAHM pre-simulation (blue is FAHM and green is ViVA+ model). This allows to analyse points 1 and 3 from the previous list (identical positioning and similar anthropometric distribution). The positioning is in fact identical for both models in all tests (the modified validation tests do not change model positioning from one test to another as previously explained). Moreover, the anthropometrical distribution of the FAHM and the ViVA+ model is very similar, although more adipose tissue in present in the lower back and buttocks of the ViVA+ model, and the FAHM has a slightly longer upper leg.

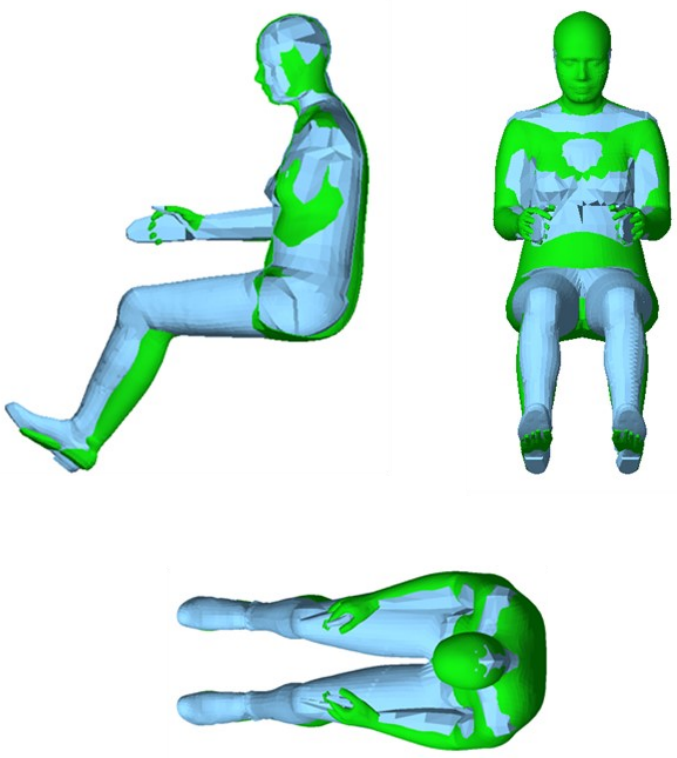

Fig. 107. ViVA+ vs FAHM positioning. Frontal, side (cut) and top view

A comparison between the standard validation tests and the modified validation tests is offered in Fig. 108 to Fig. 115. The system configuration shown in these figures is identical for the ViVA+ model.

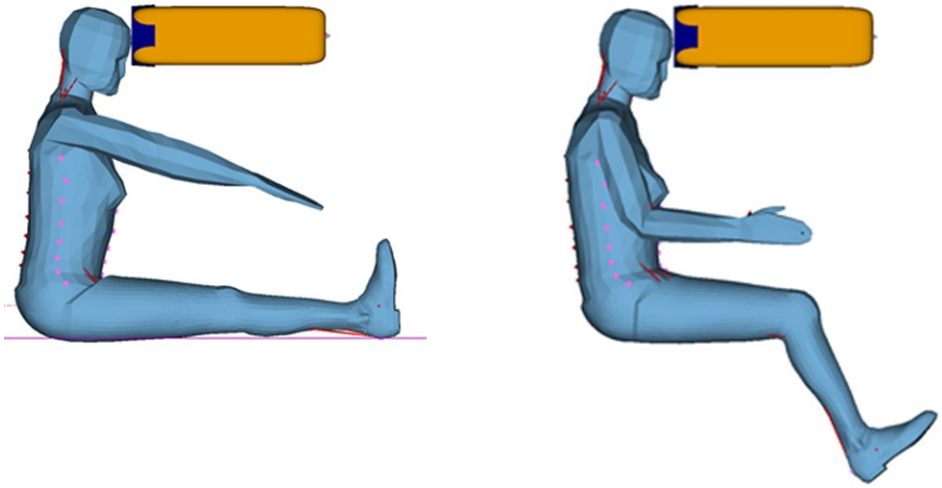

Fig. 108. Standard vs modified validation tests. Frontal impact on head

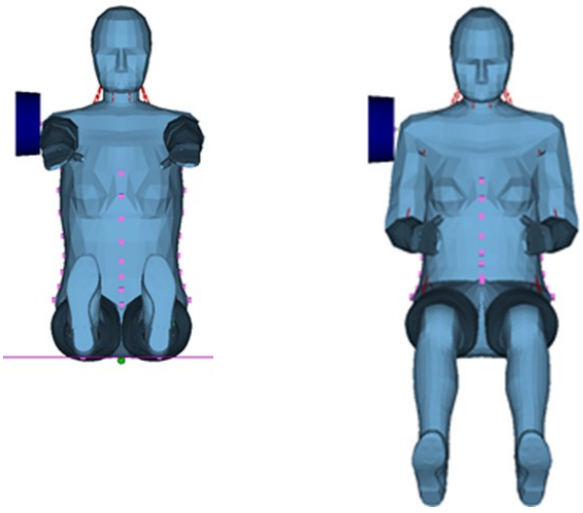

Fig. 109. Standard vs modified validation tests. Lateral impact on shoulder 1

As explained in Chapters 2 and 3, the ViVA+ model was simulated via coupled simulations of LS-Dyna with Simcenter Madymo in mpp configuration. Hence, the internal biomechanics of the model are calculated by LS-Dyna and the rest of interactions, including the contacts between the model and the Madymo environment are handled by Madymo (with an exchange of information between each tool).

Following the statement made in point 4, unknown variables associated with different simulation environments should be minimized. For this reason, the number of interactions between each tool was reduced to the minimum, by removing the gravity and the inertial

plane from most of the tests. This is the case for the frontal impact on head tests (Fig. 108), lateral impact on shoulder tests (both versions, Fig. 109 and Fig. 110), frontal and lateral impacts on thorax tests (Fig. 111 and Fig. 112) and lateral impact on abdomen tests (Fig. 114). Exceptions to this are explained below.

Additionally, the arms were removed from the contact definition between the impactor and the model, for the lateral impact on thorax tests (Fig. 112), and frontal and lateral impacts on abdomen tests (Fig. 113 and Fig. 114), to preserve the purpose of said tests (the arm were not completely removed, so that they could still have an effect on the models' responses).

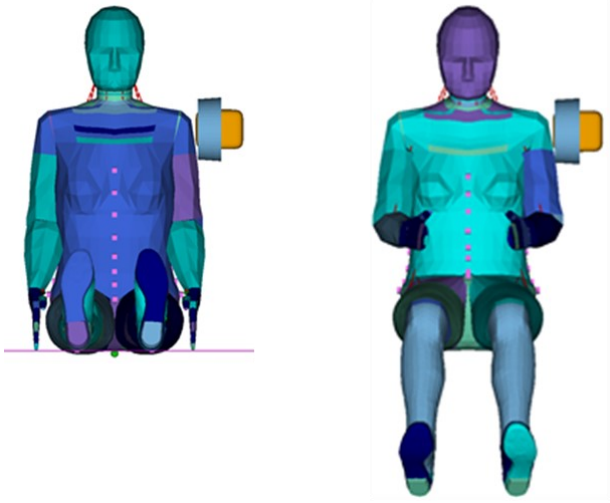

Fig. 110. Standard vs modified validation tests. Lateral impact on shoulder 2

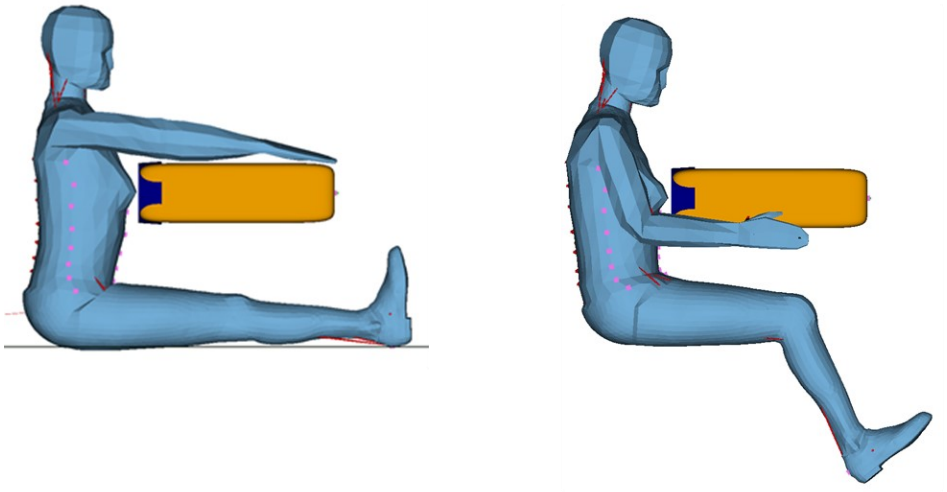

Fig. 111. Standard vs modified validation tests. Frontal impact on thorax

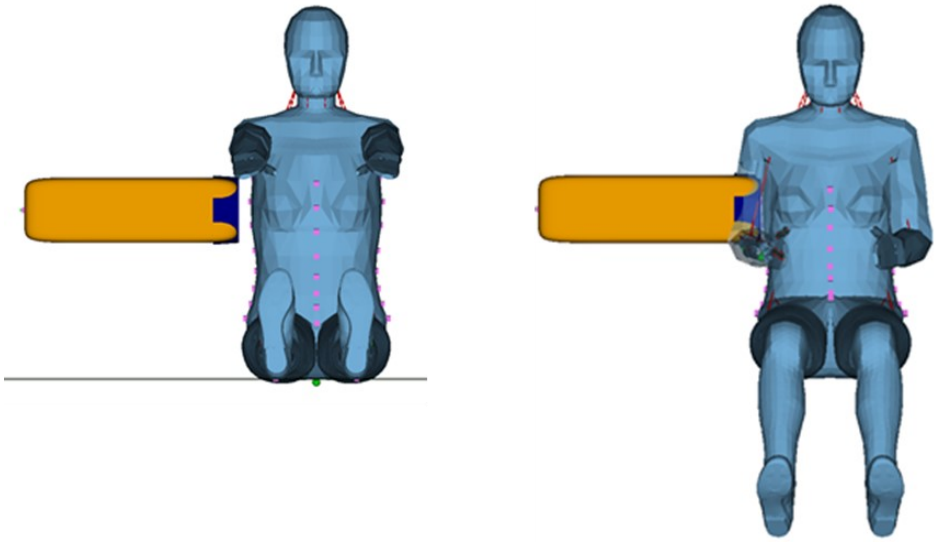

Fig. 112. Standard vs modified validation tests. Lateral impact on thorax

However, the inertial plane was kept (for both, the FAHM and ViVA+ model) for the frontal impact on abdomen tests (Fig. 113) and lateral impact on pelvis tests (Fig. 115). In both cases, the impactor is close to where the inertial plane is, and even though some intermediate simulations confirmed that the response was not significantly different for the FAHM, they were significant for the ViVA+ model regarding adipose tissue deformation (thus, not aligning with point 5 if the inertial planes were removed). On the other hand, the gravity was still removed, as no significant differences were observed in either of the models.

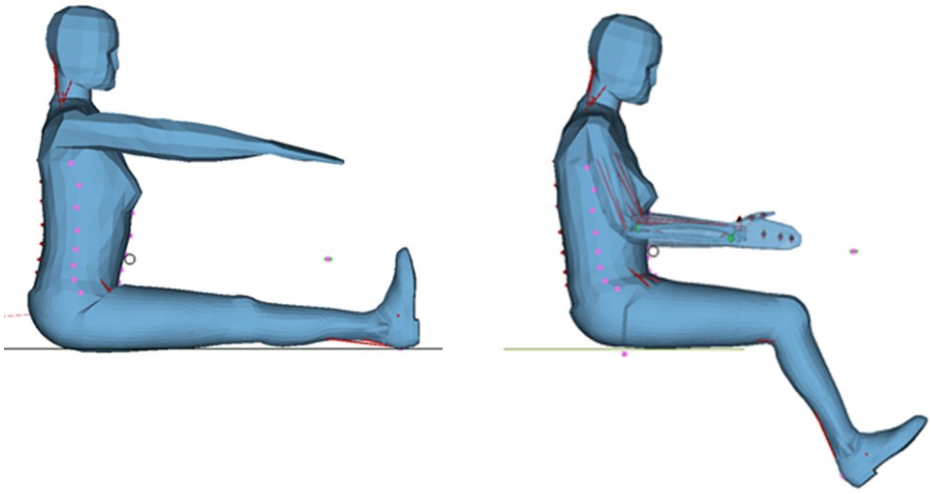

Fig. 113. Standard vs modified validation tests. Frontal impact on abdomen

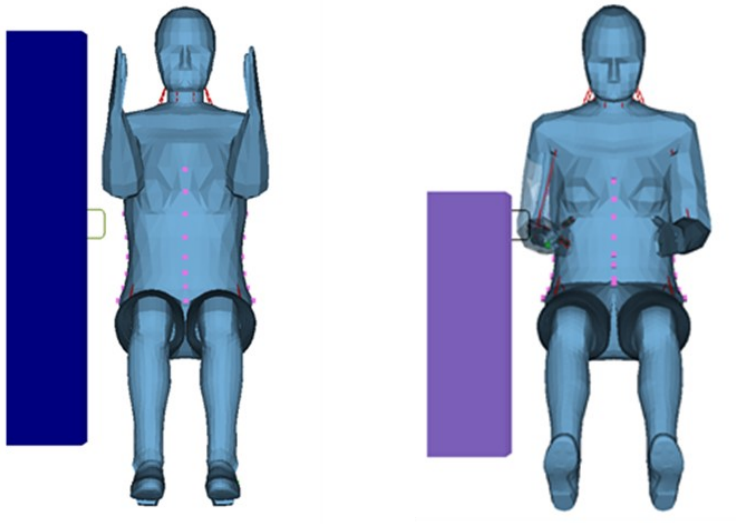

Fig. 114. Standard vs modified validation tests. Lateral impact on abdomen

In addition, the geometry of the rigid wall (not the impactor itself) from the drop-tests (lateral impact on abdomen tests, Fig. 114) was modified, to account for point 5. A difference in definition for where the arm starts for both models, made the boundary conditions identical but not equivalent, as an extra contact appeared at a certain point in the simulation for one of the models. The new geometry of the rigid wall behind the abdominal impactor prevents this issue.

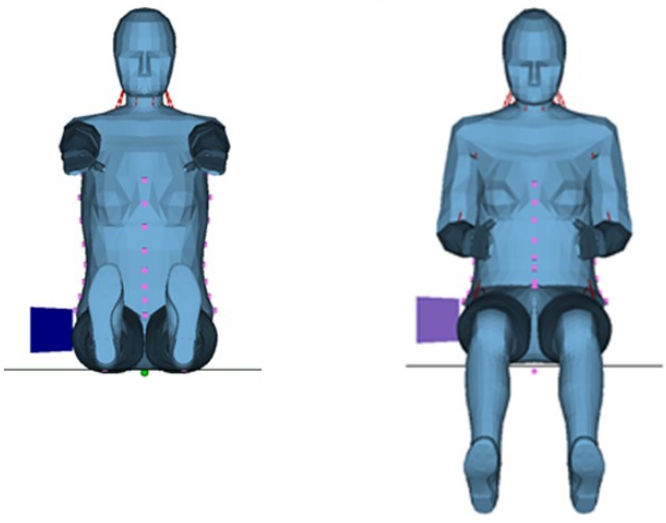

Fig. 115. Standard vs modified validation tests. Lateral impact on pelvis

Lastly, a disadvantage of these modified validation tests is that the corridors from the standard validation tests cannot be used here. Nevertheless, and as explained before, the purpose of the female corridors (that is, the normalized corridors) was of an approximation, rather than accurate curves. A further discussion of this topic is offered at the end of this subchapter.

Results

This part offers the main results obtained in all modified tests and compares the biomechanical behaviour of the FAHM and ViVA+ model, to analyse similarities and differences in dynamic and kinematic responses. In all cases, green curves represent the ViVA+ model responses, whereas the blue curves represent the FAHM responses. In addition, for the most relevant cases, 3 animation frames for both models are offered (per test) to compare their kinematic behaviours. The time-step of these frames has been defined as: peak force time, halfway through the simulation, and last time-step of the simulation.

As previously explained, these ViVA+ model responses were normalized to match the FAHM mass and seated height, in order to allow for an adequate comparison between them (point 2). The standing height of the ViVA+ model is 1.59 (against 1.63 from the FAHM, just a 2.5% difference, and so, aligned with point 1), and the normalization factors from the Mertz method for response normalization (as previously explained) used in this case are:

$$R_k = \frac{SH_{FAHM}}{SH_{ViVA+}} = \frac{0.830}{0.836} = 0.993$$

$$R_m = \frac{m_{FAHM}}{m_{ViVA+}} = \frac{69.3}{62.7} = 1.105$$

Seated height for both models is almost identical, but the FAHM is 6.6kg heavier than the ViVA+ model, emphasizing the need for this normalization for an adequate response comparison between both models.

Before the comparison between the FAHM and the ViVA+ model was analysed in the modified validation tests, these tests were simulated using the AHM, to check for possible

stability problems in the environment definition or other problems, and to analyse whether the responses were significantly different from the standard validation tests. In most cases the responses were fairly similar, or at least in the same order of magnitude. The most significant difference (but still in the same order of magnitude) was found in the frontal impact on abdomen tests, with higher peak force values and deformations. No instabilities or other problems were found in any of the tests.

Frontal impact on head (Melvin)

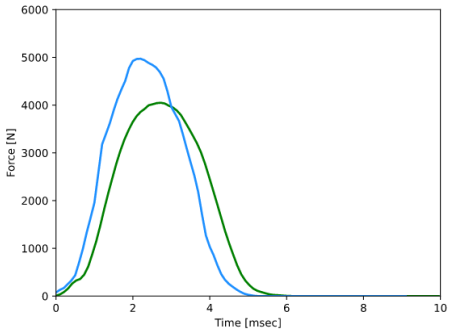

Fig. 116. Impactor force x-axis in test 2.0 m/s.

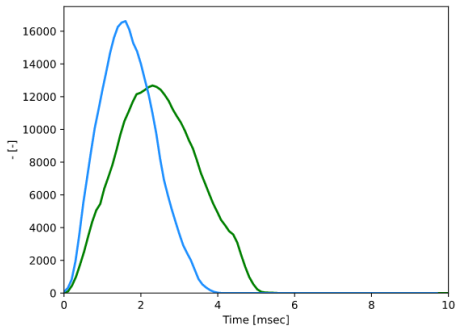

Fig. 117. Impactor force x-axis in test 5.5 m/s.

Fig. 116 and Fig. 117 show a similar response shape for both models, although the FAHM has a stiffer behaviour. Kinematic wise, the simulation time is considerably short to allow for a proper kinematic development, although up to the 10 ms both models behave identically.

Lateral impact on shoulder (ISO, and Meyer)

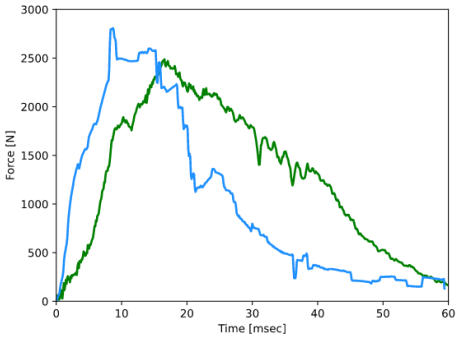

Fig. 118. Impactor force y-axis in test 4.5 m/s.

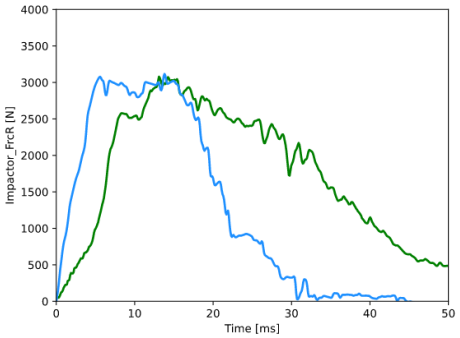

Fig. 119. Impactor force resultant in test 5.5 m/s.

Fig. 118 and Fig. 119 offer the impactor force vs time signal for the lateral impact on shoulder tests. Peak force value for both responses are significantly similar, although the shape of the response varies, indicating a stiffer contact behaviour for the FAHM.

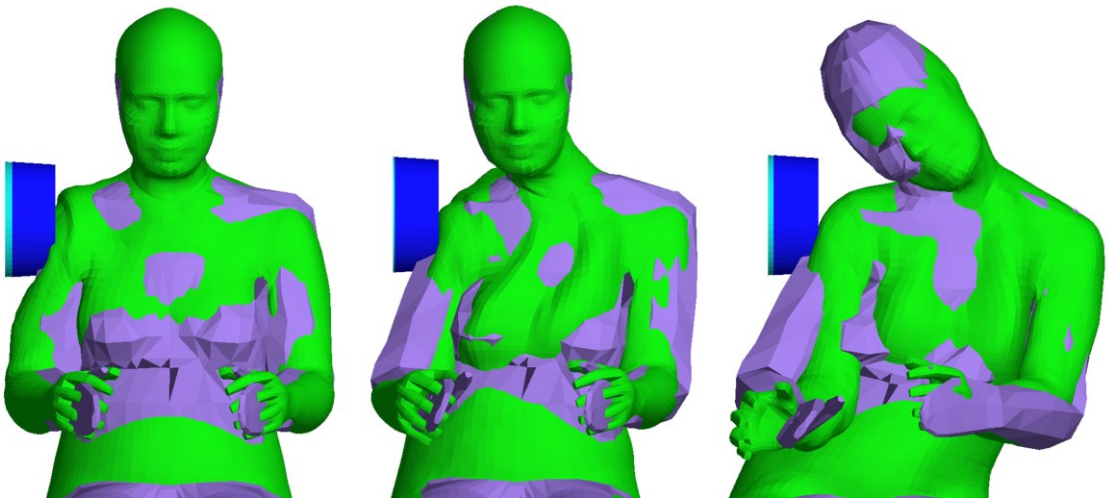

Fig. 120. Kinematics comparison in test 4.5 m/s

In terms of kinematics, Fig. 120 shows an identical response up to halfway thought the simulation, that is, 25 ms. From there, the ViVA+ has a higher displacement field, contributing to the previous hypothesis that the FAHM has a stiffer behaviour in this set of tests.

Frontal impact on thorax (Bouquet, Kroell, and Nahum)

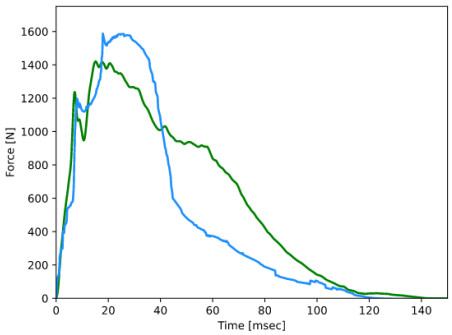

Fig. 121. Impactor force x-axis in test 3.4 m/s.

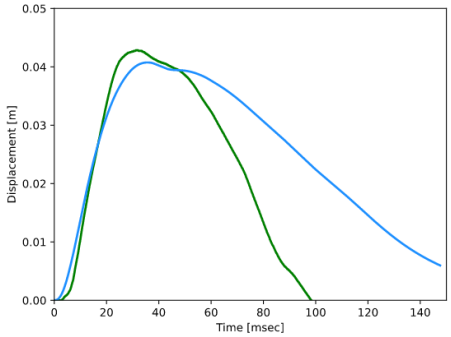

Fig. 122. Frontal thoracic deflection x-axis in test 3.4 m/s.

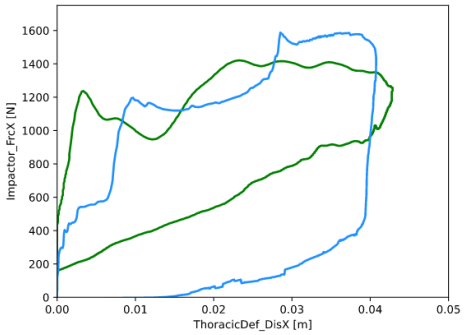

Fig. 123. Impactor force vs frontal thoracic deflection x-axis in test 3.4 m/s.

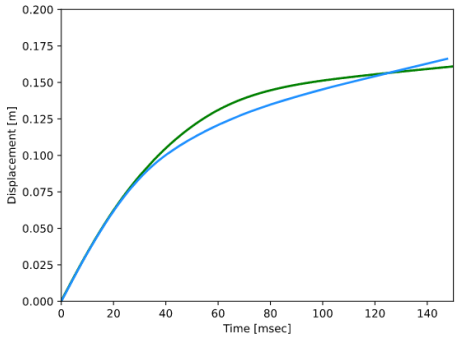

Fig. 124. Impactor displacement x-axis in test 3.4 m/s.

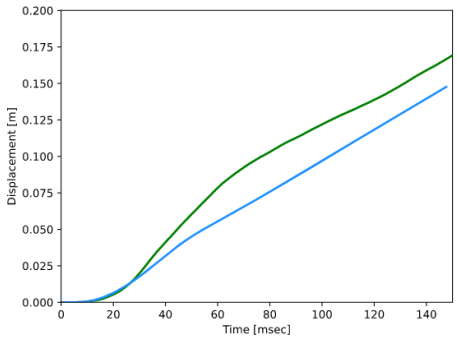

Fig. 125. T12 displacement x-axis in test 3.4 m/s.

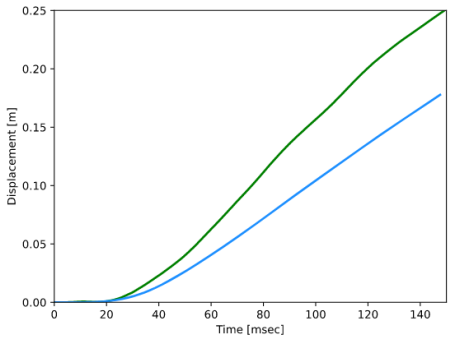

Fig. 126. T1 displacement x-axis in test 3.4 m/s.

Fig. 121 to Fig. 126 offer the results for the first of the frontal impact on thorax tests (also from the first out of three studies in this type of impact). Impactor force and displacement have very similar curves for both models.

On the other hand, T12 and T1 displacement indicates a different kinematic behaviour (although still in the same order of magnitude). The animation of Fig. 127 confirms this statement, showing a different kinematic development from slightly before the 75 ms. Both sources of information suggest a stiffer response of the FAHM.

Additionally, ribcage recovery is considerably faster in the ViVA+ model.

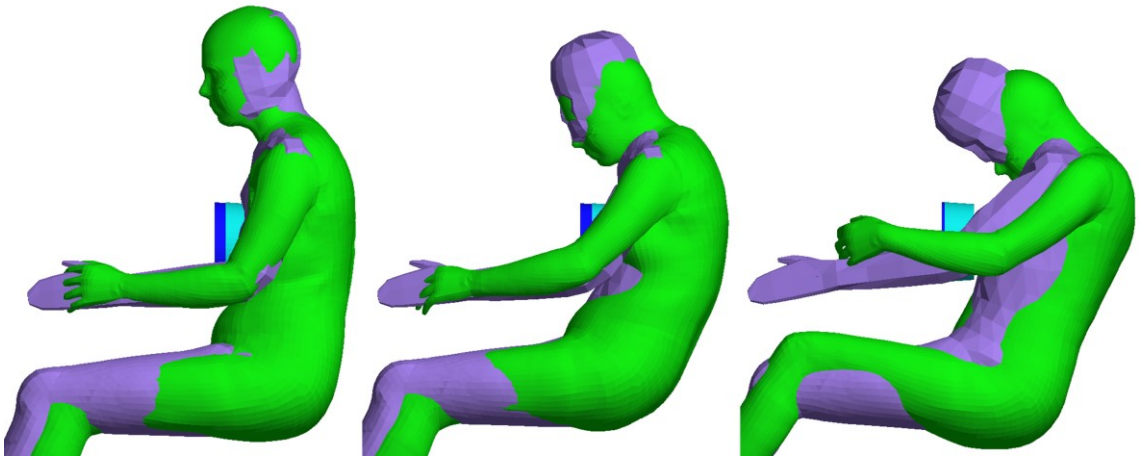

Fig. 127. Kinematics comparison in test 3.4 m/s

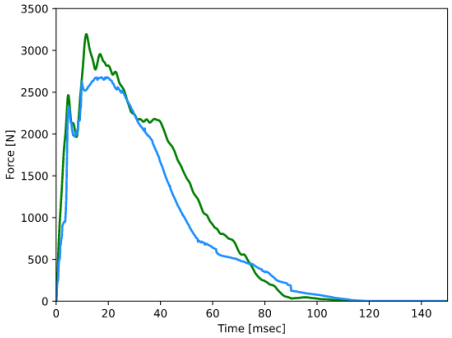

Fig. 128. Impactor force x-axis in test 5.8 m/s.

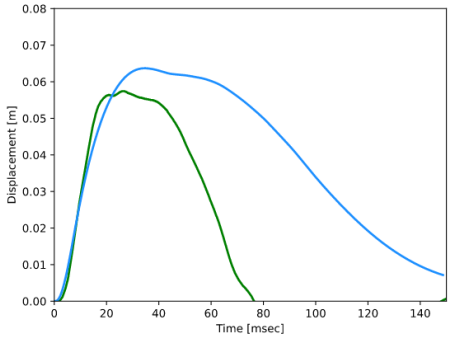

Fig. 129. Frontal thoracic deflection x-axis in test 5.8 m/s.

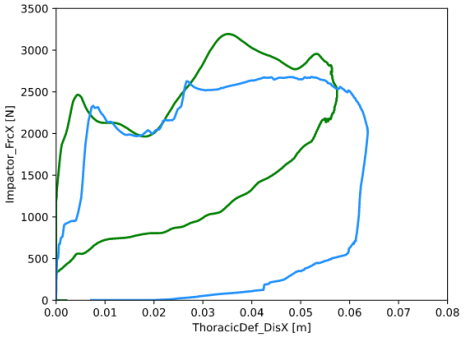

Fig. 130. Impactor force vs frontal thoracic deflection x-axis in test 5.8 m/s.

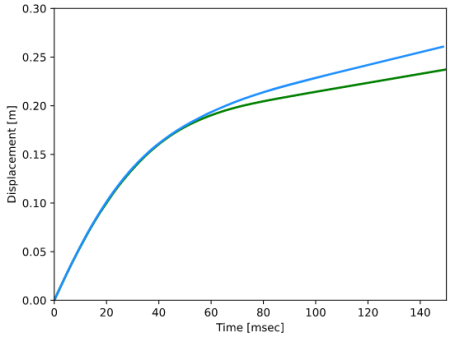

Fig. 131. Impactor displacement x-axis in test 5.8 m/s.

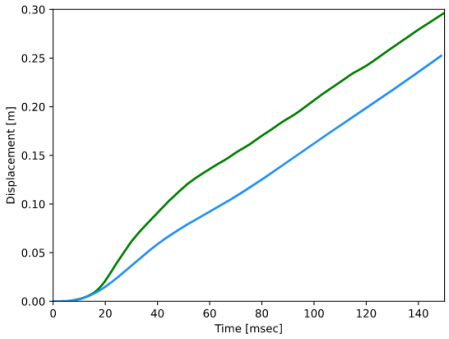

Fig. 132. T12 displacement x-axis in test 5.8 m/s.

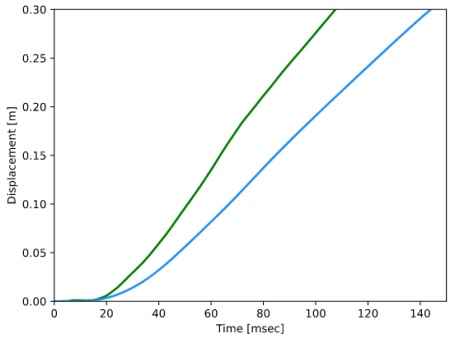

Fig. 133. T1 displacement x-axis in test 5.8 m/s.

Fig. 128 to Fig. 133 offers a similar conclusion as that drew from the lower velocity test, showing consistency and robustness in the behaviour of both models. In addition, a velocity dependent characteristic can be observed, as for this higher velocity test, the ViVA+ model's peak force increases with respect to that of the FAHM, and the thoracic deflection decreases.

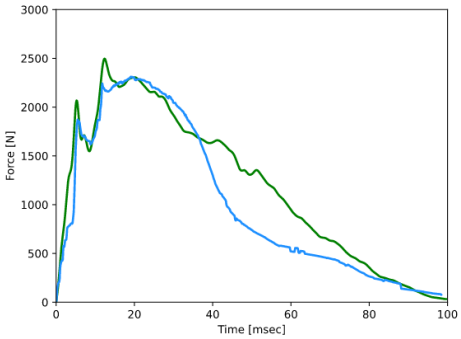

Fig. 134. Impactor force x-axis in test 4.9 m/s.

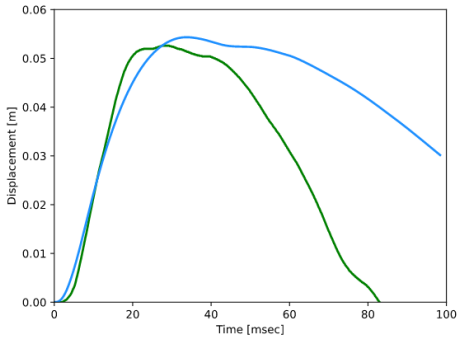

Fig. 135. Frontal thoracic deflection x-axis in test 4.9 m/s.

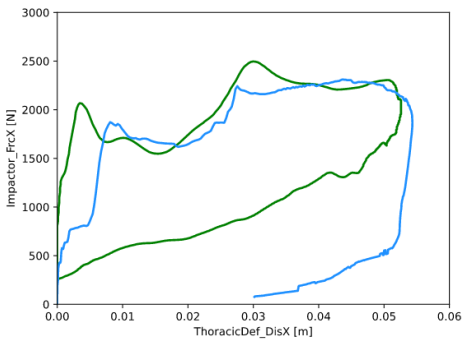

Fig. 136. Impactor force vs frontal thoracic deflection x-axis in test 4.9 m/s.

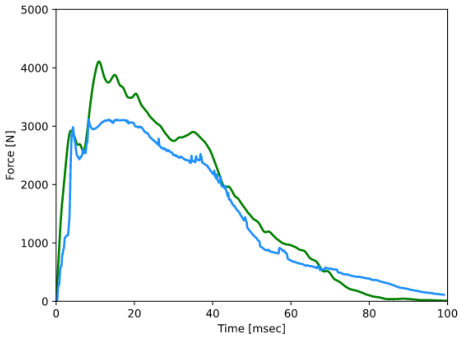

Fig. 137. Impactor force x-axis in test 6.9 m/s.

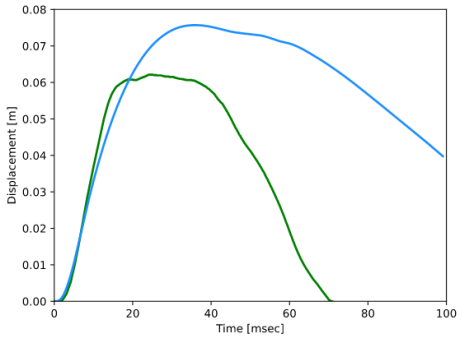

Fig. 138. Frontal thoracic deflection x-axis in test 6.9 m/s.

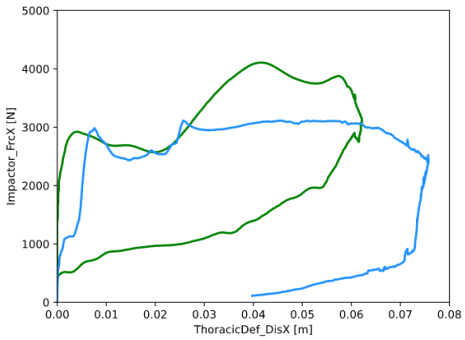

Fig. 139. Impactor force vs frontal thoracic deflection x-axis in test 6.9 m/s.

Fig. 134 to Fig. 136 show the results for the second study regarding frontal impact on thorax tests. Impactor mass in these tests stays invariant, whereas the velocity of the impactor changes. Thus, a relationship between impactor velocity and model behaviour can be established.

As in the previous cases, the differences between the responses from the ViVA+ model and the FAHM seem to be consistently proportional to velocity. Higher velocities result in a higher peak force value for the ViVA+ model with respect to the FAHM and a lower peak thoracic deflection.

Moreover, no instabilities were found in these first frontal impact on thorax tests, confirming a robust model design for both the ViVA+ model and the FAHM. In the case of the FAHM, the model is also stable independently of its positioning (as concluded from the standard and modified validation tests).

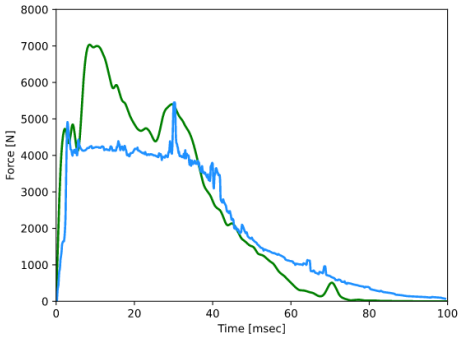

Fig. 140. Impactor force x-axis in test 9.9 m/s.

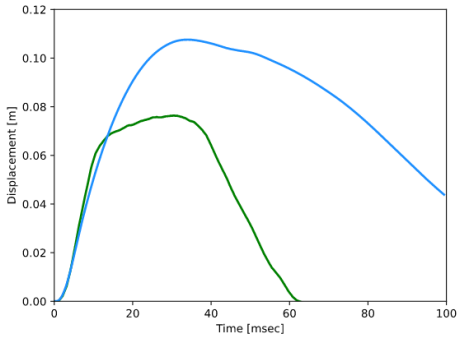

Fig. 141. Frontal thoracic deflection x-axis in test 9.9 m/s.

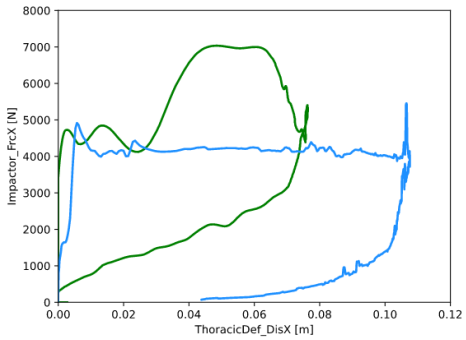

Fig. 142. Impactor force vs frontal thoracic deflection x-axis in test 9.9 m/s.

Fig. 140 to Fig. 142 show the results for the highest velocity test from the second thorax tests set. This high velocity impact test shows a significant difference in peak response and shape of the curve, and the appearance of a small peak in force for the FAHM. A possible explanation could be the same one given in the standard validation tests. However, this value also coincides with a third peak in the response of the ViVA+ model, suggesting that the FAHM response could be less stiff or with a lower damping value definition.

Lastly for these frontal impact on thorax tests, the third study uses different impactor masses and velocities. Fig. 143 shows a fairly similar response for a high impact velocity although its mass is lower than in the previous tests (now 10.4 kg vs 23.4 kg before), so the total energy stored in the impactor is lower. Fig. 144 shows a very similar response to the highest impactor velocity test for the previous study, and so, the conclusions are identical (even though the mass of the impactor is slightly smaller, with 22.2 kg).

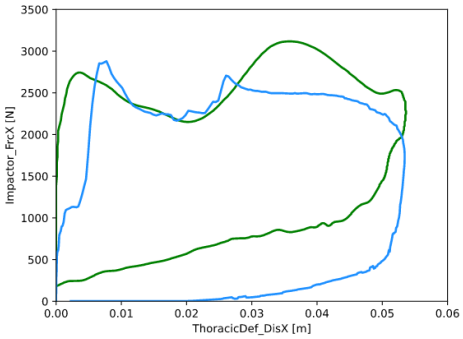

Fig. 143. Impactor force vs frontal thoracic deflection x-axis in test 7.0 m/s.

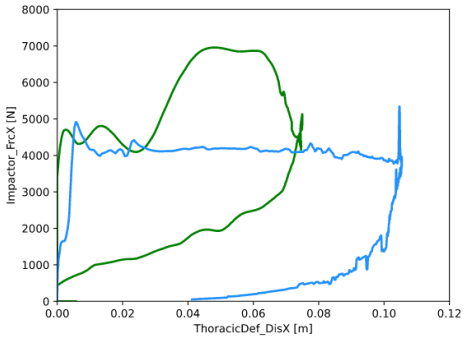

Fig. 144. Impactor force vs frontal thoracic deflection x-axis in test 9.9 m/s.

Lateral impact on thorax (Bouquet)

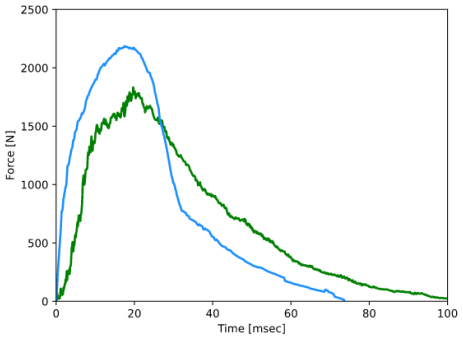

Fig. 145. Impactor force y-axis in test 3.3 m/s.

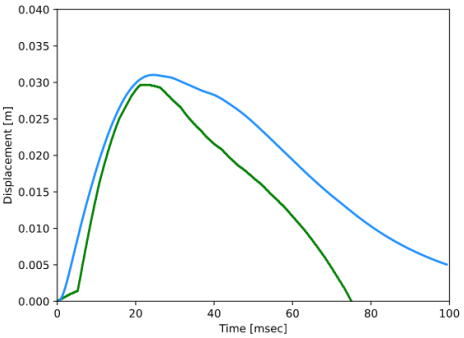

Fig. 146. Lateral thoracic deflection y-axis in test 3.3 m/s.

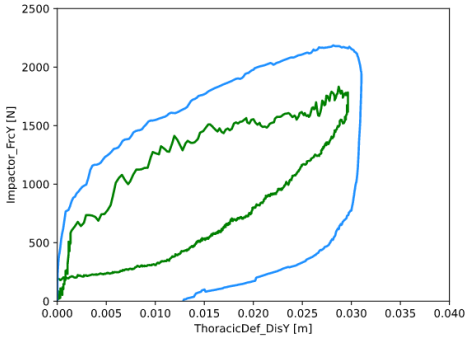

Fig. 147. Impactor force vs lateral thoracic deflection y-axis in test 3.3 m/s.

Fig. 145 to Fig. 147 offer the results for the low impactor velocity of the lateral impact on thorax tests. Results are fairly similar, although FAHM has a slightly higher peak

impactor force value and a slower ribcage recovery (but with a smaller difference between both models compared to that observed in the frontal impact on thorax tests).

In terms of kinematics the animation frames from Fig. 148 show an almost identical behaviour until halfway through the simulation. After, smaller differences appear, with a stiffer response for the FAHM.

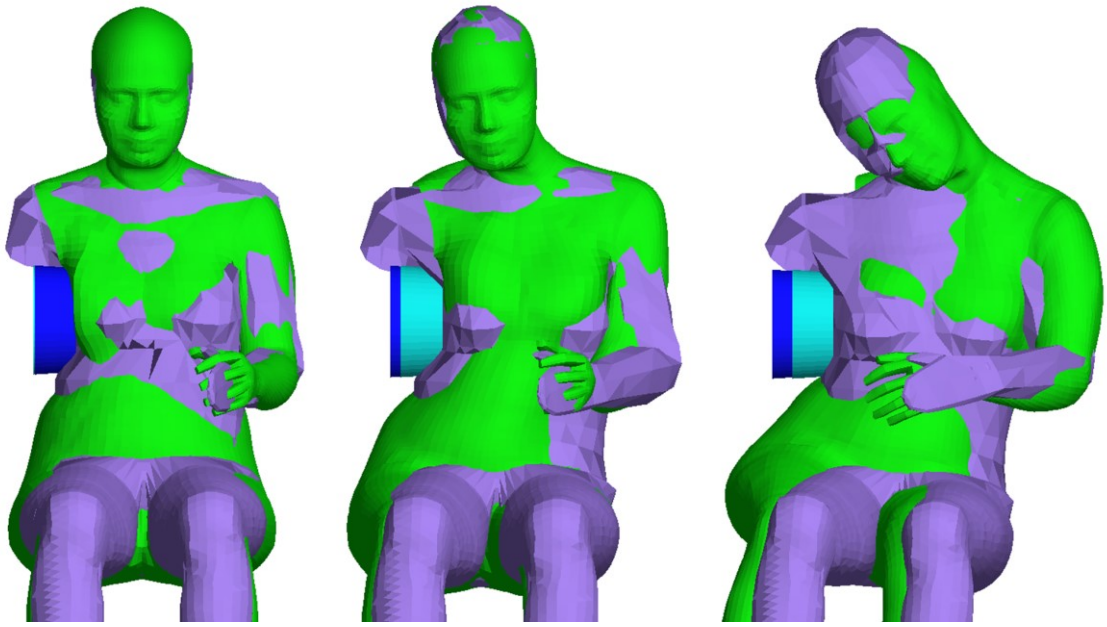

Fig. 148. Kinematics comparison in test 3.3 m/s

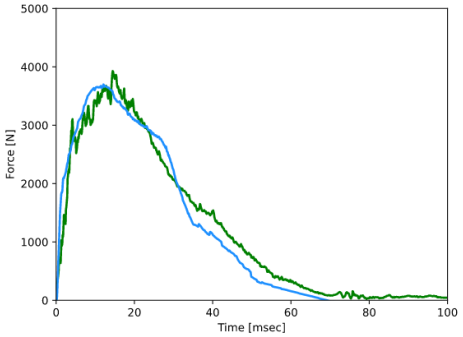

Fig. 149. Impactor force y-axis in test 5.9 m/s.

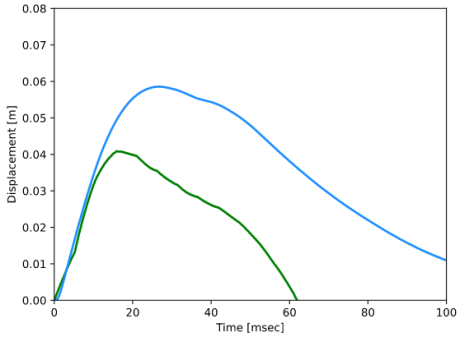

Fig. 150. Lateral thoracic deflection y-axis in test 5.9 m/s.

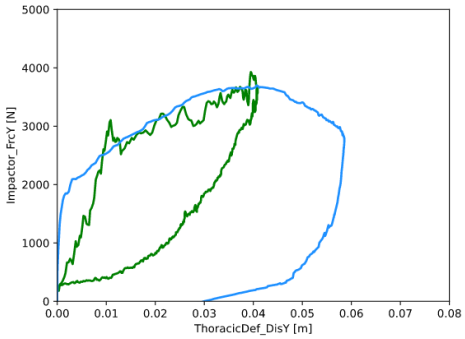

Fig. 151. Impactor force vs lateral thoracic deflection y-axis in test 5.9 m/s.

For the high impactor velocity test of this set, impactor peak force is identical, whereas regarding lateral thoracic deflection, the ViVA+ model has a significant faster ribcage recovery (similar again to that of the frontal impact on thorax tests).

Frontal impact on abdomen (Cavanaugh)

Fig. 152 to Fig. 155 offer the results for the frontal impact on abdomen tests. Contrary to the thorax overall behaviour, the ViVA+ model behaviour is stiffer and shows a lower abdominal deflection.

On the other hand, Fig. 156 shows that, like in the thorax tests, the kinematic behaviour of the FAHM is stiffer than the ViVA+ model, especially from the mid-point of the simulation.

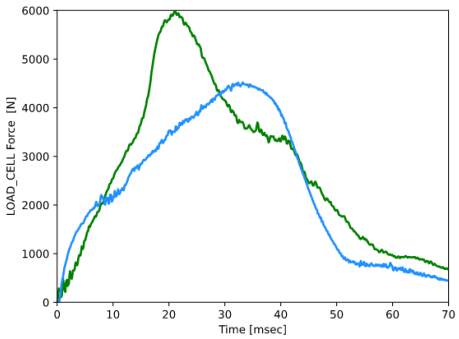

Fig. 152. Impactor force x-axis in test 6.9 m/s.

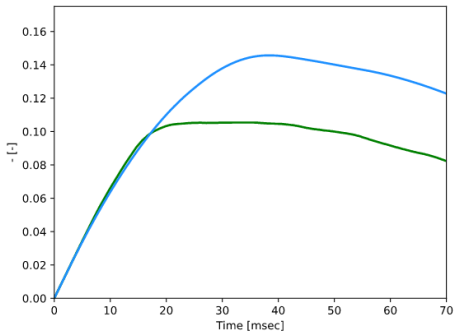

Fig. 153. Frontal abdominal deflection x-axis in test 6.9 m/s.

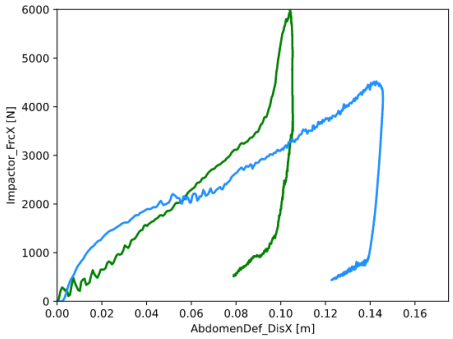

Fig. 154. Impactor force vs frontal abdominal deflection x-axis in test 6.9 m/s.

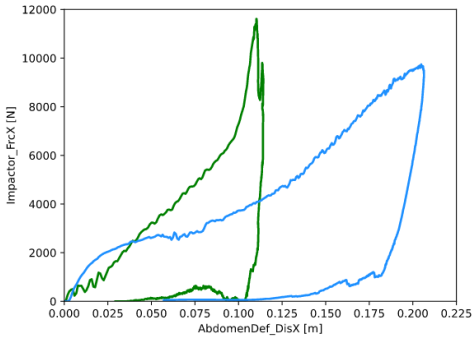

Fig. 155. Impactor force vs frontal abdominal deflection x-axis in test 9.4 m/s.

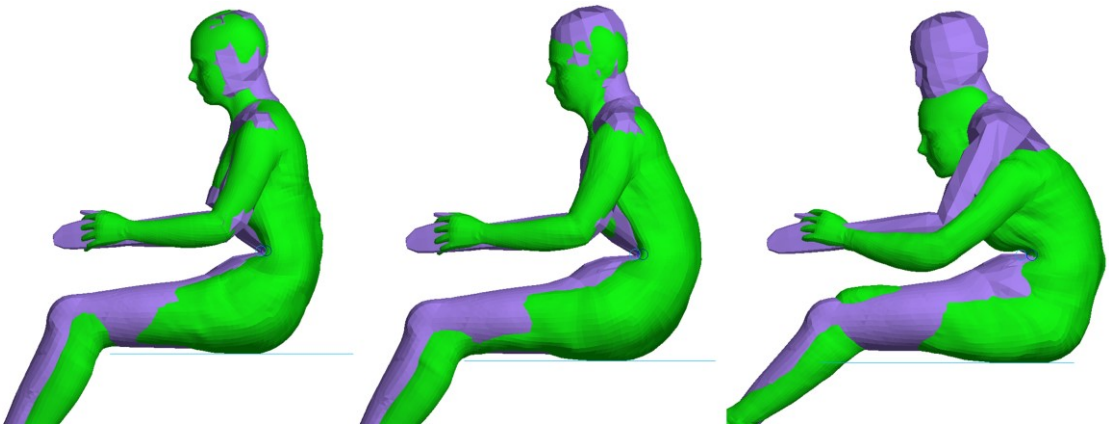

Fig. 156. Kinematics comparison in test 6.9 m/s

Lateral impact on abdomen (ISO)

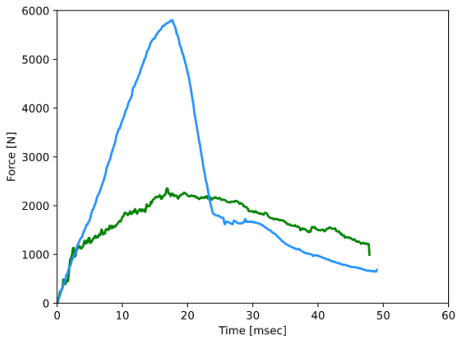

Fig. 157. Impactor force y-axis in test 4.43 m/s.

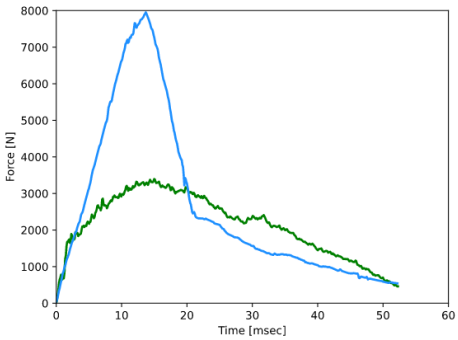

Fig. 158. Impactor force y-axis in test 6.26 m/s

The dynamic behaviour of both models for the lateral impact on abdomen tests is shown in Fig. 157 and Fig. 158. The differences in the responses are significant. However, Fig. 159

shows a fairly similar kinematic behaviour, even at the end-time of the simulation, with the exception of leg motion. The possible causes for this impactor force difference are still to be analysed.

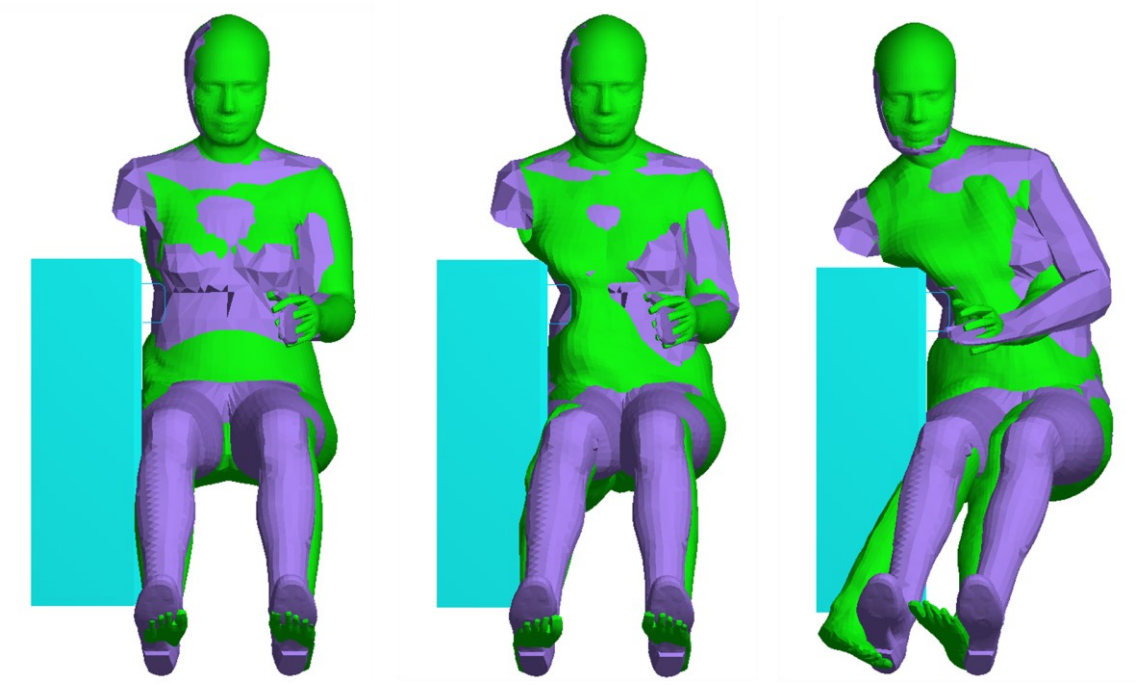

Fig. 159. Kinematics comparison in test 4.43 m/s

Lateral impact on pelvis (Bouquet)

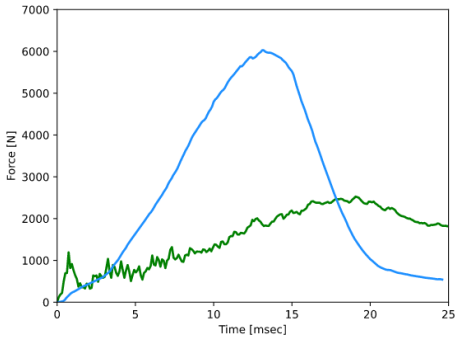

Fig. 160. Impactor force y-axis in test 3.46 m/s.

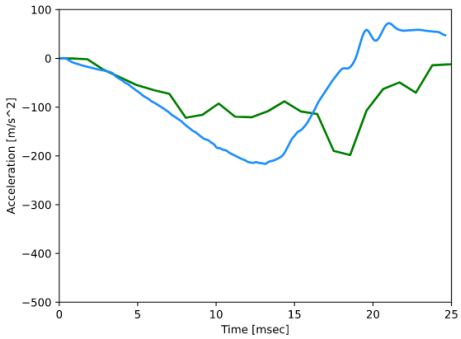

Fig. 161. Sacrum acceleration y-axis in test 3.46 m/s

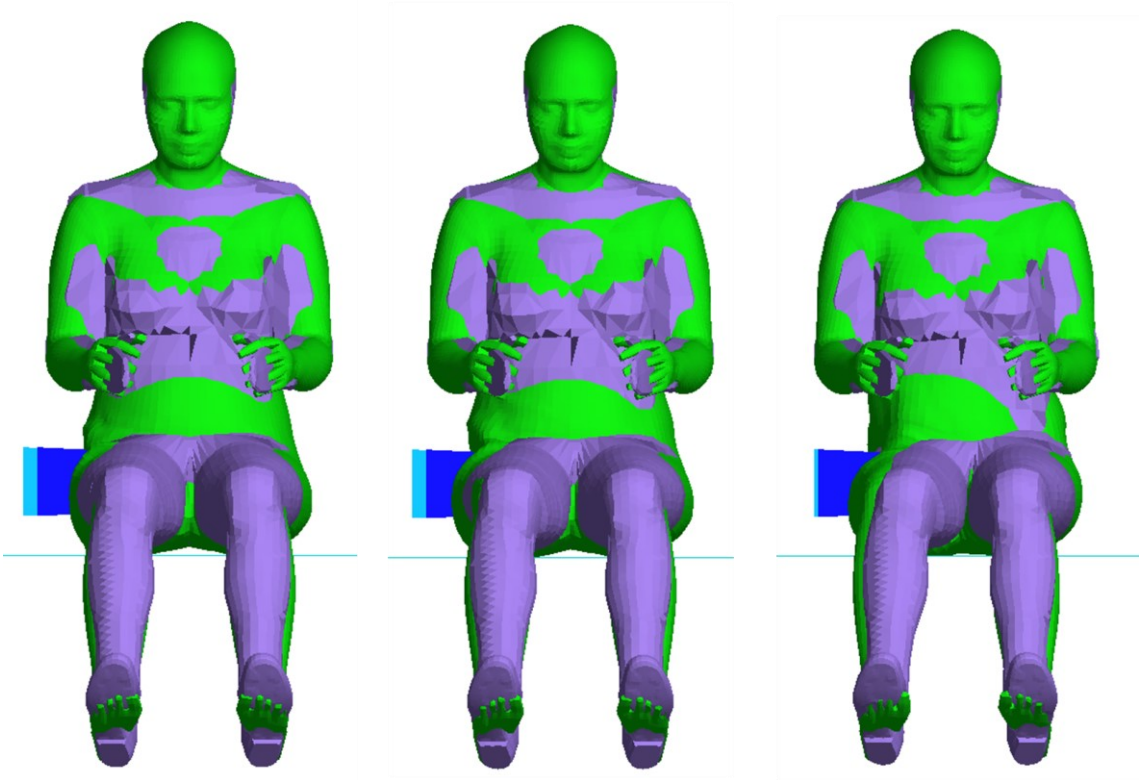

Fig. 162. Kinematics comparison in test 3.46 m/s

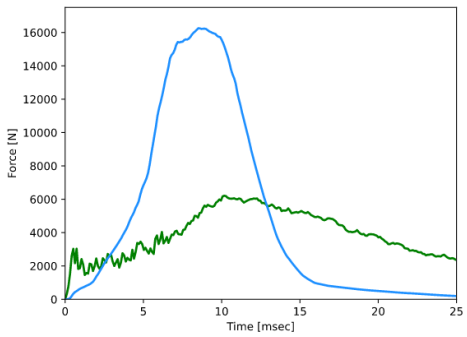

Fig. 163. Impactor force y-axis in test 6.66 m/s.

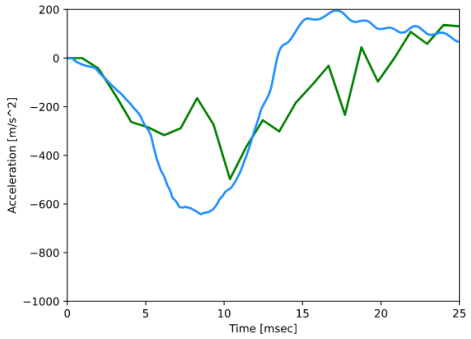

Fig. 164. Sacrum acceleration y-axis in test 6.66 m/s

Similar to the frontal impact on abdomen test, the lateral impact on pelvis tests (Fig. 160 to Fig. 164), show a significant different impactor force peak value and shape for the FAHM and the ViVA+ model. However, sacrum acceleration responses are similar for both models and so seems the kinematic behaviour (although the duration of the test does not allow for a proper kinematic development of the chain). The possible causes are also still to be analysed.

5.2.3 DISCUSSION ON LOCAL VALIDATION RESULTS

The tests performed in this subchapter, did not seek for a direct local validation. As aforementioned, achieving complete local validation (within the established criteria) was not possible at the time of documentation of this Master´s Thesis, due mainly to the lack of sufficient and adequate input data. The main objective of this subchapter was to analyse whether the biomechanical behaviour of the FAHM in the context of vehicle occupant and pedestrian safety showed robustness, coherence, and consistency at a local level. The conclusions drawn throughout the previous sections aligned with these three qualities.

Against the AHM, the FAHM showed the same response characteristic, and the observed differences were coherent and consistent with the scaling factors used for each absolute axis and model part. Moreover, no significant instabilities were found, giving the robust responses for all tests. In this sense, the FAHM behaves locally as it was expected, considering the process of development carried out.

Against the ViVA+ model, the FAHM showed a similar behaviour in the head, shoulder, and thorax impact tests. However, higher differences were observed for the abdomen and pelvis impact tests. As previously described, these parts correspond to the first links of the kinematic chain, and so, the possible differences in behaviour for the last links between both models are accumulated in these first link tests. The kinematic behaviour around the time of impact is very similar for both models, although the FAHM is stiffer in the post-impact kinematic development. In terms of dynamics, the FAHM is consistently stiffer than the ViVA+ model, but within the same order of magnitude and response consistency.

As aforementioned, the normalization of corridors in the standard validation tests should be considered as an approximation. The method used does not consider sex, and specially for local validation of female models (in cases such as frontal impact on thorax tests due to breast geometry, lateral and frontal impact on abdomen tests due to adipose tissue distribution, and lateral impact on pelvis tests due to adipose tissue distribution and pelvis

morphometry), this could be a key scaling factor, that also should change with each subsystem.

On the other hand, in the normalization of the ViVA+ model responses this problem is mitigated, as both models are female. However, differences in both models regarding for instance adipose tissue distribution (Chapter 4) could be also influencing the model responses. Additionally, the assumption of half sine-like impact responses of the model for all subsystems should be further analysed in the field.

In conclusion, the presented results are a first step towards local validation of the model's passive response, and further study is still required.

5.3 FAHM GLOBAL VALIDATION

The global validation described in this subchapter follows the same statements established and justified in the local validation subchapter:

1. PMHS experimental data should be the type used, as active response was not scaled in the FAHM development process.
2. Response global behaviour of the FAHM is unknown. It is expected to be similar to that of the AHM but manifesting overall higher deformations and lower stiffness (proportional to how it was scaled).
3. To the knowledge and resources of this study, there is no input data available regarding specific female response studies in global PMHS testing compatible with Multi-Body Dynamics.
4. The aim of this Chapter is to analyse global robustness, coherence, and consistency of the model.
5. The simulations in this subchapter are a first step towards global validation.

Due to resource limitations, the global validations were only performed with the equivalent of section 1 from the local validation tests, that is, the comparison between the FAHM and the AHM. The experimental test set selected in this study was also part of the

AHM validation process during its development. Said set is composed by three pedestrian impact vehicle tests with the same boundary conditions except for the vehicle initial velocity. The corresponding experimental tests were performed by [68].

5.3.1 AHM COMPARISON ANALYSIS II

The structure of this section is divided in two parts. First, the boundary conditions for the standard validation tests, together with the initial positioning are described. After, the results are presented and discussed.

Boundary conditions and initial positioning

The mentioned vehicle test consists of lateral impacts from a rigid vehicle at 25, 32, and 39 km/h. The Madymo simulation setup (Fig. 165) was already defined for the AHM previous to this Master's Thesis. Therefore, it was considered as optimal regarding the replication and simplification (such as the vehicle's geometry, or the rigidification of its elements to reduce computational cost) of boundary conditions from their respective experimental tests without any further analysis needed. Said tests were adapted to the FAHM, modifying the initial positioning of the model to match that of the AHM.

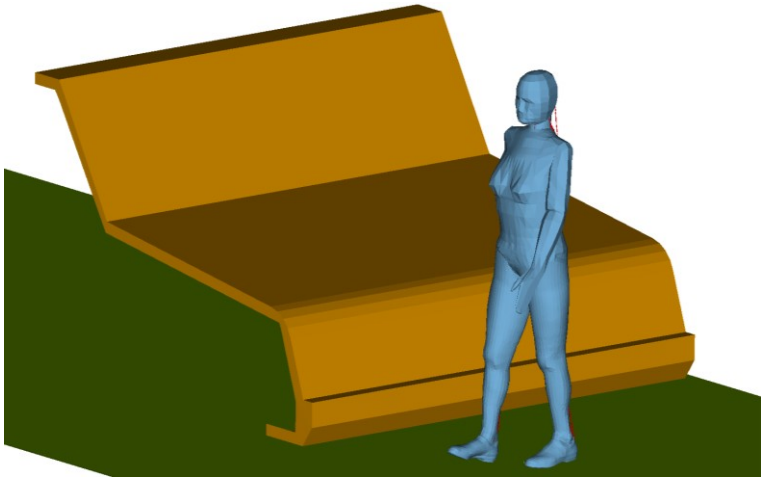

Fig. 165. Vehicle tests setup

Results

This part offers the main results obtained in the 25 km/h test and compares the biomechanical behaviour of the AHM and FAHM. The results of the 32 and 39 km/h are significantly similar to that of the 25 km/h test, and so, conclusions can be extrapolated from it. In all cases, red curves represent the AHM responses, whereas the blue curves represent the FAHM responses. Additionally, experimental curves are shown in grey (there are no experimental corridors in these tests).

These experimental curves were normalized to match the FAHM mass and height, using the same normalization factors as the ones described in section 5.2.1. They are showed in the results with dashed lines. Hence, AHM responses should be similar to solid experimental curves, and FAHM similar to dashed experimental curves. As aforementioned, this normalization should be considered as an approximation.

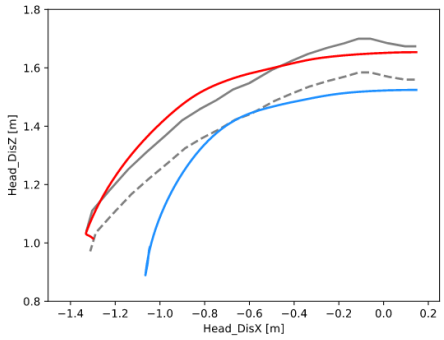

Fig. 166. Head displacement z-axis vs x-axis in 25 km/h test.

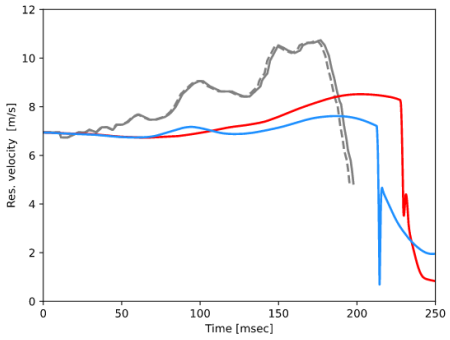

Fig. 167. Head velocity resultant in 25 km/h test

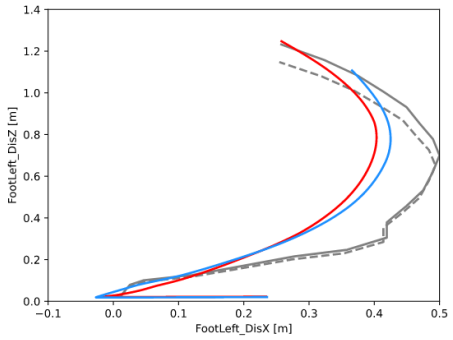

Fig. 168. Left foot displacement z-axis vs x-axis in 25 km/h test

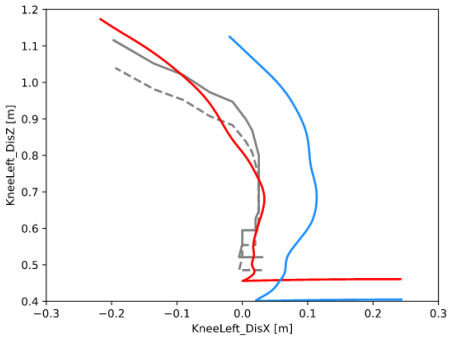

Fig. 169. Left knee displacement z-axis vs x-axis in 25 km/h test

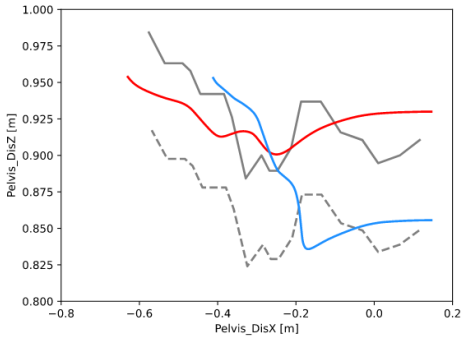

Fig. 170. Pelvis displacement z-axis vs x-axis in 25 km/h test

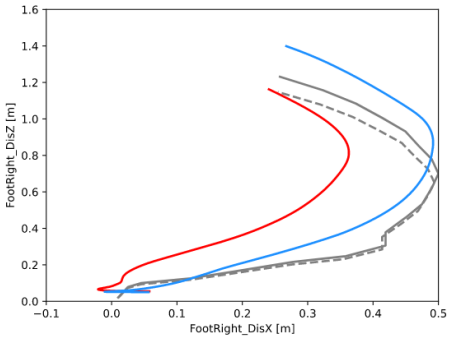

Fig. 171. Right foot displacement z-axis vs x-axis in 25 km/h test

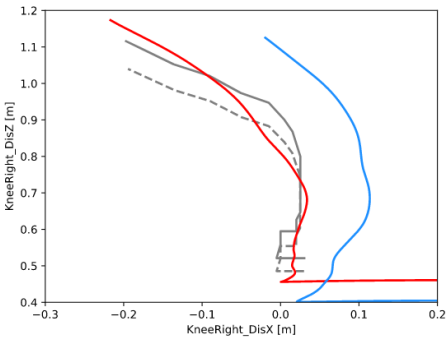

Fig. 172. Right knee displacement z-axis vs x-axis in 25 km/h test.

Fig. 166 to Fig. 172 show the most relevant results for the lateral vehicle impact at 25 km/h. The x and z-axis refer to the direction parallel to the vehicle displacement, and the vertical axis normal to the inertial plane, respectively. The different displacement and velocity values in the FAHM simulations are, as expected, scaled from that of the AHM. For some of the responses, the FAHM represents an improvement over the AHM with respect to the experimental curves (such as Fig. 168 and Fig. 171), whereas not being the case in other figures. Nevertheless, and as explained throughout this Chapter, the normalized corridors should be considered as an approximation.

On the other hand, the kinematic behaviour of the FAHM in the tests of this section is overall scaled from the AHM, confirming that the FAHM has a biomechanical global response proportional to that of the AHM, and so, that the FAHM development process was performed adequately.

5.3.2 DISCUSSION ON GLOBAL VALIDATION RESULTS

Like the local validation tests, the tests performed in this subchapter, did not seek for a direct global validation, but rather aimed to analyse the biomechanical behaviour of the FAHM in the context of vehicle occupant and pedestrian safety and in terms of robustness, coherence, and consistency. As sufficient and adequate input data regarding specific female global tests was not found at the time of documentation of this Master´s Thesis, an AHM validation vehicle test set was used, and the existent experimental curves were normalized (curves that, as already explained, should be considered as an approximation).

The FAHM showed the same response characteristic as the AHM, and the observed differences were coherent and consistent with the scaling factors used for each absolute axis and model part. Moreover, no significant instabilities were found. Subsequently, the FAHM behaves globally as it was expected, considering the process of development carried out.

In conclusion, the presented robust, consistent, and coherent results are a first step towards global validation of the model's passive response, and further study is still required.

Chapter 6. FUTURE WORK

This Master's Thesis has covered a wide range of aspects regarding the development and validation of the Simcenter Madymo Female 50th percentile Active Human Model. First, the anthropometric differences between males and females were studied in the context of Multi-Body Dynamics and Madymo software. After, a development method, together with its baseline model, and main references were analysed for this new model. Finally, the most adequate scaling, validation process, and response normalization approaches were selected and implemented.

However, there are still several challenges left for the FAHM:

Model validation

The local validation process confirmed the robustness, coherence, and consistency of the FAHM, and pointed out several response differences with respect to the ViVA+ model. However, further local validation is still needed, requiring additional PMHS female-specific impact test sets focusing on said differences.

The global validation process also confirmed the robustness, coherence, and consistency of the FAHM, but at a higher level. In this case, a comparison against the ViVA+ model was not performed since it was out of the scope and resources of this study. Identically, further global validation is needed, using PMHS female-specific vehicle and sled test sets.

Evidently, in order to use PMHS female-specific experimental data for the mentioned purposes, said data has to exist in the first place in experimental testing, and has to be compatible and coherent with MBD and Simcenter Madymo software (as discussed in Chapters 3 and 4). This Master's Thesis did not find the required data in the available literature and did not have enough resources to directly perform the experimental tests. Hence, future work can either wait for the publication of new studies relating this topic (or

search and find existent studies omitted by this Master's Thesis) or new fully-validated models, or design and perform a new set of PMHS experimental tests.

Model's active response and Injury Risk Functions

Moreover, active response, injury risk functions, and injury criteria were not modified from the AHM nor validated for the FAHM, as it was out of the scope of this study. Future work should consider a different approach for these elements to that described in the development process of this Master's Thesis, as for some of their characteristics might not be possible to scaled them directly.

Model's sex-related anthropometric features

Regarding the possible future implementation of other sex-specific anthropometric features in the FAHM, female-specific experimental data is also needed. This data is not only key for the validation process, but also for the development process since both are usually performed simultaneously in Madymo software due to its nature (as explained in Chapter 3).

Diversity for human modelling

After the abovementioned, the FAHM could be integrated in Madymo Scaler Tool, so that a wide range of Female AHM from 5th to 95th percentile groups from different anthropometric databases can be created at any moment. To facilitate this, the present Master's Thesis parameterized most of the elements of the model.

Lastly, a randomized algorithm could be implemented to the previous case, and so, considering Madymo's capabilities for extensive design space exploration, complete female anthropometric diversity studies could be performed. This could translate into a huge step towards occupant vehicle and pedestrian safety, being able to optimize any vehicle and infrastructure design for a significantly high number of sets of models representing any possible female anthropometric distributions.

Finally, the suggested steps for future work following the aforementioned are:

1. Find female-specific local experimental test data or perform the tests personally. Optimize the definition of the different subsystems of the FAHM to meet the experimental corridors.
2. Find female-specific global experimental test data or perform the test personally. Optimize the global FAHM definition to meet the experimental corridors.
3. Implement female-specific active response, injury risk functions, and injury criteria definitions, gathering sufficient input data from literature or experimental testing.
4. Find more input data regarding sex-related anthropometric features that are compatible with MBD and Simcenter Madymo software and implement the needed development and validation processes.
5. Complete the full parametrization of the model and adjust the necessary elements to make it compatible with Madymo Scaler Tool and Siemens Jack Scaling databases.
6. Integrate a randomized algorithm in Madymo Scaler Tool to work with the different local scaling factors defined in Siemens Jack Scaling databases.

Chapter 7. CONCLUSIONS

This Chapter gathers the conclusions drawn throughout this Master´s Thesis and analyses whether the mission and objectives established at the beginning of it have been completed. Additionally, a discussion on the possible impact of this study in its vision is offered.

Main conclusions and observations

Chapter 1 focused on the contextualization of the observed problem, and on the definition of the vision, mission, objectives, scope, and workflow methodology of this Master´s Thesis. Gathered literature suggests a significantly higher probability of injury and mortality for women than for men in road traffic accidents. A further analysis concluded that the main reasons behind this phenomenon are physiology, culture and behaviour, and the general lack of representation of the female anthropometry in the vehicle safety sector. This study focused on the latter, as it is directly related to the engineering sector.

Delving into this topic, it was observed that overall, the average female anthropometry is not requested by any vehicle safety assessment programme or used by any Original Equipment Manufacturer (OEM) in the sector, but also, that, with 2 exceptions, there are no Human Body Models (HBMs) or physical or virtual Anthropometric Test Devices (ATDs) available representing this group. On the one hand, these observations suggest that the average female anthropometry is considered to be covered by the average male anthropometry by the vehicle safety sector. On the other hand, it also suggests that the general lack of average female models difficult any other scenario.

At this point, the vision of this study was already defined: *to provide OEMs and vehicle safety assessment programmes (both type approval and consumer testing) with another tool to improve vehicle design (regarding comfort and safety) and vehicle safety assessment towards increasing female road user's safety, as well as to improve female injury prediction.*

From the aforementioned, said tool could only be referring to the observed general lack of average female models, and so, the mission of this study was defined: *to develop a 50th percentile female MB (Multi-Body) HBM.* With it, the objectives, scope, and the rest of elements were defined.

Chapter 2 overviewed the main technologies used in this Master´s Thesis. First, the Multi-Body Dynamics (MBD) numerical simulation solution method was presented, alongside with Simcenter Madymo software, the main software used in this study. In this subchapter, Simcenter Madymo Scaler and Siemens Jack Scaling were also introduced. After, the most complex model from Madymo software, the Active Human Model (AHM) was described, as it had been selected as male equivalent and baseline model for this study. Thus, the designation 50th percentile female MB HBM from the mission statement was updated to Female Active Human (FAHM).

In the third subchapter, the Finite Element Method (FEM) numerical simulation solution method was presented, a method also used by Simcenter Madymo software. Additionally, it is the mathematical background for LS-Dyna, the software used in coupled simulations in later stages of this Master´s Thesis. Lastly, in the last subchapter, Altair HyperMesh software was introduced as the main tool utilized for geometry morphing.

Being as this Chapter was predominantly descriptive, no conclusions were drawn, aside from the selection of Massively Parallel Processing (mpp) as the most adequate computation configuration for both Madymo and LS-Dyna in the mentioned coupled simulations.

Chapter 3 offered the State of the Art, composed by a female anthropometry analysis, a baseline model and references definition, and a Siemens Jack Scaling database selection.

The first subchapter focused on documented input data of anthropometric differences between males and females, and their applicability to a HBM in MBD and Madymo software. From the gathered literature, input data from topics such as adipose tissue distribution, cervical spine morphometry, neck muscle and behaviour, head mass, and pelvis morphometry were considered as adequate and sufficient for a partial or total

implementation in the FAHM. However, other topics found regarding ligaments and tendons strength, general biomechanical properties, general bone properties, radius anthropometric measures, tibia cortical bone properties, and ankle behaviour and Injury Risk Functions (IRFs), were considered as qualitative, insufficient for the intended purpose of this study, or not compatible with MBD characteristics and nature.

The second subchapter analysed, in the first section, other existent technological approaches to female 50th percentile models which are the Humanetics EvaRID virtual ATD, and the ViVA+ model. After, in the second section, the AHM was presented as the baseline model for this study, together with a female 50th percentile neck model from a previous Madymo study as Main Reference 1 (MR1), and the Simcenter Madymo´s facet female 5th percentile scalable model as Main Reference 2 (MR2).

In order to use MR2 as a reference for average female anthropometric distribution, an automatic scaling process via Madymo Scaler Tool and using a database from Siemens Jack Scaling was needed. Therefore, the third chapter analysed, among the databases available, the most adequate one for this Master´s Thesis. The National Health and Nutrition Examination Survey (NHANES) study from 2011 to 2014 was considered to be the most consistent with the established acceptance criteria.

Chapter 4 described the development process of the FAHM carried out. First, the most suitable approach to said process was discussed. The one selected was the scaling process similar to that used in the development of the EvaRID model, but with a different mathematical background and some exceptions. The model scaling method used is the same as that of the Madymo Scaler Tool, and the exceptions were mainly regarding thorax skin and pelvis morphometry (as a result of the female anthropometry analysis). Other differences from the female anthropometry analysis, compatible with MBD and Madymo, regarding the head-neck subsystem were already considered in MR1.

The next subchapters and sections in this chapter described the development process itself, starting from the morphing of the pelvis and thorax skin attending to their function within Madymo, and to the available tools, input data, and resources. After, the

morphometric side of the scaling process was detailed, together with the used scaling factors and other considerations. Finally, the dynamic side of the scaling process was presented, obtaining the new FAHM.

This Chapter was mainly descriptive, and so the only conclusion drawn was the consistency of the process followed, that resulted in only a 1.2% error in height, and a 4% error in total mass with respect to MR2 (a much simpler model with a very different structure).

Chapter 5 described the validation process of the FAHM. An initial overview subchapter discussed what a human model validation process implies, and what mechanisms to characterize human biomechanical response, from the existent, are more suitable to use as validation reference in this study (considering compatibility with MBD and available input quantitative data). As a result, the rest of the chapter was divided into two parts, both involving passive response validation, but the first of them focusing on the local validation and the second on the global validation.

A key element in this analysis was response normalization, introduced in this first subchapter, and utilized throughout this Chapter. The selected normalization method was that of the Mertz 1984 study, and a further discussion concluded that, in particular for the normalization of male experimental data into female, the obtained curves should be considered as an approximation, especially regarding local validation.

The first step in local validation aimed for an analysis of the robustness, consistency, and coherence of the FAHM, by means of the 'standard validation tests' and comparing each response with that of the AHM, and with the Post Mortem Human Subject (PMHS) blunt impact tests experimental corridors (that were normalized). The FAHM showed results with respect to the AHM aligned with the scaling factors used for each absolute axis and model part.

The second step in local validation benchmarked the FAHM against the ViVA+ model using the 'modified validation tests'. Experimental corridors from the 'standard validation

tests' could not be considered because of the modifications made in the boundary conditions of the tests, but the response of the ViVA+ model was normalized. As of the date of documentation of this Master´s Thesis, the ViVA+ model local validation data has not yet been published (except for the neck system), and hence, the objective of this second step was to analyse the similarities and differences in the responses of both models. Results showed a similar initial kinematic response, but an overall stiffer kinematic development for the FAHM. The dynamic response for both models was overall similar but with a stiffer behaviour of the FAHM in the abdominal and pelvic area. Additionally, the ViVA+ model showed a significantly faster ribcage recovery. In all cases, the responses of both models were within the same order of magnitude, and the observed differences were consistent.

Finally, the global validation was performed in a single step, using a test set from the 'standard validation tests'. Responses were compared between the FAHM and the AHM, and each one with the selected PMHS experimental vehicle tests (with response normalization). As in the first step of the local validation, The FAHM showed the same response characteristic as the AHM, and the observed differences were coherent and consistent with the scaling factors used for each absolute axis and model part. Regarding numerical and physical robustness, no significant instabilities were found in the FAHM.

Chapter 6 suggested future work on this FAHM, including further local and global passive response validation using as reference experimental PMHS testing found in literature or performed personally, active response development and validation, additional sex-specific anthropometric features, and full parametrization of the model for use in the Madymo Scaling Tool.

To sum up, the key conclusions of this Master´s Thesis are:

1. The mission of this study to develop the Simcenter Madymo's FAHM aims to provide the vehicle safety sector with a tool to help increase female safety as a road user, as women have a significantly higher probability of injury and mortality than men in road traffic accidents.

2. A female anthropometry analysis allowed to define the baseline model and main references for the development of the FAHM.
3. The developed FAHM showed consistency in terms of anthropometric distribution with respect to the references used.
4. A first approach to the FAHM validation was performed, obtaining consistent, coherent and robust responses both locally and globally. Additionally, a local comparison against the ViVA+ model showed overall similar responses, although some differences were also observed.
5. The suggested future work for the FAHM focus on further passive validation and implementation and validation of female-specific active response.

Achievement of the established mission and objectives

The objectives of this study, as established in Chapter 1, were:

3. To develop a Multi-Body Female 50th percentile HBM.
    a. To analyse the physiological differences across male and female anthropometries.
    b. To evaluate the most suitable human anthropometry database from the available ones.
    c. To select the most suitable HBM developing method.
    d. To build up the morphometry-related part of the model.
    e. To elaborate the dynamics-related part of the model.

4. To validate said model.
    a. To analyse possible approaches for the validation of the developed model.
    b. To perform the selected validation method.
    c. To evaluate the results obtained and the necessity for model modifications.

A discussion on the level of completion of these objectives is offered below:

- *To analyse the physiological differences across male and female anthropometries:* this objective was completed successfully in the Female Anthropometry Analysis of Chapter 3.

- *To evaluate the most suitable human anthropometry database form the available ones:* this objective was completed successfully in the Siemens Jack Database Analysis of Chapter 3

- *To select the most suitable HBM developing method*: this objective was completed successfully in the Model Development Approach of Chapter 4.

- *To build up the morphometry-related part of the model:* this objective was performed in the Model Morphometry subchapter of Chapter 4 and was considered as consistent and completed.

- *To elaborate the dynamics-related part of the model:* this objective was performed in the Model Dynamics subchapter of Chapter 4 and was considered as consistent and completed (active response was not part of the scope of this study as established in Chapter 1).

- *To analyse possible approaches for the validation of the developed model:* this objective was completed successfully in the Overview of Chapter 5.

- *To perform the selected validation method:* this objective was performed in the FAHM Local Validation and FAHM Global Validation subchapters of Chapter 5. This objective was completed in the context of the selected validation approach.

- *To evaluate the results obtained and the necessity for model modifications*: Results were aligned with what was expected, and no model modifications were made, as this step was not compatible with the selected validation approach.

Consequently, the mission of this Master´s Thesis, *to develop a 50th percentile female MB (Multi-Body) HBM*, can be considered as completed within the established scope, objectives, and acceptance criteria.

Expected impact of this Master´s Thesis on its vision

This study is not expected to impact female safety as road users in the short term, as future work is still needed for a fully developed FAHM, especially regarding passive response validation and active response modification and validation. Nevertheless, its impact in the middle or long term does not depend only on the mentioned future work. As previously explained, the observations made in the Contextualization of Chapter 1, suggest that the average female anthropometry is considered covered by the average male anthropometry by OEMs and vehicle safety assessment programmes (both type approval and consumer testing). A change in this situation is needed so that the FAHM and other female 50th percentile models can start to help improve female safety as road users.

Chapter 8. REFERENCES

[1] C. J. Kahane. Injury vulnerability and effectiveness of occupant protection technologies for older occupants and women. (Report No. DOT HS 811 766). 2013. Washington, DC: National Highway Traffic Safety Administration (NHTSA).

[2] J. Forman, G. S. Poplin, C. G. Shaw, T. L. McMurry, K. Schmidt, J. Ash & C. Sunnevang. Automobile injury trends in the contemporary fleet: Belted occupants in frontal collisions. 2019. Traffic Injury Prevention. 2019;20(6):607-612. doi: 10.1080/15389588.2019.1630825.

[3] B. Jonsson, C. Tingvall, M. Krafft & U. Bjornstig. The risk of whiplash-induced medical impairment in rear-end impacts for males and females in driver seat compared to front passenger seat. 2013. ATSS Research, Volume 37, Issue 1, Pages 8-11,https://doi.org/10.1016/j.iatssr.2013.04.001.

[4] Parliamentary Advisory Council for Transport Safety (PACTS). Safe System.

[5] M. L. Brumbelow & J. S. Jermakian. Injury risks and crashworthiness benefits for females and males: Which differences are physiological? 2021. Traffic Injury Prevention, doi: 10.1080/15389588.2021.2004312.

[6] Insurance Institute for Highway Safety (IIHS). Fatality Facts 2020: Males and Females. May 2022. Recovered, on April 4, 2022, from: https://www.iihs.org/topics/fatality-statistics/detail/males-and-females#speeding

[7] Institute for Health Metrics and Evaluation (IHME). Global Health Data Exchange tool. Recovered, on April 4, 2022, from: https://vizhub.healthdata.org/gbd-results/

[8] Gendered Innovations. Inclusive Crash Test Dummies: Rethinking Standards and Reference Models. Recovered, on April 4, 2022, from: http://genderedinnovations.stanford.edu/case-studies/crash.html#tabs-2.

[9] A. Linder, R. Thomson, M. Svensson, A. Carlsson, P. Lemmen, K. U. Schmitt & E. Tomasch. Occupant Diversity in Modelling and Evaluation Related to Soft Tissue Neck Injuries in Low Severity Impact. RS4C Conference 2013.

[10] P. Lemmen, A. Gupta, A. Lakshminarayana, A. Carlsson, M. Svensson, K. U. Schmitt, I. Levallois, A. Linder & E. Tomasch. Seat Optimisation Considering Reduction of Neck Injuries for Female and Male Occupants – Applications of the EvaRID Model and a Loading Device Representing a 50th Percentile Female. 2013.

[11] A. Linder, W. Svedberg. Occupant safety assessment in European regulatory tests: review of occupant models, gaps and suggestion for bridging any gaps. 18th International Conference Road Safety on Five Continents (RS5C 2018), Jeju Island, South Korea, May 16-18, 2018.

[12] Consumer Reports. he Crash Test Bias: How Male-Focused Testing Puts Female Drivers at Risk. 2019. Recovered, on April 4, 2022, from: https://www.consumerreports.org/car-safety/crash-test-bias-how-male-focused-testing-puts-female-drivers-at-risk/.

[13] Liu, K. & Jain, S. A Quick Tutorial on Multibody Dynamics. 2018. School of Interactive Computing. Georgia Institute of Technology.

[14] Simcenter Madymo. Theory Manual Release 2022.1, 2021.

[15] Koppens, W. P. The Dynamics of Systems of Deformable Bodies. 1989. Technische Universiteit Eindhoven.

[16] Simcenter Madymo. Utilities Manual Release 2022.1, 2021.

[17] Simcenter Madymo (2021) Active Human 50th Facet Q Model, version 3.3 (R2021.1). Quality Report Release Update QAHM50-210601, 2021.

[18] Simcenter Madymo. Human Models Manual Release 2022.1, 2021.

[19] Simcenter Madymo. Model Manual Release 2022.1, 2021.

[20] Oasys LS-Dyna Environment. Image from the video: Session 2 - Deciphering LS DYNA Contact Algorithms. Recovered, on July 7, 2022, from: https://www.youtube.com/watch?v=m1Lffd8DOPI

[21] Simcenter Madymo. Coupling Manual Release 2022.1, 2021.

[22] Gray, H. Anatomy of the Human Body. 20th edition reviewed and re-edited by Lewis W. H. 1918. Lea & Febiger.

[23] Rice University. Anatomy and Physiology. 6.3 Bone Structure. 2022 (web version). Recovered, on July 10, 2022, from: https://openstax.org/details/books/anatomy-and-physiology?Book%20details.

[24] Brown ,L. M., Gent, L., Davis, K. & Clegg, D. J. Metabolic impact of sex hormones on obesity. 2010. Brain Research. 1350: 77–85. doi:10.1016/j.brainres.2010.04.056.

[25] Frank, A. P., de Souza Santos, R., Palmer, B. F. & Clegg, D. J. Determinants of body fat distribution in humans may provide insight about obesity-related health risks. 2019. Journal of Lipid Research. 60 (10): 1710–1719. doi:10.1194/jlr.R086975.

[26] Janssen, I., Powell, L. H., Kazlauskaite, R. & Dugan, S. A. Testosterone and visceral fat in midlife women: The Study of Women's Health Across the Nation (SWAN) fat patterning study. 2010. Obesity. 18 (3): 604–10. doi:10.1038/oby.2009.251.

[27] Chidi-Ogbolu, N. & Baar, K. Effect of Estrogen on Musculoskeletal Performance and Injury Risk. 2019. Front Physiol. 9:1834. doi: 10.3389/fphys.2018.01834.

[28] Roberts, C. W., Forman, J. L. & Kerrigan, J. R. Analysis of Potential Effects of Estrogen on Ligament Stiffness and Resulting Injury Prediction Metrics. IRCOBI Conference 2019.

[29] Notelovitz, M. Androgen effects on bone and muscle. Fertility and Sterility, Volume 77, Supplement 4, 2002, Pages 34-41, doi:10.1016/S0015-0282(02)02968-0.

[30] Nieves, J. W., Formica, C., Ruffing, J., Zion, M., Garrett, P., Lindsay, R. & Cosman, F. Males Have Larger Skeletal Size and Bone Mass Than Females, Despite Comparable Body Size. J Bone Miner Res, 20: 529-535. https://doi.org/10.1359/JBMR.041005.

[31] Naganathan, V. & Sambrook, P. Gender differences in volumetric bone density: a study of opposite-sex twins. 2003. Osteoporos Int. 14(7):564-9. doi: 10.1007/s00198-003-1422-3

[32] Vasavada, A., Danaraj, J. & Siegmund, G. Head and neck anthropometry, vertebral geometry and neck strength in height-matched men and women. 2008. Journal of biomechanics, 41:114–21, doi: 10.1016/j.jbiomech.2007.07.007

[33] Stemper, B., Derosia, J., Yoganandan, N., Pintar, F., Shender, B., & Paskoff, G. Gender dependent cervical spine anatomical differences in size-matched volunteers. 2009. Biomedical sciences instrumentation, 45:149–54.

[34] Harrison, D. D., Janik, J. T., Troyanovich, S. J. & Holland, B. Comparisons of lordotic cervical spine curvatures to a theoretical ideal model of the static sagittal cervical spine. 1996. Spine, 21(6):667–675. ISSN 0362-2436.

[35] A. L. Harden, Y. Kang, R. L. Hunter, A. Bendig, J. H. Bolte IV, N. I. Eckstein, A. G. F. Smith & A. M. Agnew. Preliminary Sex-specific Relationships between Peak Force and Cortical Bone Morphometrics in Human Tibiae Subjected to Lateral Loading. IRCOBI Conference 2021.

[36] R. L. Hunter, Z. Haverfield, A. M. Agnew. Investigation of Sex-specific Effects on Variation in Cortical Bone Morphometrics of the Radius. IRCOBI Conference 2021.

[37] Klein, K. F. Use of Parametric Finite Element Models to Investigate Effects of Occupant Characteristics on Lower-Extremity Injuries in Frontal Crashes. 2015. University of Michigan.

[38] E. Brynskog, J. Iraeus, M. P. Reed & J. Davidsson. Predicting pelvis geometry using a morphometric model with overall anthropometric variables. J Biomech. 2021 Sep 20;126:110633. doi: 10.1016/j.jbiomech.2021.110633.

[39] Šavlovskis, J. & Raits, K. The Bony Pelvis & Gender Differences in Pelvic Anatomy. Anatomy Standard. Last updated: August 12, 2021. Recovered, on April 3, 2022, from: https://www.anatomystandard.com/Pelvis/Pelvis.html.

[40] Vasavada, A., Danaraj, J. & Siegmund, G. Head and neck anthropometry, vertebral geometry and neck strength in height-matched men and women. 2008. Journal of biomechanics, 41:114–21. doi: 10.1016/j.jbiomech.2007.07.007.

[41] Forman, J. L., Poplin, G. S., Shaw, C. G., McMurry, T. L. & Ash, J. L. 2018. Automobile injury trends in the contemporary fleet: belted occupants in frontal collisions. Traffic Injury Prevention.

[42] Roberts, C. W., Forman, J. L. & Kerrigan, J. R. Injury Risk Functions for 5th Percentile Females: Ankle Inversion and Eversion. IRCOBI Conference 2018.

[43] D. Kato, Y. Nakahira, N. Atsumi & M. Iwamoto. Development of Human-Body Model THUMS Version 6 containing Muscle Controllers and Application to Injury Analysis in Frontal Collision after Brake Deceleration. IRCOBI Conference 2018.

[44] M. L. Davis. Development and Full Body Validation of a 5th Percentile Female Finite Element Model. Virginia Tech - Wake Forest University. School of Biomedical Engineering & Sciences. 2017.

[45] Z. Wang, J. McInnis, L. Benfant, Z. Feng & E. Lee. THOR 5th Percentile Female ATD Design. ESV Conference 2017.

[46] A. Carlsson, F. Chang, P. Lemmen, A. Kullgren, K. Schmitt, A. Linder & M. Y. Svensson. EvaRID - A 50th Percentile Female Rear Impact Finite Element Dummy Model. IRCOBI Conference 2012.

[47] A. Carlsson. Addressing Female Whiplash Injury Protection - A Step Towards 50th Percentile Female Rear Impact Occupant Mode. Chalmers University of Technology. 2012.

[48] J. Östh, K. Brolin, M. Y. Svensson & A. Linder. A Female Ligamentous Cervical Spine Finite Element Model Validated for Physiological Loads. J Biomech Eng. 2016 Jun;138(6):061005. doi: 10.1115/1.4032966.

[49] J. Östh, M. Mendoza-Vazquez, M. Y. Svensson, A. Linder & K. Brolin. Development of a 50th Percentile Female Human Body Model. IRCOBI Conference 2016.

[50] J. Östh, M. Mendoza-Vazquez, F. Sato, M. Y. Svensson, A. Linder & K. Brolin. A female head–neck model for rear impact simulations. Journal of Biomechanics, Volume 51, 2017, Pages 49-56, https://doi.org/10.1016/j.jbiomech.2016.11.066.

[51] J. Östh, M. Mendoza-Vazquez, A. Linder, M. Y Svensson & K. Brolin. The VIVA OpenHBM Finite Element 50th Percentile Female Occupant Model: Whole Body Model Development and Kinematic Validation. IRCOBI Conference 2017.

[52] P. A. Putra, J. Iraeus, R. Thomson, M. Y. Svensson, A. Linder & F. Sato Comparison of control strategies for the cervical muscles of an average female head-neck finite element model, Traffic Injury Prevention, 20:sup2, S116-S122, 2019. doi: 10.1080/15389588.2019.1670818.

[53] John, J., Iraeus, J., Klug, C., Svensson, M. & Linder, A. Viva+ open human body models for virtual testing. In automotive CAE Grand Challenge. Hanau, Germany, 2020.

[54] Schubert, A., Erlinger, N., Leo, C., Iraeus, J., John, J. & Klug, C. Development of a 50th Percentile Female Femur Model. In IRCOBI conference proceedings. Online, 2021.

[55] Twohig, C. Development of a Female 50th Percentile Head & Neck Complex. 2020. Project Internship at Siemens. Trinity College Dublin.

[56] Mertz, H. A Procedure for Normalizing Impact Response Data. 1984. SAE Technical Paper 840884. Warrendale, PA, USA.

[57] Database Center for Life Science. BodyParts 3D Iliac crest 03 - anterior view. Recovered, on July 16, 2022, on: https://healthcare-in-europe.com/en/news/iliac-crest-reconstruction-15-patients-recruited-into-greenbric-study.html.

[58] Melvin, J. W., King, A. I. & Alem, N. M. (1985) AATD system technical characteristics, design concepts, and trauma assessment criteria. Task EF final report. University of Michigan & Highway Safety Research Institute, 1985.

[59] ISO TR9790 (1997) Road vehicles - anthropomorphic side impact dummy - lateral impact response requirements to assess the biofidelity of the dummy. ISO/TC22/SC12/WG5 (Anthropometric Test Devices), 1997, Document N455, Revision 4.

[60] Meyer, E. & Bonnoit, J. (1994) Le choc latéral sur l'épaule: mise en place d'un protocole expérimental en sollicitation dynamique. Mémoire de DEA. Laboratoire de biomécanique appliquée, faculté de Marseille, 1994.

[61] Bouquet, R., Ramet, M., Bermond, F. & Cesari, D. (1994) Thoracic and pelvis human response to impact. Proceedings of the Fourteenth International Technical Conference on Enhanced Safety of Vehicles,1994, pp.100–109.

[62] Kroell, C.K. Thoracic response to blunt frontal loading. 1976. The Human Thorax-Anatomy, Injury, and Biomechanics, 67.

[63] Kroell, C. K., Schneider, D. C. & Nahum, A. M. Impact tolerance and response of the human thorax. 1971. SAE Paper 710851, Proceedings of the 15th Stapp Car Crash Conference, pp. 163-213.

[64] Kroell, C. K., Schneider, D. C. & Nahum, A. M. Impact tolerance and response of the human thorax II. 1974. SAE Paper 741187, Proceedings of the 18th Stapp Car Crash Conference, pp. 215-253.

[65] Nahum, A. M., Gadd, C. W. & Schneider, D. C. Deflection of the human thorax under sternal impact. 1970.

[66] Nahum, A. M., Schneider, D. C. & Kroell C. K. Cadaver skeletal response to blunt thoracic impact. 1975. SAE Paper 751150, Proceedings of the 19th Stapp Car Crash Conference.

[67] Cavanaugh, J. M., Nyquist, G. W., Goldberg, S. J. & King, A. I. Lower abdominal tolerance and response. SAE Paper 861878, Proceedings of the Stapp Car Crash Conference, pp. 41-63.

[68] Ishikawa, h., Kajzer, J. & Schroeder, G. Computer simulation of impact response of the human body in car-pedestrian accidents. 1993. SAE paper 933129.

[69] Brundtland, G. Report of the World Commission on Environment and Development: Our Common Future. 1987. United Nations General Assembly document A/42/427.

[70] United Nations Information Portal on Multilateral Environmental Agreements (InforMEA). Key MEAs. Recovered, on July 4, 2022, from: https://www.thinglink.com/scene/846020646906363905?buttonSource=viewLimits

[71] United Nations. Sustainable Developed Goals. Recovered on April 2, 2022, from: https://sdgs.un.org/goals.

ANNEX I. SUSTAINABLE DEVELOPMENT GOALS

The term sustainable development appeared for the first time in 1987 [69], in the Brundtland Report, publication also known as Our Common Future. This report was developed by a committee of the United Nations intergovernmental organization. Said committee was led by the Norwegian prime minister at that time Gro Harlem Brundtland. The aim of this publication was to analyse the environmental-related consequences of economic growth and development at a global level.

The term sustainable development was defined as '*a development which meets the needs of the present without compromising the ability of future generations to meet their own needs*'. This implies, among others, the utilization of renewable or non-renewable resources according to their renewal or substitution capabilities, the guarantee to social and economic equality or to eliminate residues as they are found in the biotope of nature.

A growing political and social concern regarding the aforementioned managed to evolve progressively from awareness into action via a significant growth in the number of Multilateral Environmental Agreements (MEAs) and ultimately, into the Sustainable Development Goals. Fig. 173 shows the key MEAs signed, from the first one with an international context signed in 1971, until the last one of 2013, just before the creation of the Sustainable Development Goals.

And so, in 2015, the Sustainable Development Goals (SDGs) [71] were agreed on in the September 25 Agenda entitled Transforming our world: the 2030 Agenda for Sustainable Development. These SDGs are made up of 17 goals and 169 targets, that focused in areas such as gender equality, education, health, and culture, as shown in the Fig. 174.

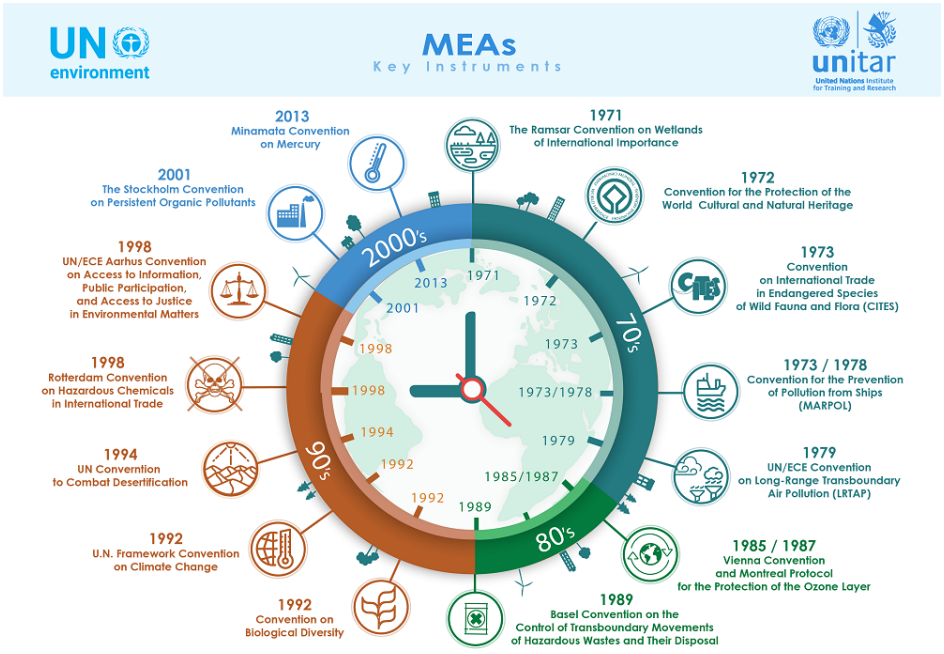

Fig. 173. Key Multilateral Environmental Agreements [70]

Fig. 174. Sustainable Development Goals [71]

The aim of this project was to develop a 50 percentile female version of the existent Simcenter Madymo's Active Human Model, the FAHM. That is, a new human virtual model for occupant vehicle and pedestrian safety that represents female average anthropometry. Thus, the areas that this study covers regarding sustainability and development are:

1. Health; aiming to improve road user's well-being by developing a tool that can be used to optimize vehicle and infrastructure design with respect to safety.
2. Gender equality: aiming to reduce the discrimination against women by providing a tool to OEMs and vehicle safety assessment programmes to be able to consider average female anthropometry in the early stages of vehicle design.

Subsequently, the three sustainable development targets most in line with this study are:

SDG 3 (Good Health and Well-Being) target 6: ***By 2020[1], halve the number of global deaths and injuries from road traffic accidents.***

As seen in the Chapter 3, there is currently only one human model representing 50 percentile female (ViVA), and one dummy model (EvaRID), both of these being FE models. Additionally, and as aforementioned, women have been demonstrated to suffer more severe injuries due to road traffic accidents than men. However, and as explained before, existent adult female FE or MB models (aside from elderly models) correspond to the 5 percentile and are considered as the most restrictive case rather than a baseline for vehicle safety design and assessment, due to its low population representation. Therefore, the development of a MB F50AHM could provide vehicle assessment programmes (such as Euro NACP) and OEMs with a better tool to enhance overall injury probability analysis on women and to improve the baseline of vehicle design process, respectively; leading to safer vehicles and less injuries and deaths in road traffic accidents.

SDG 11 (Sustainable Cities and Communities) target 2: ***By 2030, provide access to safe, affordable, accessible, and sustainable transport systems for all, improving road safety, notably by expanding public transport, with special attention to the needs of those in vulnerable situations, women, children, persons with disabilities and older persons.***

[1] Originally, this target was proposed for 2020, although eventually was changed to 2030. However, this change has not been reflected in any official form, as it would need approval of the United Nations General Assembly.

In line with the abovementioned, this study seeks to develop a female model that can be introduce in the early stages of vehicle safety related design processes, due to its high population representation. Consequently, overall road safety could be improved, especially among the female population.

SDG 5 (Gender Equality) target 1: ***End all forms of discrimination against all women and girls everywhere.***

Evidently, the fact that women's anthropometry is being considered covered by male's anthropometry for vehicle safety design, except for a marginal representation of the population that only acts as a restrictive case to comply, is a form of discrimination that this study envisions to eradicate.